2008

Real time imaging of live cell ATP leaking or release events by chemiluminescence microscopy

Yun Zhang
Iowa State University

Real time imaging of live cell ATP leaking or release events by chemiluminescence microscopy

by

Yun Zhang

A dissertation submitted to the graduate faculty

in partial fulfillment of the requirements for the degree of

DOCTOR OF PHILOSOPHY

Major: Analytical Chemistry

Program of Study Committee:
Edward S Yeung, Major Professor
Robert S. Houk
Gregory J. Phillips
Nicola L. Pohl
Klaus Schmidt-Rohr

Iowa State University

Ames, Iowa

2008

To my parents

To my husband and daughter

TABLE OF CONTENTS

ABSTRACT

The purpose of this research was to expand the chemiluminescence microscopy applications in live bacterial/mammalian cell imaging and to improve the detection sensitivity for ATP leaking or release events.

We first demonstrated that chemiluminescence (CL) imaging can be used to interrogate single bacterial cells. While using a luminometer allows detecting ATP from cell lysate extracted from at least 10 bacterial cells, all previous cell CL detection never reached this sensitivity of single bacteria level. We approached this goal with a different strategy from before: instead of breaking bacterial cell membrane and trying to capture the transiently diluted ATP with the firefly luciferase CL assay, we introduced the firefly luciferase enzyme into bacteria using the modern genetic techniques and placed the CL reaction substrate D-luciferin outside the cells. By damaging the cell membrane with various antibacterial drugs including antibiotics such as Penicillins and bacteriophages, the D-luciferin molecules diffused inside the cell and initiated the reaction that produces CL light. As firefly luciferases are large protein molecules which are retained within the cells before the total rupture and intracellular ATP concentration is high at the millmolar level, the CL reaction of firefly luciferase, ATP and D-luciferin can be kept for a relatively long time within the cells acting as a reaction container to generate enough photons for detection by the extremely sensitive intensified charge coupled device (ICCD) camera. The result was inspiring as various single bacterium lysis and leakage events were monitored with 10-s temporal resolution movies. We also found a new way of enhancing diffusion D-luciferin into cells by dehydrating the bacteria.

Then we started with this novel single bacterial CL imaging technique, and applied it for quantifying gene expression levels from individual bacterial cells. Previous published result in single cell gene expression quantification mainly used a fluorescence method; CL detection is limited because of the difficulty to introduce enough D-luciferin molecules. Since dehydration could easily cause proper size holes in bacterial cell membranes and facilitate D-luciferin diffusion, we used this method and recorded CL from individual cells each hour after induction. The CL light intensity from each individual cell was integrated and gene expression levels of two strain types were compared. Based on our calculation, the overall sensitivity of our system is already approaching the single enzyme level. The median enzyme number inside a single bacterium from the higher expression strain after 2 hours induction was quantified to be about 550 molecules.

Finally we imaged ATP release from astrocyte cells. Upon mechanical stimulation, astrocyte cells respond by increasing intracellular Ca^{2+} level and releasing ATP to extracellular spaces as signaling molecules. The ATP release imaged by direct CL imaging using free firefly luciferase and D-luciferin outside cells reflects the transient release as well as rapid ATP diffusion. Therefore ATP release detection at the cell surface is critical to study the ATP release mechanism and signaling propagation pathway. We realized this cell surface localized ATP release imaging detection by immobilizing firefly luciferase to streptavidin beads that attached to the cell surface via streptavidin-biotin interactions. Both intracellular Ca^{2+} propagation wave and extracellular ATP propagation wave at the cell surface were recorded with fluorescence and CL respectively. The results imply that at close distances from the stimulation center (<120 μm) extracellular ATP pathway is faster, while at long distances (>120 μm) intracellular Ca^{2+} signaling through gap junctions seems more effective.

CHAPTER 1. GENERAL INTRODUCTION

Dissertation Organization

This dissertation begins with a general introduction of the history and recent progress in cell imaging, chemiluminescence detection and ATP analysis with a list of cited references. The following chapters are arranged in such a way that published papers and a manuscript to be submitted are each presented as separate chapters. Cited literature, tables and figures for each paper or manuscript are attached to the end of each chapter. A general conclusion chapter summarizes the work and provides some perspective for future research.

Cell Imaging

Overview

In 1665, the English scientist Robert Hooke looked at a thin slice of cork through a compound microscope. He observed tiny, hollow, roomlike structures, which he called 'cells' because they remind him of the rooms that monks live in.[1] Since this first look at a cell in human history, scientists have been fascinated by viewing cells through microscopes. Early observations in the nineteenth century were mainly limited to morphological descriptions of visible structures, missing the chemical molecular details. Entering into the twentieth century, molecular imaging to study biochemistry and genetics inside cells has been made possible by the explosive progress in microscope techniques and imaging devices. Firstly, in the mid1950s the introduction of phase contrast microscope, for which Zernike won the Nobel Prize in 1955, as well as polarization and differential interference contrast (DIC) microscopy,

solved the problem of low contrast for cellular components in bright-field optics. Taking advantage of differences in optical density, refractive index, and phase differences the new microscopes revealed fine cellular structural details.[2] Secondly, the revolutionary introduction of the fluorescence microscope and discovery of fluorescent dyes during the 1930s urged scientific workers to shift the interest from pure morphology to specific nucleic acids, proteins, and carbohydrates inside cells.[3] Nowadays, fluorescent probes for imaging cell organelles, lipids and membranes, endocytosis, ion channels, signal transduction, and cell proliferation are readily commercially available.[4] In addition, the old photomicrography using films to document images has now been replaced by the modern charge coupled device (CCD) cameras. Cell images are no longer static, snapshot pictures, but are in vivid movies that record the dynamic movements of each individual cell. These technical advances have greatly accelerated the pace of development and are targeting research toward answering more profound biological questions. It has been forecast that the challenge for the twenty-first century is "to understand how these casts of molecular characters (genomes and expressed proteins) work together to make living cells and organisms, and how such understanding can be harnessed to improve health and well-being."[5]

Microscopy Techniques

Cells are small in size, as mammalian cells around 10 μm, and bacteria only about 1 μm. Without the help of a microscope, the naked human eyes can not observe such tiny creatures. The basic components of a modern microscope usually include an illumination light, an objective that magnifies the sample, a condenser system, and two oculars. The quality of the image is described by resolution, which is determined by the numerical

aperture of the objective and the substage condenser. For a microscope with perfect alignment and matching objective and condenser, the limit of resolution is defined by the Rayleigh formula:[6]

$$\text{Resolution (r)} = 0.61\lambda/\text{NA}$$

Where r is the resolution, NA is the microscope numerical aperture, λ is the imaging wavelength. When using a 100× oil immersion objective with NA = 1.25 and tungsten halogen bulb illumination (spectrum centered at λ = 550 nm, green light), the calculated resolution is 270 nm, which is good enough for most cell imaging work.

Several types of transmission microscopes are available for cellular structure and morphology imaging. The bright field microscope is most commonly used because of the low cost, but the contrast is not good, as cells are nearly transparent lacking big refractive index differences. Therefore it is usually used in combination with cell fixation and staining.[7] The phase contrast microscope enhances the image contrast by changing the phase of the central beam by ¼ of a wavelength, then cells that have varying thickness and slight differences in refractive index from the surrounding medium act as diffraction gratings, and the diffracted rays are brought to focus at the ocular where they reinforce the central rays, producing a bright cell image.[2] The strong contrast phase images can show clear cell structures without staining. Differential interference contrast (DIC) microscopy provides even better contrast for transparent specimens. It is optically far more complicated than the phase contrast system to create true interference.[2, 8] In short, the light passes through the polarizer and is split into two perpendicularly plane-polarized beams by a Wollaston or Nomarski prism. The two beams passing through the specimen are separated by an extremely short distance, e.g. 0.22 μm for a 100× NA 1.25 objective/ Nomarski condenser, and are recombined by the objective

and the second Wollaston or Nomarski prism. An analyzer, which is a second polarizer, is oriented 45° with the first polarizer. Slight phase differences in the cell specimens cause tiny optical path differences of the two polarized beams and after destructive or constructive interference finally appear as shadow cast images. DIC microscope can view structural details near the resolution limit, and furthermore with electronic contrast enhancement by video cameras, 25-nm diameter microtubules were reported to be visible by Allen et al.[9]

Fluorescence microscopy also serves the role to look at cell morphology using fluorescent tracers,[10-12] but the more important applications are in tracking specific molecules and studying biochemistry inside cells. Fluorophores are connected to specific proteins or nucleic acids through amine or thiol modifications, or bind with Ca^{2+}, $Ma^{2+}$and other metal ions, in order to detect organelles, lipids and membranes, ion channels etc., and to study signal transduction and metal ion flows with fluorescence imaging.[13-16] The most widely used fluorescence microscopy system is epi-fluorescence. It has the advantage of high efficiency and simplicity of operation because the objective also functions as the condenser. A high illumination mercury lamp is used to excite the sample, and then emitted light travels back through the same objective, followed by a dichroic mirror that changes its optical path to the detector.[2, 17] While the conventional fluorescence microscopy is used wildly in clinical and fundamental biochemical research, there are circumstances when its applications are hampered by intrinsic problems. For example, in conventional wide-field microscopes the depth of field for a 100× NA 0.95 objective is 0.2 μm, but image depth is 80 mm because of diffraction,[18] rendering that image details are superimposed within the plane of focus, and structural details are obscured by halos from out-of-focus light. To solve this problem confocal microscope was developed using point illuminating and a pinhole in the focal plane

to eliminate out-of-focus light.[19] With this new technique cells can be imaged in thin slices of about 0.5 μm with a high NA objective and reconstructed to reveal the three-dimensional structure.[20, 21] Besides confocal microscopy, there are many more new technologies that have emerged in recent decades targeting different issues in fluorescence microscopy, among them fluorescence resonance energy transfer (FRET), total internal reflection fluorescence microscopy (TIRFM), two-photon excitation microscopy (TPEM), fluorescence lifetime imaging microscopy (FLIM), etc. Excellent reviews of the principles and applications of these technologies can be found in the literature.[17, 19, 22-35]

Chemiluminescence microscopy is not as popular as fluorescence microscopy mainly because of the high sensitivity detector requirement for observing ultra low level light, but it is gaining more interest because (1) the intensified charge coupled device (ICCD) camera was produced to capture ultra low light,[36] and (2) luciferase as a reporter enzyme has the advantages of no background, no photobleaching, and no photo damage to cells.[37] The instrumentation is just like a conventional light microscope without using the light source. We have chosen to use this technique in the work presented here because we have a single photon sensitivity level ICCD camera, meanwhile we are interested in studying ATP related cell activities, which are best probed with the chemiluminescence reaction of firefly luciferase. Reviews of detailed methods and applications using this technique will be presented in a later section.

Imaging Devices

Photon detectors applicable for cell imaging can be classified into single channel or multichannel detectors. The photomultiplier tube (PMT) is the most sensitive single channel

detector. The schematic map is show in Figure 1 (bottom).[38] A photon strikes the cathode and generates a photoelectron, which then strikes the first dynode with enough energy to release two to five secondary electrons. Each secondary electron is accelerated and strikes the next dynode to release another two to five electrons. The multiplication process continues until the anode is reached, where the current is measured with a gain usually around 10^4 to 10^7.[39] Dark current mainly comes from thermal emission from the dynodes, and could be reduced by setting the PMT temperatures below 0°C. Because of the high gain and low noise, PMT is very useful for ultra-low-light detection. But the result is one dimensional, unless a scanning microscope is used, such as a confocal microscope, to obtain two dimensional cell images.

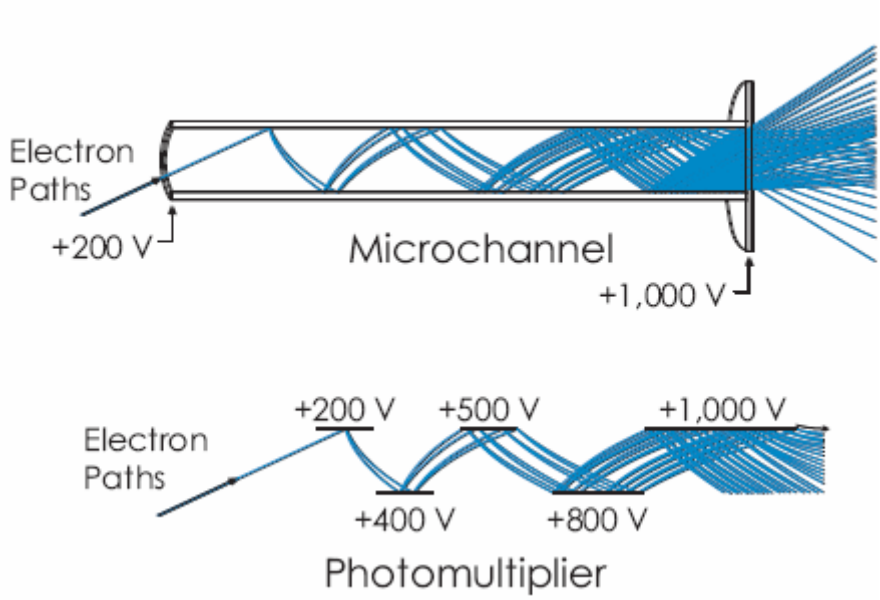

Figure 1. Schematic map of a microchannel plate (top), and a photomultiplier (bottom). Cited from reference 38.

To record images with excellent spatial information, the traditional way was to project the image on to color films. Since the invention of digital photography in 1969 by Willard Boyle and George E. Smith at AT&T Bell Labs,[2, 40] the CCD camera has now

become the standard imaging device finding the most widespread application.[41, 42] A CCD camera is composed of two parts, a photoactive region with a capacitor array sitting on top of a thin insulating oxide layer on top of a *p* type silicon substrate, and the transmission region of a shift register.[39] When the gate or shutter at the front of CCD camera is open, the image is projected on the array, causing electron accumulation in each pixel well in an amount proportional to the incident light intensity and exposure time. A control circuit in the transmission region creates a potential well that is used to shift the charge to a high speed shift register for readout by the output amplifier. The result is scanned row by row and shown as a two dimensional digital image. While CCD cameras are excellent for fluorescence detections, the usage is limited in ultra low light chemiluminescence detection. Since there is no signal multiplication component as in PMT, CCD has to increase the exposure time to gather enough light signal, which at the same time increases the noise. For ultra low light imaging, sometimes the noise itself accumulated long enough has exceeded the dynamic range of CCD chip.

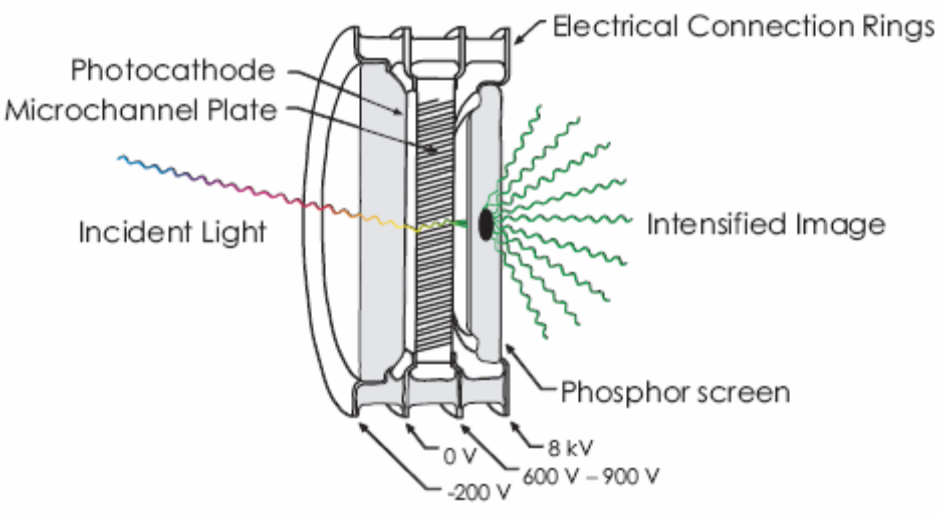

Figure 2. Components of an image intensifier tube. Cited from reference 38.

The ICCD camera overcomes the limitation by integrating an intensifier in front of the CCD chip. Figure 2 displays the components of an image intensifier.[38] Incident photons strike the photocathode and cause electrons to be released. The electrons are accelerated and multiplied when passing through the microchannel plate (MCP). The multiplication process is similar to that in the PMT (Figure 1 top). Multiplied electrons hit the phosphor screen and cause it to release photons, which are then imaged by the CCD camera behind it. ICCD functions like a two dimensional PMT, with extremely high sensitivity. The major source of dark current is also thermal emission on the photocathode; therefore it is necessary to cool the intensifier chip as well as the CCD to reduce dark noise.

Chemiluminescence Detection

Introduction

The term 'luminescence' was created by Eilhardt Wiedemann in 1888 to describe 'cold light' emission, the light excited from means other than thermal heating. According to the manner of excitation, he classified luminescence phenomena into six categories: photoluminescence, electroluminescence, thermoluminescence, triboluminescence, cristalloluminescence, and chemiluminescence.[43, 44] Chemiluminescence (CL) was defined to be light emission caused by a chemical reaction.

Chemiluminescence light is generated in reactions of two mechanisms. A substrate and an oxidant in the presence of some cofactors and sometimes a catalyst, react to form a product or intermediate in an electronically excited state. Then the excited state product or intermediate relaxes to the ground state with emission of a photon, or in the other mechanism the excited species transfers the energy to a fluorophore, which then relaxes to the ground

state with photon emission.[43] Many factors influence the CL quantum efficiency and reaction rate, including the chemical structure and concentration of substrate and catalyst, temperature, pH and ionic strength, the hydrophobicity of the solvent and solution composition, and the presence of energy transfer acceptors. In favorable conditions, the most efficient CL system—ATP and firefly luciferase has a high quantum efficiency (QE) of 0.88.[45] Another bioluminescence system, bacterial luciferase can reach QE = 0.27.[46] Bioluminescence (BL) systems as CL from living organisms generally have a higher QE than non-BL systems, which at best can only approach 0.02.[47]

Since the CL reaction rate is a function of the chemical concentration, CL detection is suitable for quantitative analysis. CL can be coupled with chromatography,[48, 49] capillary electrophoresis,[50, 51] or immunoassay[52-54] as the analytical detection technique, providing qualitative or quantitative information on a wide range of samples in the gas or liquid phases. For organic analysis, compounds such as diacylhydrazides, indoles, acridines and acridans, polydimethylaminoethylenes, anthracenes, and aroyl peroxides have strong CL that can be measured directly;[43] a substantial number of other compounds with weak CL or no CL may be oxidized or thermally excited and transfer the energy to acceptor fluorophore to emit CL, such cases including drugs like penicillin,[55] cephalothin sodium,[56] hydrocortisone,[57] and etc. Inorganic ions can also be detected with CL methods based on their catalytic or inhibiting behaviors, e.g. detection limit of Co(II),[58] Cu(II),[59] Cr(III)[60] can reach pg/mL, although selectivity is usually poor in such analysis. Enzyme linked immunosorbent assay (ELISA) for determining antigen/antibody[61, 62] and DNA analysis[63-67] were also reported to use CL as the detection method.

Firefly luciferase CL system

The firefly luciferase system is the most commonly used CL system. The reaction mechanism is shown schematically in Figure 3.

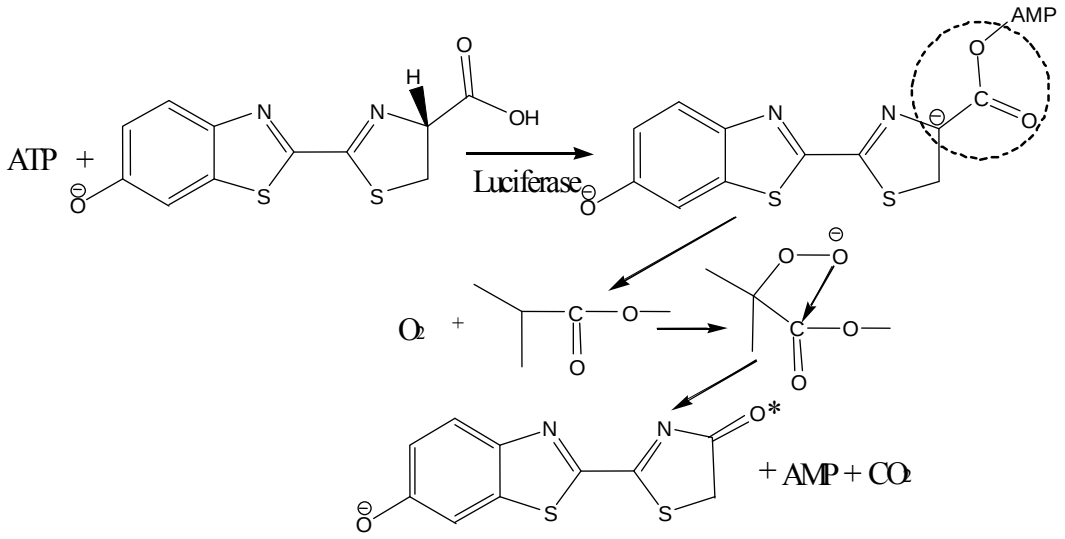

Figure 3. Firefly luciferase reaction mechanism.

Substrate D-luciferin is adenylated in the presence of the enzyme firefly luciferases and the cofactors ATP, Mg^{2+}. Luciferyl adenylate is oxygenated at its tertiary carbon (circled in Figure 3), forming a hydroperoxide intermediate. The hydroperoxide forms a very unstable 4-membered dioxetanone ring by splitting off AMP. Then the dioxetanone quickly decomposes into excited oxyluciferin and CO_2. [47, 68] Excited state oxyluciferin falls to the ground state accompanied by CL emission light. The overall reaction is as follows:

$$ATP + O_2 + \text{D-Luciferin} \rightarrow AMP + PP_i + CO_2 + \text{oxyluciferin} + \text{light (560 nm)}$$

The optimum reaction condition is at pH 7.75,[69] and a temperature of 25°C.[70] The emission is a broad peak with the maximum at 560 nm.[45] The structure of luciferase was determined by Conti et al. and reported in 1996 *Structure*.[71] It has a molecular weight of 61,000.[72] Firefly luciferase appears to be slow enzyme, with a specific activity k_{ES} of 0.1 U

mg^{-1} (1 U = 1 μmol substrate min^{-1}).[73, 74] According to our calculation, each firefly luciferase molecule produces ~21 photons in 2 minutes.[75]

Firefly luciferase CL reaction is broadly employed in sensitive detection of ATP. A detection limit of 10^{-11} M ATP can be reached at optimized conditions.[76] Therefore any ATP concentration change related cell activities can be sensitively detected with this CL system. Helped by the advances in genetic technology, the new trend during the past two decades is to utilize the system together with cell imaging techniques in fundamental cell biology study. Luc gene, the cDNA encoding the firefly luciferase cloned by Ed Wet et al. in 1985,[72] can serve as the reporter gene in various vectors and fusion constructs for studying gene delivery and regulation in live cells and organisms. For instance, James et al. showed in 1993 that after mechanical injury to the smooth muscle Rb-1 cell there is an expression increase of the Luc fused to the 5'-flanking region of the rabbit collagenase gene containing a wild type promotor;[77] Kennedy et al. reported in 1999 that in MIN6 β-cells the expression of Luc fused to insulin promoter is induced by glucose through increases in intracellular Ca^{2+} concentration in presence of insulin or the Ca^{2+} channel inhibitor verapamil.[78] Many more applications of firefly luciferase imaging in bacteria, plant and animal cells or tissues are summarized in literature reviews.[79-82]

Another frequently used reporter is green fluorescent protein (GFP), a fluorescent reporter.[83] Compared to GFP, firefly luciferase as a CL reporter has several advantages. First, no external light source is required in CL detection, so background from scattered stray light is eliminated, meanwhile problems associated with incident light such as instable excitation external source and interference from nonselective excitation process are avoided. This has also made the instrumentation simple— no lamp or excitation filter is needed. Second, after

expression GFP requires a maturation time generally around 2-4 h for the protein folding into a fluorescent chromophore formation.[83] Firefly luciferase expression in cells does not require this process therefore is suitable for real time imaging of fast dynamic cell activities. Additionally, CL detection does not photobleach the fluorophore, or cause photo damage to cells or organisms, hence is the method of choice for long term live cell or organism observations. Plus, firefly luciferase CL reaction is very specific and selective; no autofluorescence is present like in fluorescence detections.

However this remarkable CL system also has some drawbacks, such as the high requirement for sensitivity, and limitation in introduction of substrate D-luciferin into cells. It was suggested to use low pH,[84] or membrane-permeable luciferin esters that will hydrolyze into luciferin inside mammalian cells[85] to overcome this limitation. We recently proposed a novel way of improving luciferin diffusion by drying the bacteria cells.[75, 86]

ATP

ATP: the Energy Currency

Adenosine triphosphate (ATP) is a complex molecule that consists of a nucleoside adenosine and a tail of three phosphate groups. It was first discovered by Karl Lohmann in 1929.[87] After years of studies of its structure, production and consumption in cells, in 1941 Fritz Albert Lipmann proposed ATP to be the main molecule for chemical energy storage and there is a cycle within the cell that circulates ATP.[88]

ATP is found in all living cells, whether of microbial or eukaryotic origin. It is called the 'energy currency' because ATP is involved in virtually every activity of the cells or organisms by providing energy when it removes one or two of its phosphate-oxygen groups,

leaving adenosine diphosphate (ADP) or adenosine monophosphate (AMP). Then ADP is converted back to ATP in cellular respiration processes. In eukaryotic aerobic metabolism, one molecule of glucose is break down to CO_2 and generates 36-38 molecules of ATP, of which 2 are from glycolysis in cytoplasm, and 34-36 from oxidative decarboxylation of pyruvate and the Krebs cycle in mitochondria.[89]

The importance of using ATP as the index of biomass was recognized as early as 1968 by NASA groups for detection of life on other planets.[90] The ATP concentration inside the cell is typically 1–10 mM.[91] Depending on the cell volume, the ATP amount ranges from around 10^{-18} mol per cell in bacteria to 10^{-15} mol per cell in mammalian cells.[92] By extracting microbial ATP using chemical extractants or preferably non-chemical extraction procedures such as rapid heating or ultrasonic homogenization, then detecting ATP with a luminometer using firefly luciferase assay, 10+ bacterial cells could be tested in a 1 ml assay with a sensitive 10^{-11} M detection limit luminometer.[76] This method is widely used in clinical studies for detecting trace amount of microorganisms as it is faster and more convenient then the traditional cell culture method. We improved the method, and have proved that employing the advanced cell imaging technique ATP CL could be monitored from each individual bacterial cell.[86]

ATP as the Signaling Molecule

ATP not only plays the central role in the energy status of cell, but also serves as an important regulator of cell functions. ATP is small, rapidly diffusing, highly unstable and low in abundance in the extracellular environment. Those properties make it an ideal extracellular signaling molecule. This important signaling role of ATP and its metabolic products ADP,

AMP and adenosine was proposed in 1972 by Burnstock since he observed their release from putative purinergic nerves as neurotransmitters.[93] Numerous other tissues were reported to respond to extracellular adenosine and ATP in the following decades.[94-97] By now the roles of nucleotides and nucleosides as extracellular signaling molecules have been well established.[98]

Release of ATP regulates various cell autocrine and paracrine functions by activating purinergic membrane receptors P2.[95] P2 receptors have been divided into P2X ligand-gated ion channel and P2Y G protein coupled receptor families. P2X purinergic receptors were proposed to mediate contractile effects of ATP on smooth muscle.[99] They have two transmembrane domains with extensive extracellular loop, a structure similar to the inward rectifier potassium channel and the epithelial sodium channel.[100] Interaction of ATP causes influx of Ca^{2+} within milliseconds, followed by a rapid inactivation of the depolarizing current.[95] These receptors are widely distributed in the central nervous system and many types of smooth muscle. P2Y purinergic receptors were originally identified to mediate relaxant effects of ATP on smooth muscle.[99] They are a group of G-protein coupled receptors that regulate through second messenger responses. One receptor type exists on turkey drythrocytes was reported to respond to ATP/ADP by activating phopholipase C to induce inositol triphosphate (IP3) signaling pathway leading to mobilization of calcium.[101, 102] Another receptor type was reported by Okajima and coworkers on rat hepatocytes to inhibit adenylyl cyclase but has no effect on phospholipase C.[103] The existence of receptors of different second messenger pathways proves that there are multiple subtypes within the P2Y family. In fact, seven subtypes of P2X receptors and six subtypes of P2Y receptors have been

clones and characterized.[104] Each subtype of receptors exists in certain tissues and has different responding activities to ATP and other nucleotide signaling molecules.

ATP Detection

Extensive studies have focused on ATP function as the signaling molecule to regulated cell activities, but many questions remains to be the answered. For example, the underlying mechanism of ATP release is still a mystery. An effective, sensitive way of detecting intracellular/extracellular ATP from live cells is required. Of the current available ATP detection techniques, bioluminescence based method is the most widely used one. Luminometers with PMTs incorporated can monitor nanomolar level extracellular ATP changes from the bulk solutions outside cells in real time, but the one-dimensional result lacks spatial information. Multichannel video detector CCD/ICCDs allow user to acquire spatial and temporal information of dynamic live cell ATP release events in real time with 1-s temporal resolution, and the sensitivity is similar to luminometer detection. Amperometric detection provides an alternative approach for the challenging task of cellular level ATP detection. Using a three enzyme reactor that recycles ATP a modified graphite flow-through electrode was able to detect 1 nM to 5 μM ATP with amperometric method.[105] However this technique is limited by the stability and reliability of the generated analytical signal. False positives may come from interfering substances. Other less commonly used ATP detection methods include ^{31}P NMR,[106] scanning electrochemical microscopy,[107] and patch clamp technique.[108]

Our Goal

While fluorescence live cell imaging has been advancing at a fast pace during the past two decades, chemiluminescence live cell imaging lags behind because of the limitations in instrumentation sensitivity and high cost. From this introduction we could see that CL detection contributes as the best cellular ATP imaging technique. The role of ATP in cell metabolism and function regulation has been extensively studied, but is far from completely elucidated. More sensitive CL imaging method with added features like localized cell surface ATP detection will greatly help chemists, biochemists and biologists in the fundamental research of studying biochemistry inside cells. This has been our goal throughout the work presented in the following chapters.

References

(1) In *Encyclopaedia Britannica,* 15 ed.; Vol. 6, pp 44.

(2) Robert F. Smith; D. Sc.; S., D. R. M. *Microscopy and Photomicrography*, Second ed.; CRC Press, Inc.: Ithaca, New York, 1994.

(3) Elli Kohen; Hirschberg, J. G. *Cell Structure and Function by Microspectrofluorometry*; Academic Press, Inc.: San Diego, California, 1989.

(4) Haugland, R. P. *The Handbook: A Guide to Fluorescent Probes and Labeling Technologies*, Tenth ed.; Invitrogen Corp., 2005.

(5) Rieder, C. L.; Khodjakov, A. *Science* **2003**, *300*, 91-96.

(6) Ronald Jowett Oldfield; Oldfield, R. *Light Microscopy: An Illustrated Guide*; Elsevier Health Sciences, 1994.

(7) Foster, B. *Optimizing Light Microscopy for Biological and Clinical Laboratories*; Kendall/Hunt Publishing Company: Dubuque, IA, 1997.

(8) Salmon, E. D. *Trends in Cell Biology* **1995**, *5*, 154-158.

(9) Allen, R. D. *Annual Review of Biophysics and Biophysical Chemistry* **1985**, *14*, 265-290.

(10) Ledley, F. D.; Soriano, H. E.; Omalley, B. W.; Lewis, D.; Darlington, G. J.; Finegold, M. *Biotechniques* **1992**, *13*, 580-&.

(11) Tajbakhsh, S.; Vivarelli, E.; Cuselladeangelis, G.; Rocancourt, D.; Buckingham, M.; Cossu, G. *Neuron* **1994**, *13*, 813-821.

(12) Serbedzija, G. N.; Bronnerfraser, M.; Fraser, S. E. *Development* **1989**, *106*, 809-&.

(13) Giloh, H.; Sedat, J. W. *Science* **1982**, *217*, 1252-1255.

(14) Tsien, R. Y.; Rink, T. J.; Poenie, M. *Cell Calcium* **1985**, *6*, 145-157.

(15) Weiss, S. *Science* **1999**, *283*, 1676-1683.

(16) White, J. G.; Amos, W. B.; Fordham, M. *Journal of Cell Biology* **1987**, *105*, 41-48.

(17) Stephens, D. J.; Allan, V. J. *Science* **2003**, *300*, 82-86.

(18) Kenneth R. Spring; Davidson, M. W.; Nikon MicroscopyU, pp http://www.microscopyu.com/articles/formulas/formulasfielddepth.html.

(19) Xue Feng Wang; Herman, B. *Fluorescence imaging spectroscopy and microscopy*; John Wiley & Sons, Inc.: New York, NY, 1996.

(20) Chacon, E.; Harper, I. S.; Reece, J. M.; Herman, B.; Lemasters, J. J. *Biophysical Journal* **1993**, *64*, A106-A106.

(21) Chacon, E.; Reece, J. M.; Nieminen, A. L.; Zahrebelski, G.; Herman, B.; Lemasters, J. J. *Biophysical Journal* **1994**, *66*, 942-952.

(22) Axelrod, D. *Methods in Cell Biology* **1989**, *30*, 245-270.

(23) Axelrod, D. *Traffic* **2001**, *2*, 764-774.

(24) Axelrod, D.; Burghardt, T. P.; Thompson, N. L. *Annual Review of Biophysics and Bioengineering* **1984**, *13*, 247-268.

(25) Bastiaens, P. I. H.; Squire, A. *Trends in Cell Biology* **1999**, *9*, 48-52.

(26) Bergman, A.; Jortner, J. *Chemical Physics Letters* **1972**, *15*, 309-&.

(27) Berland, K. M.; So, P. T. C.; Gratton, E. *Biophysical Journal* **1995**, *68*, 694-701.

(28) Clegg, R. M. *Methods in Enzymology* **1992**, *211*, 353-388.

(29) Eckstein, J. N.; Ferguson, A. I.; Hansch, T. W. *Physical Review Letters* **1978**, *40*, 847-850.

(30) Gadella, T. W. J.; Jovin, T. M.; Clegg, R. M. *Biophysical Chemistry* **1993**, *48*, 221-239.

(31) Krichevsky, O.; Bonnet, G. *Reports on Progress in Physics* **2002**, *65*, 251-297.

(32) Saile, V. *Applied Optics* **1980**, *19*, 4115-4122.

(33) Sanders, R.; Draaijer, A.; Gerritsen, H. C.; Houpt, P. M.; Levine, Y. K. *Analytical Biochemistry* **1995**, *227*, 302-308.

(34) Selvin, P. R. *Biochemical Spectroscopy* **1995**, *246*, 300-334.

(35) Wu, P. G.; Brand, L. *Analytical Biochemistry* **1994**, *218*, 1-13.

(36) Hayakawa, T.; Kinoshita, K.; Miyaki, S.; Fujiwake, H.; Ohsuka, S. *Photochemistry and Photobiology* **1986**, *43*, 95-97.

(37) de Ruijter, N. C. A.; Verhees, J.; van Leeuwen, W.; van der Krol, A. R. *Plant Biology* **2003**, *5*, 103-115.

(38) Princeton Instruments, pp Introduction to Image Intensifiers for Scientific Imaging, @ www.piacton.com.

(39) James D. Ingle; Crouch, S. R. *Spectrochemical Analysis*; Prentice Hall, 1988.

(40) Johnstone, B. *We Were Burning : Japanese Entrepreneurs and the Forging of the Electronic Age*; Basic Books, 1999.

(41) Epperson, P. M.; Sweedler, J. V.; Bilhorn, R. B.; Sims, G. R.; Denton, M. B. *Analytical Chemistry* **1988**, *60*, A327-&.

(42) Sweedler, J. V.; Bilhorn, R. B.; Epperson, P. M.; Sims, G. R.; Denton, M. B. *Analytical Chemistry* **1988**, *60*, A282-&.

(43) Ana M. García-Campaña; Baeyens, W. R. G. *Chemiluminescence in analytical chemistry* Marcel Dekker, Inc.: New York, NY, 2001.

(44) Wiedemann, E. *Ann Phys Chem* **1888**, *34*, 446-463.

(45) Seliger, H. H.; Mcelroy, W. D. *Archives of Biochemistry and Biophysics* **1960**, *88*, 136-141.

(46) Hastings, J. W.; Riley, W. H.; Massa, J. *Journal of Biological Chemistry* **1965**, *240*, 1473-&.

(47) Brolin, S.; Wettermark, G. *Bioluminescence Analysis*; VCH: Weinheim, New York, Basel, Cambridge, 1992.

(48) Kwakman, P. J. M.; Brinkman, U. A. T. *Analytica Chimica Acta* **1992**, *266*, 175-192.

(49) Nakashima, K.; Imai, K. *Molecular Luminescence Spectroscopy*; Wiley: New York, 1993.

(50) Tsukagoshi, K.; Okumura, Y.; Nakajima, R. *Journal of Chromatography A* **1998**, *813*, 402-407.

(51) Wu, N. *Journal of Chromatography* **1993**, *639*, 383-383.

(52) Bowie, A. R.; Sanders, M. G.; Worsfold, P. J. *Journal of Bioluminescence and Chemiluminescence* **1996**, *11*, 61-90.

(53) Robards, K.; Worsfold, P. J. *Analytica Chimica Acta* **1992**, *266*, 147-173.

(54) Lewis, S. W.; Price, D.; Worsfold, P. J. *Journal of Bioluminescence and Chemiluminescence* **1993**, *8*, 183-199.

(55) Chen, S.; Yan, G.; Schwartz, M. A.; Perrin, J. H.; Schulman, S. G. *Journal of Pharmaceutical Sciences* **1991**, *80*, 1017-1019.

(56) Schulman, S. G.; Perrin, J. H.; Guo, F. Y.; Chen, S. X. *Analytica Chimica Acta* **1991**, *255*, 383-385.

(57) Aichinger, I.; Gubitz, G.; Birks, J. W. *Journal of Chromatography* **1990**, *523*, 163-172.

(58) Ling, M. F.; Lu, M. G. *Fenxi Huaxue* **1986**, *14*, 941-943.

(59) Zhang, Z. J.; Dong, W., B. *Kexue Tongbao* **1984**, *29*, 447-480.

(60) Zhang, Z. J.; Lu, J. R. *Huaxue Tongbao* **1984**, *5*, 25-29.

(61) Weeks, I.; Campbell, A. K.; Woodhead, J. S. *Clinical Chemistry* **1983**, *29*, 1480-1483.

(62) Weeks, I.; Beheshti, I.; Mccapra, F.; Campbell, A. K.; Woodhead, J. S. *Clinical Chemistry* **1983**, *29*, 1474-1479.

(63) Beck, S.; Koster, H. *Analytical Chemistry* **1990**, *62*, 2258-2270.

(64) Chiu, N. H. L.; Christopoulos, T. K. *Analytical Chemistry* **1996**, *68*, 2304-2308.

(65) Tizard, R.; Cate, R. L.; Ramachandran, K. L.; Wysk, M.; Voyta, J. C.; Murphy, O. J.; Bronstein, I. *Proceedings of the National Academy of Sciences of the United States of America* **1990**, *87*, 4514-4518.

(66) Balaguer, P.; Terouanne, B.; Boussioux, A. M.; Nicolas, J. C. *Analytical Biochemistry* **1991**, *195*, 105-110.

(67) Nelson, N. C.; BenCheikh, A.; Matsuda, E.; Becker, M. M. *Biochemistry* **1996**, *35*, 8429-8438.

(68) Shimomura, O. *Bioluminescence : chemical principles and methods* World Scientific Publishing Co. Pte. Ltd.: Hackensack, NJ, 2006.

(69) Lundin, A.; Rickardsson, A.; Thore, A. *Analytical Biochemistry* **1976**, *75*, 611-620.

(70) Mcelroy, W. D.; Strehler, B. L. *Archives of Biochemistry* **1949**, *22*, 420-433.

(71) Conti, E.; Franks, N. P.; Brick, P. *Structure* **1996**, *4*, 287-298.

(72) Dewet, J. R.; Wood, K. V.; Helinski, D. R.; Deluca, M. *Proceedings of the National Academy of Sciences of the United States of America* **1985**, *82*, 7870-7873.

(73) Schram, E.; Ahmad, M.; Moreels, E. *Bioluminescence and Chemiluminescence Basic Chemistry and Analytical Applications*; Academic Press: New York, 1981.

(74) Wulff, K.; Haar, H.-P.; Michal, G. *Luminescent Assays Perspectives in Endocrinology and Clinical Chemistry*; Raven Press: New York, 1982.

(75) Zhang, Y.; Phillips, G. J.; Yeung, E. S. *Analytical Chemistry* **2008**, *80*, 597-605.

(76) P.E. Stanley; B.J. McCarthy; Smither., R. *ATP luminescence : rapid methods in microbiology* Oxford [England] ; Boston : Blackwell Scientific Publications ; Brookline Village, Mass. : Distributors, USA, Publishers' Business Services 1989.

(77) James, T. W.; Wagner, R.; White, L. A.; Zwolak, R. M.; Brinckerhoff, C. E. *Journal of Cellular Physiology* **1993**, *157*, 426-437.

(78) Kennedy, H. J.; Rafiq, I.; Pouli, A. E.; Rutter, G. A. *Biochemical Journal* **1999**, *342*, 275-280.

(79) Contag, C. H.; Bachmann, M. H. *Annual Review of Biomedical Engineering* **2002**, *4*, 235-260.

(80) Contag, C. H.; Ross, B. D. *Journal of Magnetic Resonance Imaging* **2002**, *16*, 378-387.

(81) Greer, L. F.; Szalay, A. A. *Luminescence* **2002**, *17*, 43-74.

(82) Rehemtulla, A.; Stegman, L. D.; Cardozo, S. J.; Gupta, S.; Hall, D. E.; Contag, C. H.; Ross, B. D. *Neoplasia* **2000**, *2*, 491-495.

(83) Tsien, R. Y. *Annual Review of Biochemistry* **1998**, *67*, 509-544.

(84) Wood, K. V.; Deluca, M. *Analytical Biochemistry* **1987**, *161*, 501-507.

(85) Craig, F. F.; Simmonds, A. C.; Watmore, D.; McCapra, F.; White, M. R. H. *Biochemical Journal* **1991**, *276*, 637-641.

(86) Zhang, Y.; Phillips, G. J.; Yeung, E. S., 2007; Vol. 79, pp 5373-5381.

(87) Lohmann, K. *Naturwissenschaften* **1929**, *17*.

(88) Lipmann, F. *Adv. Enzymol.* **1941**, 99.

(89) Donald Voet; Voet, J. G. *Biochemistry*, Second ed.; John Wiley and Sons: New York, 1995.

(90) Levin, G. V.; Usdin, E.; Slonim, A. R. *Aerospace Medicine* **1968**, *39*, 14-&.

(91) Beis, I.; Newsholme, E. A. *Biochemical Journal* **1975**, *152*, 23-32.

(92) Lundin, A. *Applications of firefly luciferase.*; Raven Press: New York, 1982.

(93) Burnstoc.G *Pharmacological Reviews* **1972**, *24*, 509-&.

(94) Elmoatassim, C.; Dornand, J.; Mani, J. C. *Biochimica Et Biophysica Acta* **1992**, *1134*, 31-45.

(95) Dubyak, G. R.; Elmoatassim, C. *American Journal of Physiology* **1993**, *265*, C577-C606.

(96) Zimmermann, H. *Trends in Neurosciences* **1994**, *17*, 420-426.

(97) Harden, T. K.; Boyer, J. L.; Nicholas, R. A. *Annual Review of Pharmacology and Toxicology* **1995**, *35*, 541-579.

(98) Burnstock, G. *Neuropharmacology* **1997**, *36*, 1127-1139.

(99) Burnstock, G.; Kennedy, C. *General Pharmacology* **1985**, *16*, 433-440.

(100) North, R. A. *P2 Purinoceptors: Localization, Function and Transduction Mechanisms* **1996**, *198*, 91-109.

(101) Berrie, C. P.; Hawkins, P. T.; Stephens, L. R.; Harden, T. K.; Downes, C. P. *Molecular Pharmacology* **1989**, *35*, 526-532.

(102) Boyer, J. L.; Downes, C. P.; Harden, T. K. *Journal of Biological Chemistry* **1989**, *264*, 884-890.

(103) Okajima, F.; Tokumitsu, Y.; Kondo, Y.; Ui, M. *Journal of Biological Chemistry* **1987**, *262*, 13483-13490.

(104) Ralevic, V.; Burnstock, G. *Pharmacological Reviews* **1998**, *50*, 413-492.

(105) Yang, X. R.; Pfeiffer, D.; Johansson, G.; Scheller, F. *Analytical Letters* **1991**, *24*, 1401-1417.

(106) McLaughlin, A. C.; Takeda, H.; Chance, B. *Proceedings of the National Academy of Sciences of the United States of America* **1979**, *76*, 5445-5449.

(107) Kueng, A.; Kranz, C.; Mizaikoff, B. *Biosensors & Bioelectronics* **2005**, *21*, 346-353.

(108) Mobasheri, A.; Gent, T. C.; Nash, A. I.; Womack, M. D.; Moskaluk, C. A.; Barrett-Jolley, R. *Osteoarthritis and Cartilage* **2007**, *15*, 1-8.

CHAPTER 2. REAL-TIME MONITORING OF SINGLE BACTERIAL CELL LYSIS EVENTS BY CHEMILUMINESCENCE MICROSCOPY

A paper published in Analytical Chemistry*

Yun Zhang, Gregory J. Phillips, Edward S. Yeung

ABSTRACT

The small size of bacteria makes it difficult to study the biochemistry inside single cells. The amount of material inside is limited, therefore an ultra sensitive method is required to interrogate single cells. Using a sensitive ICCD detector to record chemiluminescence (CL) from an optimized firefly luciferase-ATP bioluminescence reaction system, we report for the first time real time imaging of lysis of single bacterial cells with 10-s temporal resolution. Movies are generated to visualize how the cell membrane was damaged by phage lysis, antibiotics attack, or dehydration, as well as the wall repair and cell recovery processes. The results show single-cell variations that are not obtainable from bulk measurements, confirming that CL microscopy of luciferase-expressing bacteria is a powerful tool for studying the fundamental biology of cells.

---

* Reprint with permission from Analytical Chemistry **2007,** 79(14), 5373-5381.

INTRODUCTION

Bacteria cause serious diseases, including tuberculosis, typhoid fever, cholera, gonorrhea, staphylococcal dysentery, and many more, that were among the leading causes of death back in the pre-antibiotic years. The appearance of antibiotic "miracle drugs" in the mid-20th century once led the optimism that infectious diseases can be fully controlled and prevented. However, because of growing bacterial resistance to existing drugs, up until now infectious diseases are still the second-leading cause of death worldwide and the third-leading cause of death in economically advanced countries.[1] Developing new bactericidal drugs and thoroughly understanding antimicrobial actions continues to be a concern for researchers. Currently the most commonly used methods for measuring biocide behavior include minimum inhibitory concentration assay, turbidity assay, disk diffusion assay, etc. All of these utilize broth dilution or agar dilution method for detection, in which the death of bacteria was indicated by the drop of optical absorbance in the broth medium or the decrease of colony numbers on the agar plate. Optical density (OD) or plate count only represents bacterial group property. For single bacterial cells, no valuable information can be revealed. In order to evaluate bactericidal response and to study the mechanism at the single-cell level, a system that is capable of monitoring single bacterial cell lysis events in real time is needed.

For centuries, optical microscopy has been providing cell morphological details of live cells undergoing state changes. Additionally, it is now possible to monitor real-time gene expression and protein activities in single living cells with the help of modern fluorescence or chemiluminescence (CL) microscopes, thus making visualizing the biochemistry inside cells feasible.[2] The rapid expansion of the single-cell imaging field in the last 20 years is due to the development of ultra-low-light detection devices[3-5] and the use of reporter genes.[6] Luc,

which encodes the DNA that expresses firefly luciferase, is one of the most important reporter genes that have been extensively used in bioanalysis.[7] The reaction of firefly luciferase and adenosine triphosphate (ATP) is facilitated by the enzymatic action of luciferase to catalyze the oxidation of the substrate luciferin in the presence of one or more cofactors, among them oxygen, ATP, and metal ions:[8]

$$ATP + O_2 + \text{D-Luciferin} \rightarrow AMP + PP_i + CO_2 + \text{oxyluciferin} + \text{light (560 nm)}$$

A product of this reaction is light, which is detected by optical devices. This reaction has a fast response and extremely high sensitivity; a detection limit of 10^{-19} mol luciferase or 10^{-10} M ATP can be reached at optimized conditions.[9] Besides, there is an interesting characteristic of the substrate luciferin: as an amphipathic molecule due to its carboxyl group, the molecule is charged at physiological pH, thus preventing easy passage across bacterial cell membrane. At lower pH, when the luciferin molecules are protonated, they can easily pass into bacteria.[10] This implies that the size of luciferin molecules is right at the critical point for permeation into bacterial cells. If the pH is controlled at physiological condition and the test bacteria expresses firefly luciferase, even slight damage on the cell membrane will lead to luciferin passage and result in light output. Therefore, we chose CL detection of firefly luciferase reaction for testing cell membrane leakage, which is indicative of bactericidal effects. Compared to the detection of a decrease in light intensity due to fluorescent probe leakage, detection of flashes of light from extracellular luciferin that diffused inside is easier and more sensitive, with the additional advantages of extremely low background and simple instrumentation.

The firefly luciferase reporter system has been applied in plant or animal cell imaging studies with diverse applications,[3, 11, 12] but rarely in single bacterial cell imaging. Following

Hill et al.'s report on imaging of bioluminescence from individual bacteria in 1994,[13] only a few articles on single bacterial cell CL imaging have been published and only on protein expression levels. Moreover, all those papers used bacteria strains expressing bacterial luciferase (lux) from Vibrio fischeri and V. harveyi instead of firefly luciferase. The overall bacterial luciferase light production reaction is:[14]

$$FMNH_2 + RCHO + O_2 \rightarrow FMN + H_2O + RCOOH + \text{light (490 nm)}$$

The main reason is that this type of bacteria is luminous without the need to add the lux substrate, decanal, because of the presence of the full operon.[15] However, the intrinsic low sensitivity of the bacterial luciferase reaction inevitably brought on problems of long exposure times and the need for high expression level promoters.[16] Also, no triggering from "off" to "on" state is possible, since the luminous bacteria is always "on". So, that system is not useful in the application to cell lysis measurements.

In this work, we show that bacteria expressing firefly luciferase is a superior choice for studying bacterial lysis events. We introduced Luc gene into Escherichia coli (E. coli) strain BL21 with the highly expressive promoter Ptac. Eukaryotic firefly luciferase was expressed inside the bacteria and reacted with intrinsic ATP and permeated luciferin under carefully controlled conditions in various bactericidal environments. For the first time, single bacterial cell lysis responses to phage lysis, antibiotics attack and dehydration are recorded with an ultra sensitive intensified charge-coupled device (ICCD) with essentially single-photon detection sensitivity. Using this system, chemiluminescence can be used for ATP detection as low as 5×10^{-10} M with less than one second exposure time, so that even low CL levels from single bacterial cells can be unequivocally detected with an exposure time as short as 5 seconds. Furthermore, brightfield optical images could be recorded alternately with

the CL images in a modified instrument for comparing optical shape changes with CL registered leakage.

EXPERIMENTAL SECTION

Materials. Luciferase from firefly Photinus pyralis, D-luciferin, ATP, luciferase from Vibrio fischeri, ®-nicotinamide adenine dinucleotide (NADH), flavin mononucleotide (FMN), NADH-FMN oxidoreductase, decanal, Luria-Bertani (LB) medium, penicillin G, ampicillin, poly-L-lysine were purchased from Sigma-Aldrich (St. Louis, MO). Hanks' balanced salt solution (HBS), phosphate buffered saline (PBS) were purchased from Invitrogen (Carlsbad, CA). 100 mM isopropyl- ® –D-thiogalactopyranoside (IPTG) solution were purchased from EMD Biosciences (San Diego, CA). The plasmid pBESTluc™ was obtained from Promega (San Luis Obispo, CA). All chemical reagents were used without further purification.

Bacteria Strains and Transformation. E. coli strain BL21 competent cells (EMD Biosciences) and pBESTluc™ plasmids were used for transformation following standard protocols.[17] The introduced pBESTluc™ vector contains the gene Luc under control of Ptac promoter, with ampicillin resistance. Transformed bacteria were grown in LB broth, supplemented with 100 μg/ml ampicillin, at 30 °C with vigorous shaking. Overnight culture was diluted 100 fold and grown until the early-log phase (OD_{600}~0.2). Then the inducer, 100 mM IPTG, was added to make a final concentration of 200 μM. The bacteria continued growth and expression for about 2 hours to reach the mid-log phase (OD_{600}~0.5-0.8). Then bacteria were harvested and prepared for detection.

Instrumentation. The imaging system consists of an inverted light microscope

(Nikon Diaphot 300, Fryer, Edina, MN) and a complex electron-multiplying microchannel plate (MCP) coupled ICCD (EEV 576 × 384, Princeton Instruments, Trenton, NJ) attached to the camera amount of the microscope. The ICCD camera was operated at –30 °C and read out at 430 kHz with 12-bit resolution. Gain of the intensifier chip was set at 10. A 20× objective (N/A 0.5, Nikon, Japan) was used for standard calibration tests; a 100× oil immersion objective (N/A 1.25, Nikon, Japan) was used for single bacteria imaging. To keep the proper temperature for *in vivo* cell experiments, a heated stage insert (World Precision Instruments, Sarasota, FL) was placed on the microscope stage. For all bacterial cell experiments, the temperature was set at 30 °C. Bacterial cells were incubated in o-ring chambers on cover slips for microscopic observation. The chamber was created by sticking Teflon o-rings (Small Parts Inc., Miami Lakes, FL) to poly-L-lysine coated cover slips under sterile operations. The positively charged poly-L-lysine coating helps bacteria cells to stick on the surface. In standard calibration tests when chemical reagents were added into the buffer, a 50 µl syringe (Hamilton, Reno, NV) was used. To keep the position consistent, the syringe tip was always placed right above the solution surface and in the microscope optical path.

For alternate detection of brightfield optical images and chemiluminescence images, a mechanical Uniblitz shutter (Edmund Optics, Barrington, NJ) was put in the microscope stage in the microscope optical path. The shutter cut off light from the tungsten lamp when the CL image was collected, and opened to provide the light source when the optical image was captured. A pulse generator (Quantum Composers, Bozeman, MT) controlled both the shutter controller and the ICCD controller to synchronize the acquisition of the two different images. Each detection cycle was 16 s and composed of one CL image and one optical image.

That is, a 10 s exposure for chemiluminescence was recorded followed by a 2.5 s delay, then a 5 ms exposure for brightfield and 3.495 s delay, then another CL frame, etc.

Standard ATP and NADH Calibration. In all standard calibration tests, 10 µl standard solution (ATP or NADH) was injected by syringe into 20 µl reaction mixture in o-ring chambers. The ATP reaction mixture was composed of 167 nM firefly luciferase and 200 µM luciferin. The NADH reaction mixture contained 0.4 µM bacterial luciferase, 2.1 µM FMN, 0.002 Unit NADH-FMN oxidoreductase, and 0.3 mM decanal. All chemicals were dissolved in HBS buffer. ATP standard solutions with concentrations ranging from 10^{-7} to 10^{-9} M, and NADH standard solutions with concentration ranging from10^{-6} to 10^{-7} M were added into respective mixture buffers. Light generated by the reactions was recorded by the ICCD detector in sequential frames of 0.5 s exposure time. The dead time between two consecutive frames was about 0.5 s. In every experiment, each recorded as one movie, the first 10 frames were regarded as background since ATP/NADH standards were added at frame 11. Each data point was the average intensity of all pixels in the frame.

***In Vivo* Bacteria CL Monitoring.** Induced luciferase expressing bacteria BL21 were grown to mid-log phase. 200 µl of culture was placed in o-ring chambers and incubated on the heated stage for 5 min. Then the medium was discarded and the chamber was rinsed with 200 µl PBS buffer twice. D-luciferin was dissolved in pH 5.0 sodium-citrate buffer (100 mM) to make a 200 mM solution. 200 µl of this solution was added to the rinsed chamber. CL light from single bacterial cells attached to the poly-L-lysine coated surface was recorded with 5-s, 10-s, 15-s, 20-s, and 30-s exposure times. Optical cell images were recorded before and after each CL movie at 5-ms exposure time.

Bacteriophage T7 Lysis. Bacteriophage T7 (ATCC BAA-1025-B2™) were

propagated following the ATCC protocols. E. coli strain BL21 (non-transformed) was used as the host. The surface of an agar plate was covered with 2.5 ml of melted 0.5% agar that contained one or two drops of the freshly grown host in the early-log phase. The freeze-dried phage was rehydrated with 1 ml nutrient broth plus 0.5% NaCl and placed on top of the soft-agar surface. After one day of incubation, the surface was scraped off and centrifuged at 5000 rpm for 10 min to preconcentrate the cellular debris and agar. The supernatant was passed through a .22 µm Millipore filter and the filtrate stored at 4 °C. For the bacteria lysis experiment, 200 µl of the phage T7 filtrate was well mixed with 1 ml luciferase expressing BL21 culture in the mid-log phase. The mixture was incubated at 30 °C for 5 min. 100 µl of this mixture was mixed with 100 µl luciferin HBS buffer (400 µM), and then placed in the chamber on the heated microscope stage. ICCD camera recorded alternating optical and CL images for about an hour.

Bacteria Antibiotic Resistance. Luciferase expressing bacteria BL21 were induced with IPTG at the early log phase (OD_{600} = 0.15). The culture continued growing for precisely 3 hours and was then harvested at the mid-log phase. Bacteria culture, antibiotics (penicillin-G or ampicillin) solution, and 600 µM luciferin HBS buffer were mixed 1:1:1. The final concentration of antibiotics was 200 mg/L or 500 mg/L. 200 µl of the mixture was placed in the o-ring chamber on the heated microscope stage. The ICCD camera recorded CL movies for 2-3 h at 10-s exposure time. Optical images were recorded between CL images at 5-ms exposure time.

Bacteria Dehydration. 10 µl culture of induced luciferase expressing bacteria BL21 at the mid-log phase was mixed with 10 µl luciferin HBS solution (400 µM). The mixture was placed in the o-ring chamber on the heated microscope stage. The ICCD camera

recorded CL from bacteria while water evaporated from the buffer and the bacteria dried out. The process took about 30 min before the CL signal from bacteria decreased. Then another 20 µl HBS buffer was added to the chamber. The dehydration process was repeated and CL was again recorded at the same 10-s exposure time. Optical images were recorded at 5-ms exposure time.

RESULTS AND DISCUSSION

Comparison of Firefly and Bacterial Luciferase Reactions. The reasons why firefly or some marine bacteria glow in the dark are well known. The two systems share some common features: both require an enzyme, luciferase, to induce the other compound, luciferin, to emit light. However, the reaction paths are different. The firefly luciferase reaction has a higher quantum efficiency of 0.88 compared to the bacterial luciferase quantum efficiency of 0.27.[18] The bacterial luciferase substrate $FMNH_2$ is available from NADH in the presence of the NADH-FMN oxidoreductase enzyme:[19] $FMN + NADH \rightarrow FMNH_2 + NAD^+$. Based on that, ATP and NADH are the two indispensable factors in the respective reactions. We used ATP/NADH as the limiting reagents in standard calibration tests. By measuring CL profiles and intensities upon adding ATP/NADH to the corresponding reaction mixtures at optimized (saturation) concentrations, we were able to determine the reaction speed, efficiency and sensitivity of the two systems.

As shown in Figure 1, the light intensity from ATP reactions rapidly increased to a maximum within 1-2 s after adding ATP at time point 10 s. Then the system went into a second stage when the signal decreased relatively slowly over time. In contrast in NADH reactions, the increase of signal was not immediate: it took almost 20 s after the addition of

NADH to reach the maximum, then the signal slowly decreased. A second difference was that the peak height for ATP (150 nM) reaction was almost 100 times higher than that of the NADH (500 nM) reaction. The detection limits were 5×10^{-10} M ATP and 2.5×10^{-7} M NADH, respectively. These results demonstrate that compared to the NADH-bacterial luciferase reaction, the ATP-firefly luciferase reaction has faster kinetics, generates more light with higher quantum efficiency, and gives a much better detection limit. Therefore, the ATP-firefly reaction system is the one better suited for single-cell imaging applications.

The insets in Figure 1 are standard calibration curves of peak heights against concentrations. The linearity of the reactions is fair, with a correlation coefficient of 0.994 for ATP over 3 orders of magnitude and 0.993 for NADH over 2 orders of magnitude. Because every addition of ATP/NADH caused slight variations in peak profiles, linearity was not perfect in these data sets.

Monitoring CL from Live Single Bacterial Cells. Imaging luminous bacteria colonies on a plate is not difficult for conventional cameras,[20] but visualizing the faint light from a single bacterial cell on the microscope is challenging. The successful detection of single luminescent bacterial cell is based on an ultra sensitive optical detector—ICCD camera. Three key factors—enhancement of the light signal by the MCP intensifier plate, reduction of dark current background by cooling the ICCD at –30 °C, and removal of stray light by placing the whole system in a completely dark environment—all worked together to make it possible to record a CL image with an exposure time of only 5 s (Figure 2).

Light was produced when neutral, protonated extracellular D-luciferin molecules managed to pass the bacterial membrane and react with ATP and luciferase inside. With the abundant ATP concentration (at 10^{-3} M) inside cells,[21] CL from bacteria lasted for at least 5

hours without impairing the cell viability in our experiments. In Figure 2, CL images of different exposure times were compared. The images showed an increase in signal-to-noise ratio and in resolution when the exposure time increased from 5 s to 30 s. This is because noise from dark current was averaged out over a longer exposure time and more signal was collected over time. It should be noted that the ICCD camera has a very small dynamic range because of the MCP, and does not produce good optical images in general. Although 30-s images have the best contrast, we used 10 s exposure time in subsequent bacteria lysis detection to obtain an optimal temporal resolution for dynamic events.

Monitoring Bacteriophage T7-Induced Bacteria Lysis. Because of growing prevalence of antibiotic resistant microbes, researchers are searching for new generations of therapeutics against bacterial infection, including the new weapon of bacteriophages.[22] The viruses, as bacteria's natural enemies, penetrate into the bacterium, feed on the host cell, self-replicate using bacterial DNA, and finally break out at a certain stage to release progeny virions.[23] They are harmless to humans, and evolve with bacteria; therefore, they are considered the ultimate antibacterial therapy.

Bacteriophage lysis mechanisms have been well studied.[24] Two proteins play essential roles in bacteriophage lysis: endolysins and holins. Endolysin is the muralytic enzyme that degrades the cell wall, while holin is believed to be the protein clock that controls phage lysis timing, which is claimed to be "programmed" to optimize evolution.[25] Holins are small proteins that accumulate in the membrane until at a specific time the proteins form holes and the membrane suddenly becomes permeabilized to the fully folded endolysin. Subsequently, endolysins destroy the integrity of the murein wall, and cause bursting of the unprotected cells due to the high internal osmotic pressure. The overall

process is described, but the details, i.e. nature of the hole, what makes the lysis clock tick, etc., still have to be elucidated.

Bacteriophage T7 was reported to lyse E. coli cells in 25 min after infection at 30 °C.[24] In our experiments on the microscope stage, the growth conditions were not at optimum, so lysis events were actually observed to span longer times, starting from about 25 min until almost an hour. The previously reported OD data show the phage lysis as a single sharply decreasing peak[24], because the one by one cell membrane disruption was reflected as a decline in overall cell optical density. But the CL from bacteria lysis was read as light bursts from single bacterial cells (Figure 3). Light is produced after endolysin disrupts the cell wall, when luciferin molecules can get inside the cells and initiate CL reaction, and ends when the bacteria totally bursts and luciferase diffuses away. So, the cells that are luminous are those in a state between the start of leakage and the final disruption of the cell. After the CL faded away, the bacterial cells were also found to disappear in the optical images. From the CL and optical images, information on holin controlled phage lysis timing, bursting details and morphology changes was registered for every cell.

Each bacterial cell lysis is an independent event, with its own specific timing and manner of membrane disruption. To differentiate the events from cell to cell, we analyzed 16 cell lysis events from one movie (see Supporting Information), and summarized the results in Figure 4. For about half of the cells, CL only showed up in one frame. The bacteria disappeared in the optical images immediately following the light burst. The whole lysis process took less than 16 s. Other cells took a longer time to lyse (> 50 s), and the debris remained visible for a couple of cycles (>100 s). However, the CL intensity of most cells fall in the range between 80 and 160. This probably reflects the total amount of ATP in each cell,

which should be fairly constant. These data show that phage lysis is a heterogeneously distributed dynamic process.

Monitoring Bacteria Resistance to Antibiotics. The transformed BL21 bacteria gained antibiotic resistance from the plasmid pBESTluc™. Therefore, this type of bacteria can survive the attack of β-lactam antibiotics. β-lactams, including penicillins and cephaolosporins, attack and acylate the active site of transpeptidase, the enzyme that acts in crosslinking glycan strands, to inhibit bacterial wall synthesis.[26] The transformed bacteria with ampicillin resistance can produce β-lactamases, which inactivates antibiotics by hydrolysis of the four-membered β-lactam ring in penicillins to overcome the antimicrobial effect and survive.[27] Penicillin is the name of a large group of antibiotics, including penicillin G and ampicillin. By applying these two antibiotics to bacteria, we can visualize the membrane damage and the repair process of antibiotic resistant bacteria under the attack of the antibiotics.

Penicillin G and ampicillin were added to actively growing bacteria culture to a final concentration of 200 or 500 mg/L. Suddenly surrounded by such a high concentration of antibiotics, the bacterial cell wall was attacked and started to leak. So the bacteria were observed to be increasingly luminous during the first half hour, as shown in Figure 5. Then, antibiotic resistance began to work, and the cell wall was gradually repaired and leakage was prevented. This is shown in Figure 5 as a decrease of light intensity. This process was not evident from the optical images, as the integrity or morphology of bacteria did not change at all.

There is an interesting observation: bacteria responded differently to penicillin G and ampicillin (Figure 6). It is apparent that the penicillin G attack was more effective—quickly

reaching the maximum of about 600 at around 40 min. In comparison, the ampicillin attack of bacteria led to the most leakage at around 70 min, but with similar peak height. The different timing to maximum leakage implies that the bactericidal effects of penicillin G and ampicillin are different, with penicillin G being the faster killing drug to this bacterial strain.

However, the two concentrations studied (200 or 500 mg/L) did not show any difference, probably because they were already at the saturation level. Also, all cells in the observation area showed similar peak profiles, in terms of peak shapes and widths. This implied similar response behaviors for bacteria towards the antibiotics. In all cases, the increase in CL lasted no longer than 20 min, leading to the conclusion that the resistance systems were triggered to hydrolyse the drugs and the bacteria started to repair the cell wall immediately following the onset of leakage. Furthermore, CL peak widths, the indicator of membrane damage time, in all cases were less than 40 min.

The above results were confirmed by comparison to the control experiments shown in Figure 6 (C1/C2). When no antibiotics were added, there was basically no CL signal. As for the few bumps in C1 and C2 of Figure 6, one can infer that cell membranes are transforming during growth.

Monitoring Bacteria Leakage during Dehydration. It has been reported that dehydration-induced phase transitions of membranes from a liquid-crystalline to a gel phase would lead to various alterations, including transient permeability that results in leakage of the contents of cells to the surrounding medium.[28] The phase transition was detected by measuring the leakage of fluorescent probes, or alternatively, by measuring changes in vibrational frequency and bandwidth of the CH_2 bands with infrared spectroscopy.[29] In this work, we demonstrate that such leakage can be monitored by CL detection down to the single

bacterial cell level.

Figure 7 shows the sequential CL images of bacteria undergoing dehydration. In the first 20 min, as the buffer volume was shrinking because of water evaporation, the bacterial membrane gradually became slightly permeable and many bright spots from luminous bacteria cells appeared. When the water was completely gone and the cell membrane underwent phase transition, and membrane leakage led to a strong burst of CL light from the bacterial cells. This intense light-producing process lasted less than 10 min. Then, with the phase transition completed, CL light diminished. Optical images of the cells after dehydration also showed such a difference. The contrast was greatly reduced, indicating changes in the refractive index.

The dehydration process is repeatable on the same batch of bacterial cells, as shown in Figure 8. The whole process was displayed as a plot of the average intensity of pixels around a single cell against time. The first CL peak from leakage occurred at around 20 min. That decreased to baseline as the phase transition was completed and the cell dried. Then at 32 min, the same volume of buffer was again added to rehydrate the cells. 20 min later, a second CL peak from leakage appeared again. The presence of a second peak demonstrated that the decrease in CL after the first peak was not because of luciferase leaking out or because of complete cell disruption. Otherwise, there would be no enzyme for the CL reaction during the second dehydration. Retention of the larger proteins such as luciferases means that bacteria may preserve large molecules like proteins or DNA during dehydration, so once rehydrated some time later, the cells can recover and thrive again. This phenomenon is not surprising, as it has been reported previously that some organisms, like fungal spores, yeast cells etc., may persist without water for decades.[30] The reasons why some cells may

survive drying but not others are under investigation.[31, 32]

CONCLUSIONS AND PROSPECTS

We have demonstrated the utility of CL microscopy in monitoring real time leakage events of single bacterial cells. Whether they are caused by phage, antibiotics, or dehydration, so long as the cell events accompany membrane leakage, they are detectable via chemiluminescence from the firefly luciferase reactions. Additional advantages include simple instrumentation (simply connecting an ICCD camera to a microscope), elimination of the light source (avoiding stray light problems), and long-time observation (no light-induced damage to cells). Previously,[33] we have studied the lysis of non-transformed cells and bacteria by bathing them in buffer that contained luciferin and luciferase. There, ATP that was released reacted while diffusing away from the cell. The sensitivity here is much higher since the reagents are all confined inside the intact cell to increase their local concentrations.

Combining this tool with other biological techniques, we can investigate the timing of holin control mechanisms in phage lysis, membrane damage and repair mechanisms under bactericidal drug attack, membrane stabilization mechanisms of dehydration survival, and other fundamental biological processes. Instead of looking at a group of cells, we can study individual behaviors of single bacterial cells. Moreover, since sample culture volume is small, this method is promising in antibacterial drug studies when available bacteria cells are limited, e.g., when working with rare bacteria.

There are also deficiencies in the present approach. The resolution of the optical images presented here is not good because of the intrinsic inhomogeneous background and the shallow electron well depth of the ICCD. If higher quality optical images are necessary in

certain studies, one possible solution is to use another cooled CCD camera for collecting optical images. Coupling laser-induced-fluorescence detection is also appealing. This may be implemented by introducing a laser beam through another shutter. Detection combining fluorescence, chemiluminescence and optical brightfield in one will be a most powerful way to investigate biological events.

ACKNOWLEDGMENTS

E.S.Y. thanks the Robert Allen Wright Endowment for Excellence for support. The Ames Laboratory is operated for the U.S. Department of Energy by Iowa State University under Contract No. DE-AC02-07CH11358. This work was supported by the Director of Science, Office of Basic Energy Sciences, Division of Chemical Sciences and by the National Institutes of Health.

REFERENCES

(1) Nathan, C. *Nature* **2004**, *431*, 899-902.

(2) Wouters, F. S.; Verveer, P. J.; Bastiaens, P. I. H. *Trends in Cell Biology* **2001**, *11*, 203-211.

(3) Wang, Z.; Haydon, P. G.; Yeung, E. S. *Analytical Chemistry* **2000**, *72*, 2001-2007.

(4) Ma, Y.; Shortreed, M. R.; Li, H.; Huang, W.; Yeung, E. S. *Electrophoresis* **2001**, *22*, 421-426.

(5) Gruenhagen, J. A.; Lovell, P.; Moroz, L. L.; Yeung, E. S. *Journal of Neuroscience Methods* **2004**, *139*, 145-152.

(6) Rutter, G. A.; Kennedy, H. J.; Wood, C. D.; White, M. R. H.; Tavare, J. M. *Chemistry and Biology* **1998**, *5*, R285-R290.

(7) Greer, L.; Szalay, A. *Luminescence* **2002**, *17*, 43-74.

(8) Deluca, M.; McElroy, W. D. *Methods in Enzymology* **1978**, *57*, 3-15.

(9) Gruenhagen, J. A.; Lai, C.-Y.; Radu, D. R.; Lin, V. S.-Y.; Yeung, E. S. *Applied Spectroscopy* **2005**, *59*, 424-431.

(10) Wood, K. V.; DeLuca, M. *Analytical Biochemistry* **1987**, *161*, 501-507.

(11) Sala-Newby, G. B.; Taylor, K. M.; al., e. *Immunology* **1998**, *93*, 601-609.

(12) Gallie, D. R.; Lucas, W. J.; al., e. *Plant Cell* **1989**, *1*, 301-311.

(13) Hill, P. J.; Eberl, L.; Molin, S.; Stewart, G. S. A. B. In *Bioluminescence and Chemiluminescence: Fundamentals and Applied Aspects. Proceedings of the 8th International Symposium on Bioluminescence and Chemiluminescence*; Campbell, A. K., Kricka, L. J., Stanley, P. E., Eds.; Wiley: Chichester, 1994, pp 629-632.

(14) Hastings, J. W.; Baldwin, T. O.; Nicoli, M. Z. *Methods in Enzymology* **1978**, *57*, 135-152.

(15) Engebrecht, J.; Simon, M.; Silverman, M. *Science* **1985**, *227*, 1345-1347.

(16) Sternberg, C.; Eberl, L.; Poulsen, L. K.; Molin, S. *J. Biolumin. Chemilumin.* **1997**, *12*, 7-13.

(17) Sambrook, J.; Russell, D. W. *Molecular Cloning: A Laboratory Manual*, Third Edition ed.; Cold Spring Harbor Laboratory Press: Cold Spring Harbor, NY, 2001.

(18) Brolin, S.; Wettermark, G. *Bioluminescence Analysis*; VCH: Weinheim, New York, Basel, Cambridge, 1992.

(19) Jablonski, E.; DeLuca, M. *Biochemistry* **1977**, *16*, 2932-2936.

(20) Langridge, W.; Escher, A.; al., e. *J. Biolumin. Chemilumin.* **1994**, *9*, 185-200.

(21) Arciuco, G.; Lin, J. H.; Takano, T.; Liu, C.; Jiang, L.; Gao, O.; Kang, J.; Nedergaard, M. *Proceedings of the National Academy of Science (USA)* **2002**, *99*, 9840-9845.

(22) Thiel, K. *Nature* **2004**, *22*, 31-36.

(23) Adams, M. H. *Bacteriophages*; Interscience Publishers, Inc.: New York, 1959.

(24) Young, R. *Bacteriophage Lysis: Mechanism and Regulation. Microbiological Reviews*, 1992.

(25) Wang, I.; Smith, D. L.; Young, R. *Annu. Rev. Microbiol.* **2000**, *54*, 799-825.

(26) Spratt, B. G.; Cromie, K. D. *Rev. Infect. Dis.* **1988**, *10*, 699-711.

(27) Yoneyama, H.; Katsumata, R. *Biosci. Biotechnol. Biochem.* **2006**, *70*, 1060-1075.

(28) Crowe, L. M.; Womersley, C.; Crowe, J. H.; al., e. *Biochim. Biophys. Acta* **1986**, *861*, 131-140.

(29) Crowe, J. H.; Crowe, L. M.; Hoekstra, F. A. *J. Bioenerg. Biomem.* **1989**, *21*, 77-91.

(30) Potts, M. *Microbiol. Rev.* **1994**, *58*, 755-805.

(31) Crowe, J. H.; Carpenter, J. F.; Crowe, L. M. *Annu. Rev. Physiol.* **1998**, *60*, 73-103.

(32) Crowe, J. H.; Hoekstra, F. A.; Crowe, L. M. *Annu. Rev. Physiol.* **1992**, *54*, 579-599.

(33) Aspinwall, C. A.; Yeung, E. S. *Anal. Bioanal. Chem.* **2005**, *381*, 660-666.

FIGURE CAPTIONS

Figure 1. ATP and NADH reaction time courses and (inset) standard calibration curves. (A) ATP. Final ATP concentration:150 nM; (B) NADH. Final NADH concentration: 500 nM. Both ATP and NADH were added at time 10 s.

Figure 2. Images of single bacterial cell chemiluminescence. (A) Brightfield optical image. Exposure time: 5 ms. (B-F) Chemiluminescence images. Exposure times: (B) 5 s, (C) 10 s, (D) 15 s, (E) 20 s, (F) 30 s. The scale bar in the first image corresponds to 10 μm.

Figure 3. Alternating optical and chemiluminescence imaging of bacteriophage T7 lysis. Time zero was 47 min after phage was added to the bacteria culture. The arrow points to a bright spot at 19.5 s that corresponds to a bacteria particle marked at 0 s and 16 s in the optical images. After the burst at 19.5 s, the bacterial cell disappeared in the next optical image at 32 s. The scale bar in the first image corresponds to 10 μm.

Figure 4. Distribution of bacteria lysis time and burst intensities. (A) Chemiluminescence light burst durations. (B) Time from CL disappearance to optical disappearance. (C) Burst intensity, measured by averaging light intensities of pixels around the bacteria (about 10 pixels). When the chemiluminescence lasted several frames, the most intense one was counted.

Figure 5. Monitoring ampicillin resistant bacteria under penicillin-G attack. The first row are optical images taken with 5-ms exposure time. The second row are CL images with 10-s exposure time. The contrasts of CL images are all adjusted to the same level. The CL intensity first turned brighter, then dark again as time passed. The scale bar in the first image corresponds to 10 μm.

Figure 6. Monitoring bacterial cell leakage under ampicillin and penicillin-G attack. (A1, A2) ampicillin. A1: 200 mg/L. A2: 500 mg/L. (P1, P2) penicillin-G. P1: 200 mg/L. P2: 500 mg/L. (C1, C2) Controls of normally growing bacteria, no antibiotics added.

Figure 7. Monitoring bacteria lysis during dehydration. The first image is an optical image of bacteria before dehydration. Between 13-25 min, bacteria dehydrated and CL from leakage of luciferin into the cells was observed. The optical image at 32 min showed the bacteria when dried. Then, another 20 μl buffer was added and the optical image at 33 min showed rehydrated bacteria. The scale bar in the first image corresponds to 10 μm.

Figure 8. Repetitive dehydration of bacteria. The first dehydration process was completed in the first 30 min. Then, additional buffer was added as the arrow indicated. The subsequent CL images showed a second peak at around 50 min corresponding to a second dehydration event.

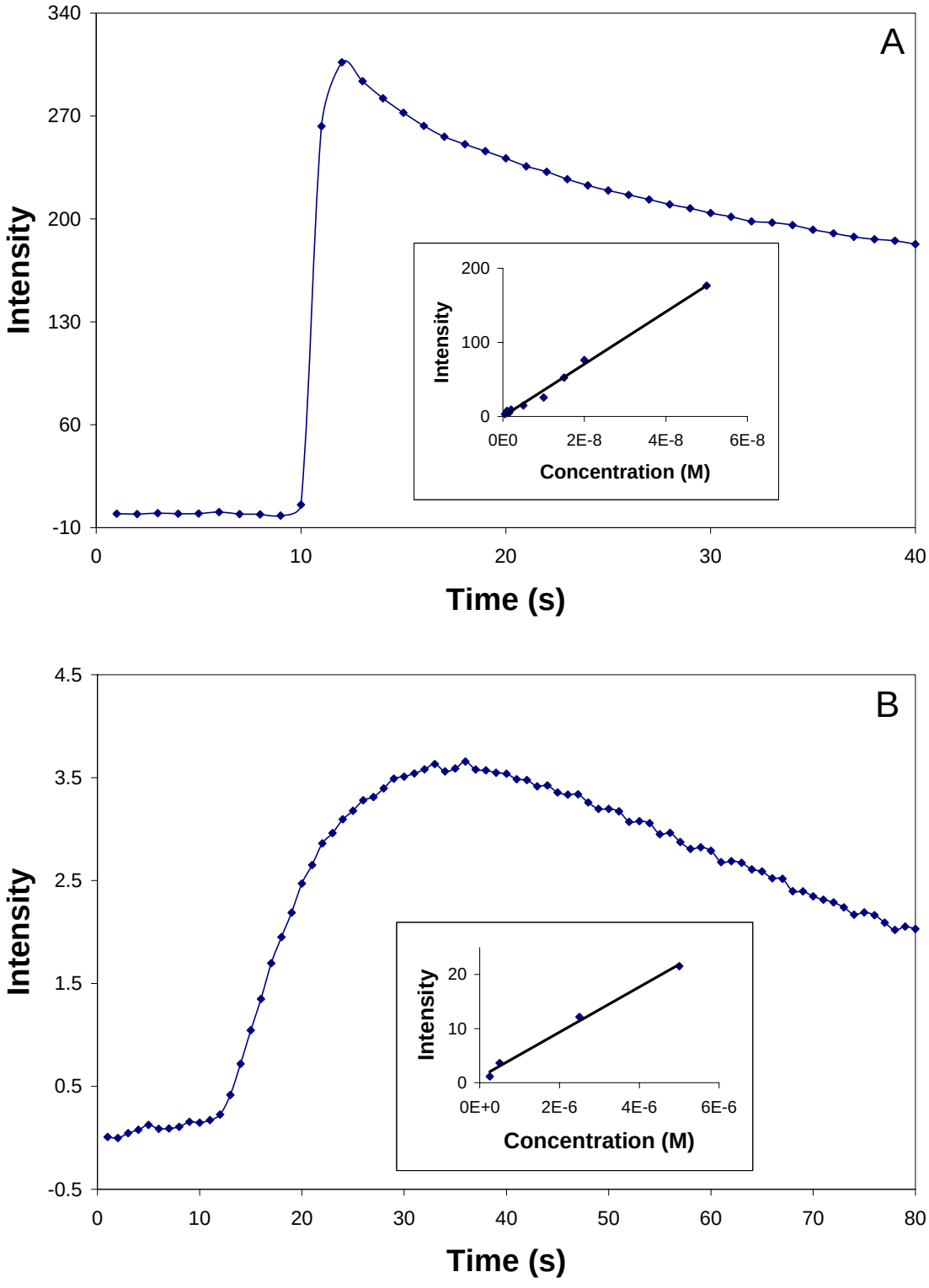

Figure 1.

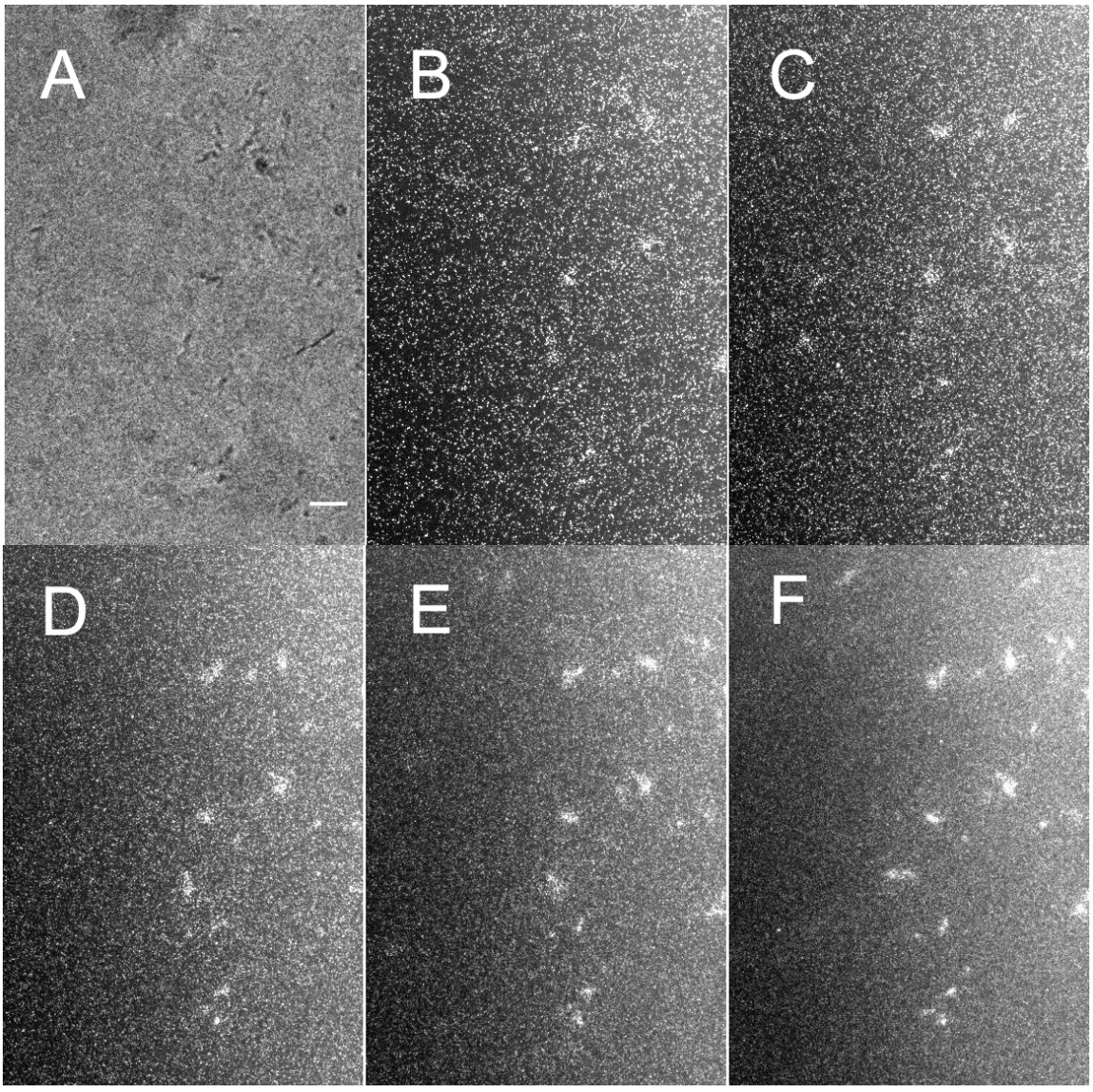

Figure 2.

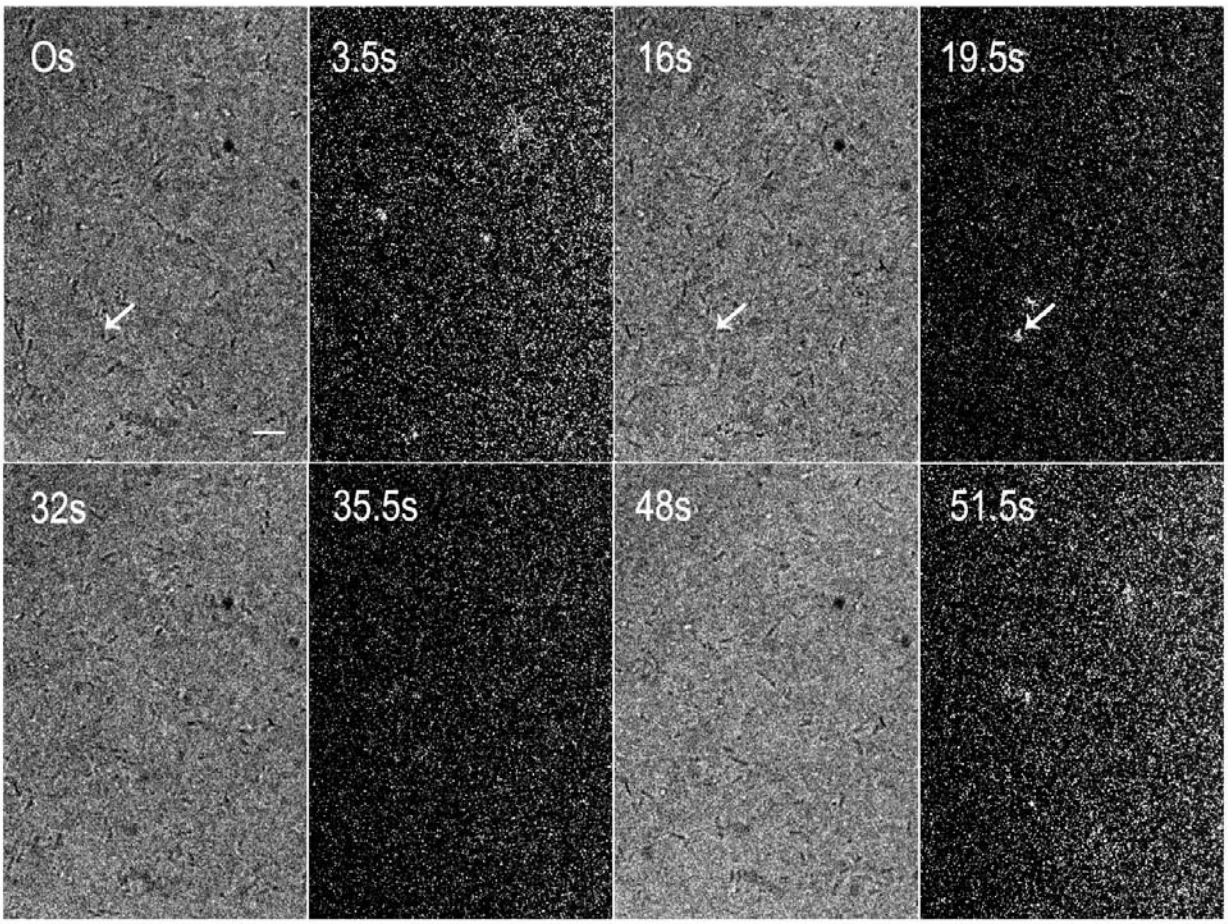

Figure 3.

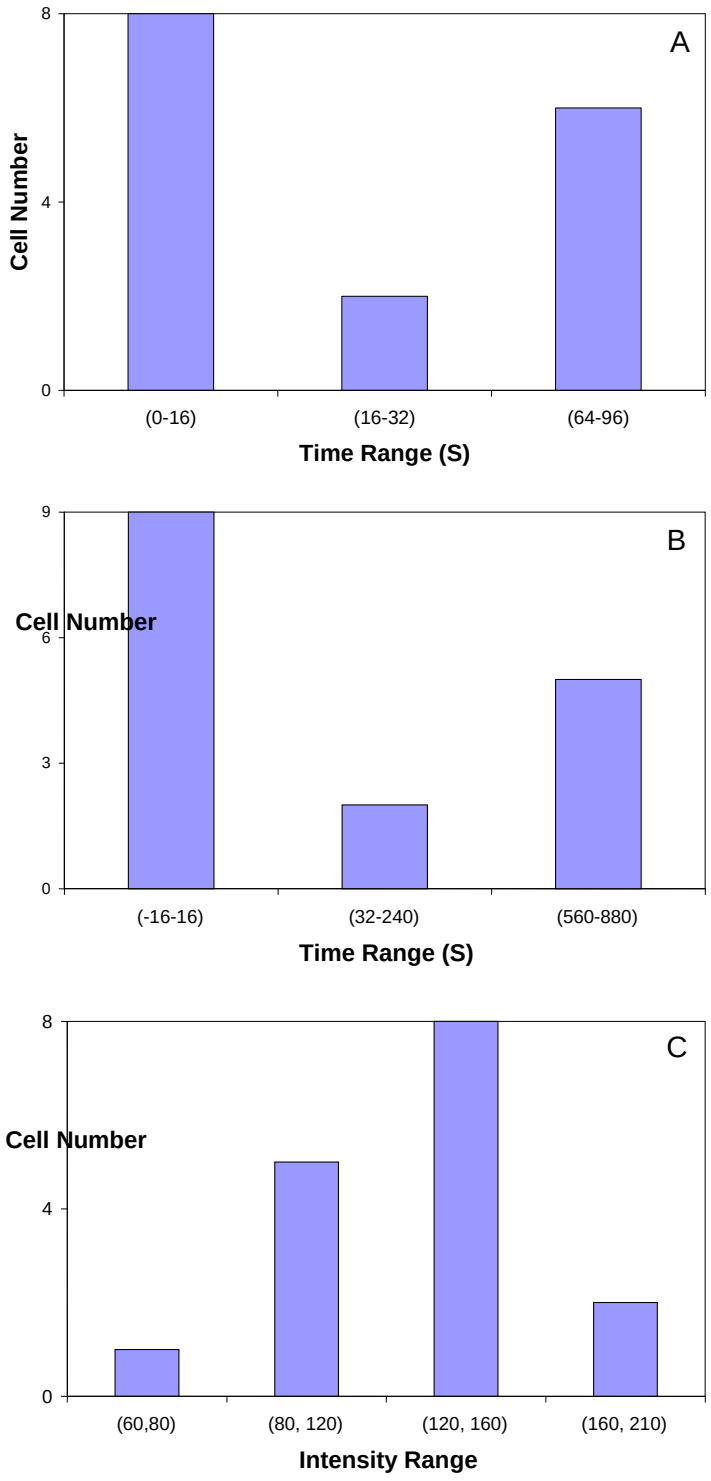

Figure 4.

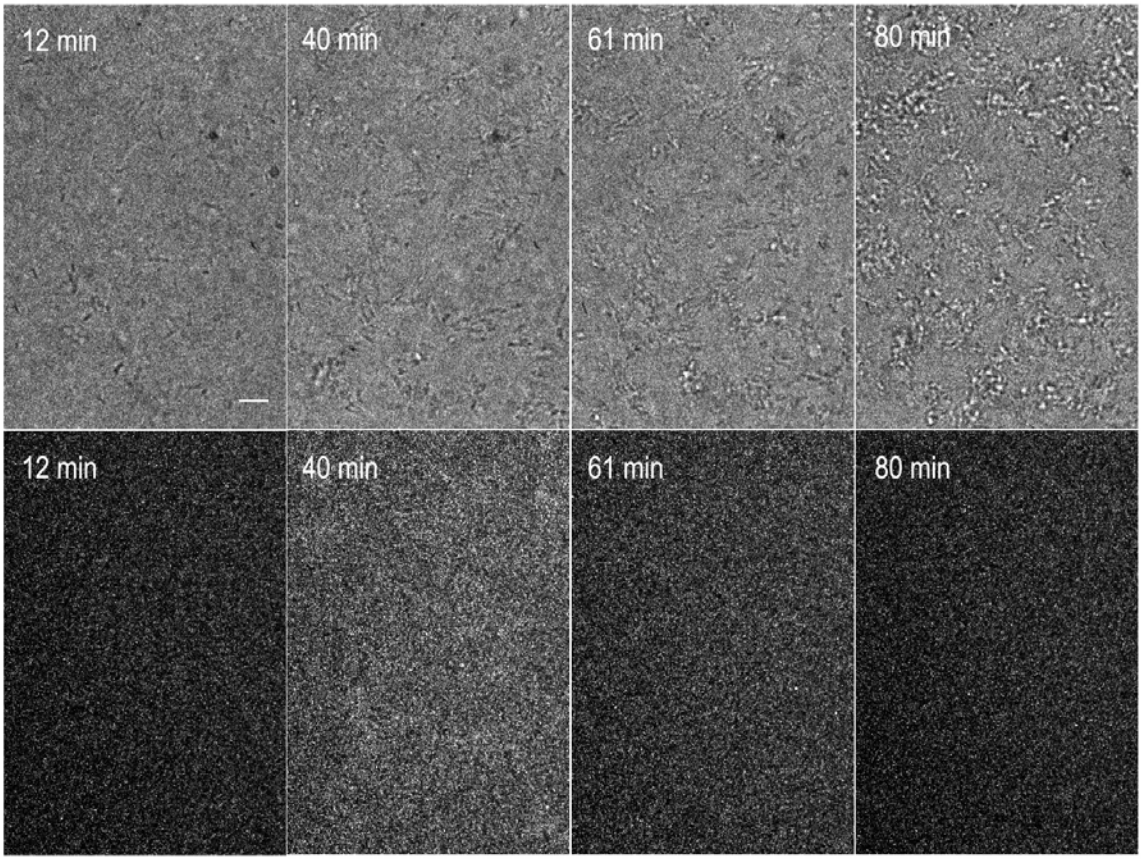

Figure 5.

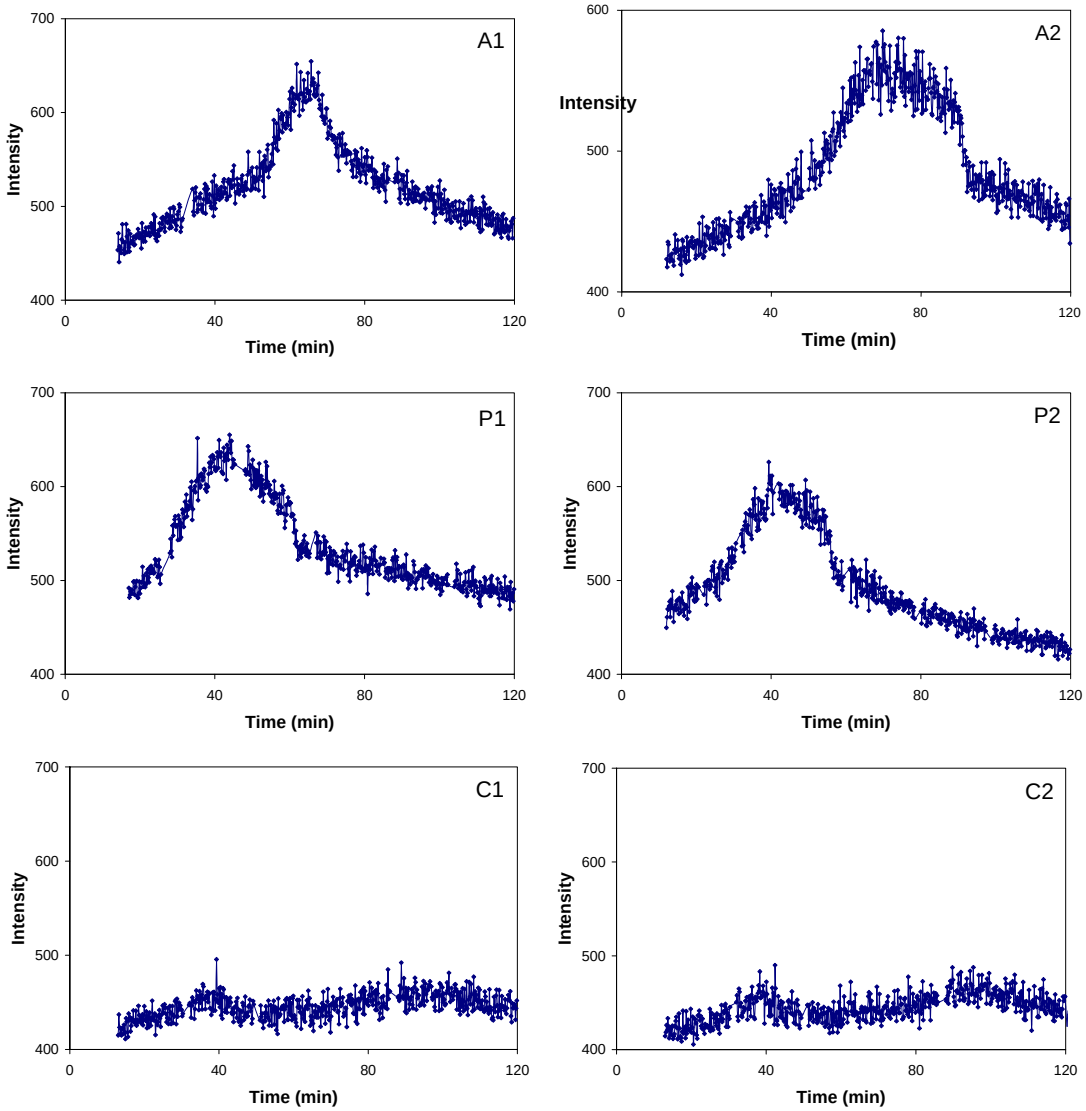

Figure 6.

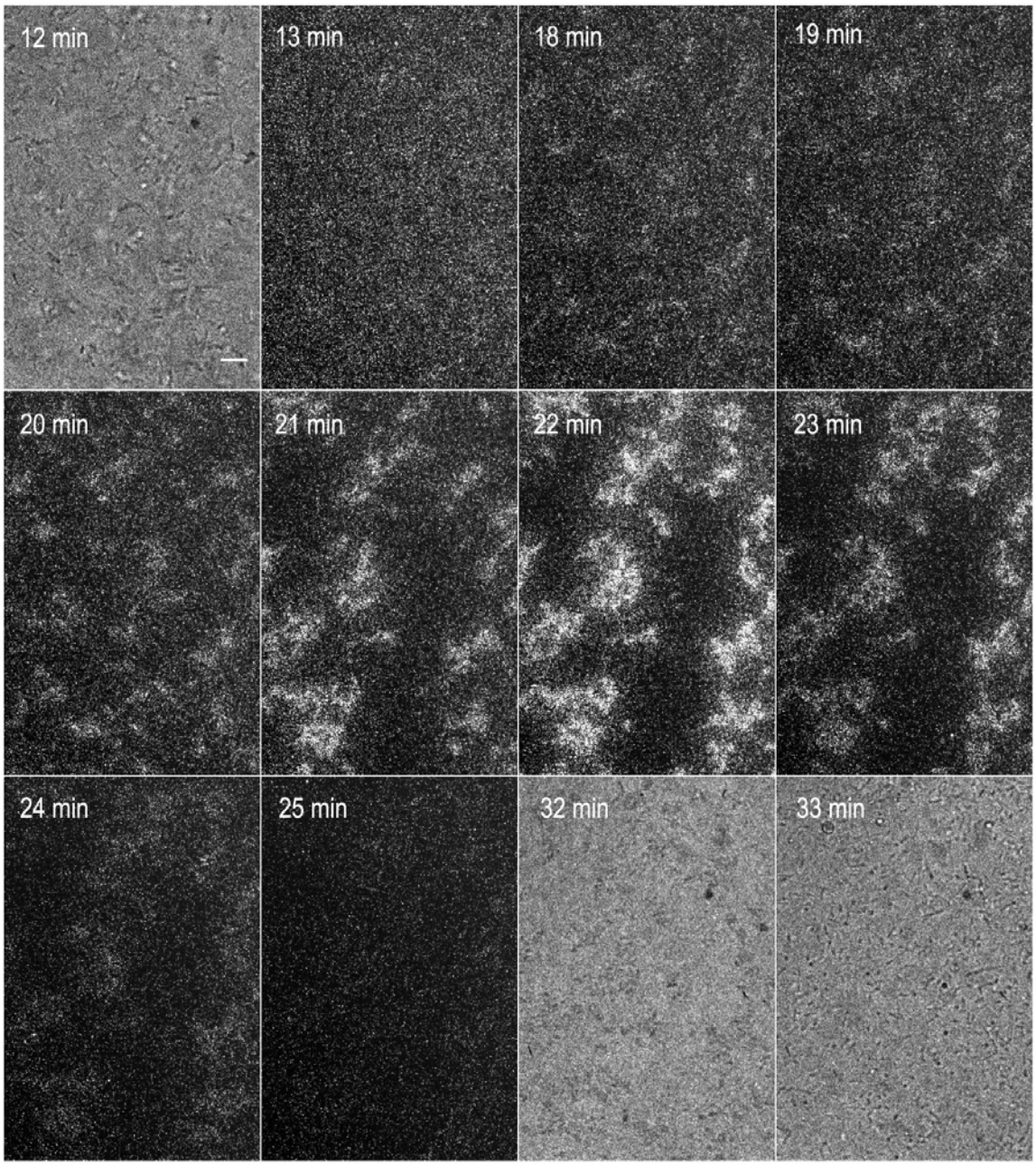

Figure 7.

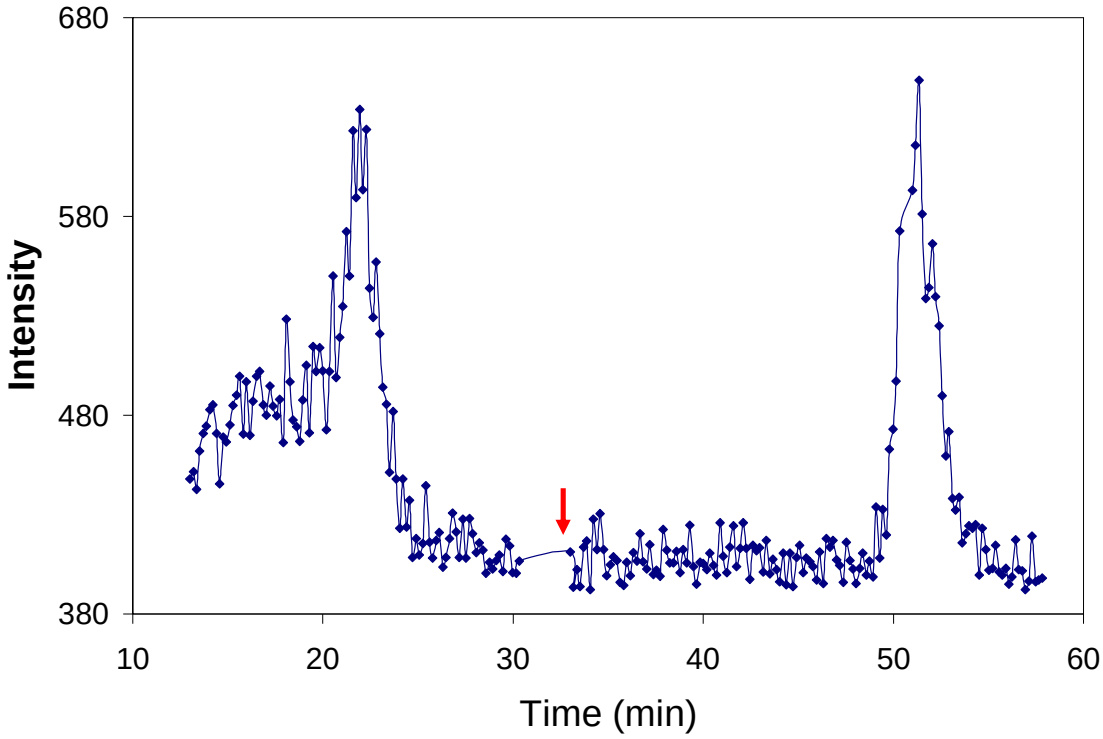

Figure 8.

CHAPTER 3. QUANTITATIVE IMAGING OF GENE EXPRESSION IN INDIVIDUAL BACTERIAL CELLS BY CHEMILUMINESCENCE

A paper published in Analytical Chemistry*

Yun Zhang, Gregory J. Phillips, and Edward S. Yeung

ABSTRACT

Recent gene expression studies at the single bacterial cell level have primarily used green fluorescent protein (GFP) as the reporter. However, fluorescence monitoring has intrinsic limitations, such as GFP maturation time, high background and photobleaching. To overcome those problems, we introduce the alternative approach of chemiluminescence (CL) detection with firefly luciferase as the probe. Firefly luciferase is roughly 100 times more efficient and is faster in generating CL than bacterial luciferase but requires the introduction of luciferin, a species that is not native to bacteria. The difficulty of luciferin diffusion into the cells was solved by making use of cell membrane leakage during bacteria dehydration. In this scheme, the overall sensitivity of the system approaches the single protein molecule level. Quantitative studies of gene expression in BL21 and XLU102 bacteria can thus be performed.

---

* Reprint with permission from Analytical Chemistry **2008,** 80(3), 597-605.

INTRODUCTION

In the past decade, rapidly advancing live-cell imaging technologies have greatly enhanced our understanding of gene expression. The gene expression process is believed to be inherently stochastic because the repressors and transcriptional factors randomly bind on or off. At the same time, the initiation, elongation, and termination levels of transcription and translation fluctuate randomly.[1] Since every cell within a population is inherently different, the transient transcriptional activities can only be correctly described by monitoring gene expression within a single cell. Fluorescence methods using green fluorescent protein (GFP) or its derivatives as the reporter to quantify the expressed protein levels is the most commonly used approach. In most cases, however, single molecules of GFP are generally undetectable *in vivo* due to background fluorescence. Furthermore, fluorescent proteins are well known for their long maturation periods.[2] While biological processes take place in seconds to minutes, fluorescent proteins takes hours to become fluorescent after the protein synthesis, e.g., GFP has a maturation time of two hours.[3] This makes probing fast dynamic biological processes impossible. Recently Xie and colleagues reported interrogating protein expression in individual mammalian cells with single-molecule sensitivity by using a fluorescence enzyme assay.[4] Since enzyme activities vary[5, 6] and fluorophors are subject to photobleaching, the fluorescence signal is only semiquantitative.[7]

Here, we try to solve the obstacles by imaging gene expression in single bacterial cells with a different approach, namely chemiluminescence (CL) detection. The light-producing reaction of the enzyme firefly luciferase with the substrate luciferin in the presence of oxygen and ATP has long been used for real-time, low-light imaging of gene expression in living cells and organisms.[8] Firefly luciferase as the reporter starts its catalytic

activity immediately following synthesis, i.e. without a delay time. It is one of the most efficient biological enzymes, with a quantum yield of 0.88 photons per molecule of substrate reacted.[9] A detection limit of 10^{-19} mol firefly luciferases can be reached with commercial instruments. However, bacterial luciferase rather than firefly luciferase has been used exclusively in gene expression imaging of single bacterial cells. The main reason lies in the difficulty of introducing the substrate luciferin into the bacteria. Unlike mammalian cells, the pores on the bacterial cell membrane are so small that the charged luciferin molecules could not pass through the cell membrane at physiological pH. At acidic pH, the permeability is improved as the carboxyl group of the amphipathic molecule is protonated, so that the neutral molecules can pass inside and react with the intracellular luciferase and ATP to produce light.[10] Still, the emission is so weak that conventional instruments cannot detect it at the single bacterial cell level. As shown in our recent reports,[11-15] an ultra-sensitive intensified CCD (ICCD) camera with single-photon sensitivity can be used in such situations.

This article reports another approach for passing luciferin inside the bacterium. During dehydration the bacterial cell membrane became permeable owing to the phase transition from liquid crystalline phase to gel phase. Hence, luciferin molecules, despite their charge, could easily penetrate into those bacteria cells expressing firefly luciferase and give intense CL emission.[16] This process occurs at physiological pH, and the collected light was much more intense than that at acidic pH. The higher CL signal implies that permeation through the membrane is much more efficient in introducing luciferin into the cell than diffusion of the neutral molecules across the membrane at acidic pH. By calibrating the light intensity with standards, we are able to quantify the number of reporter firefly luciferase molecules. Such gene expression studies are not affected by photobleaching or background

auto-fluorescence, and reflect the real-time reporter protein levels because firefly luciferase needs no maturation time. We explored the gene expression of two types of *Escherichia coli* strains, both transformed with plasmids containing *Luc*, which encodes the DNA that expresses firefly luciferase, under the control of *araBAD* promoter (P_{araBAD}). The promoter is induced by arabinose and is repressed by both catabolite repression in the presence of glucose or by competitive binding of the anti-inducer fucose.[17] Very low background levels of expression were reported since this *araBAD* system is tightly controlled. One of the strains we used is a normal BL21 strain and the other is a special strain (XLU102) that is deficient in both arabinose transport and arabinose degradation, with the diffusion of arabinose facilitated by the expressed LacY proteins (LacY A177C).[18] The gene expression patterns of the two types of bacterial strains at different times of the growth period were recorded to demonstrate differences in expression levels and to reveal heterogeneities.

EXPERIMENTAL SECTION

Materials. Luciferase from firefly Photinus pyralis, D-luciferin, adenosine triphosphate (ATP), Luria-Bertani (LB) medium, ampicillin, and L-arabinose were purchased from Sigma-Aldrich (St. Louis, MO). Hanks' balanced salt solution (HBS), phosphate buffered saline (PBS), pBAD TOPO TA Expression Kit were purchased from Invitrogen (Carlsbad, CA). The medium used was LB supplemented with 100 μg/ml ampicillin. The plasmid pBESTluc™ was obtained from Promega (San Luis Obispo, CA). All chemical reagents were used without further purification.

Bacteria Strains and Plasmids. The *Luc* gene was amplified from plasmid pBESTluc™ using PCR and the primers for the 5'-end of the gene (5'-

ATGGAAGACGCCAAAAAC-3') and the 3'-end of the gene (5'-CGCTGAATACAGTTACATTTTA-3'), and then ligated with pBAD-TOPO vector following the Invitrogen manual. Since the DNA insert has two directions, the following procedures must be employed to choose the plasmids with the right insert orientation. First, the constructed pBAD-TOPO was transformed into competent *E. coli* DH5〈. Then 8 colonies of the transformed *E. coli* cells were picked and grown at 30 °C in LB with ampicillin overnight. The next day, the culture was diluted 100 fold and grown until the early-log phase (OD_{600}~0.2) before the inducer 2% L-arabinose was added. The induced bacteria culture continued to grow and reached the mid-log phase (OD_{600}~0.5-0.8) in about 2 h. Then the culture was harvested and tested for CL by the bacteria cell CL detection method described below. 3 out of 8 colonies, which contained the correct orientation of the insert, showed positive CL light. Those verified as correct plasmids pBADluc were extracted and used in later experiments.

The *E. coli* strain XLU102 was constructed to avoid the observed lack of effective regulation of the *araBAD* promoter when using sub-saturating concentrations of arabinose.[17] XLU102 was constructed by elimination of the *bla* gene that encode ampicillin resistance from ECF530[19] by λ Red-based homologous recombination (Duncan, S., Lu, X. and G. J. Phillips, unpublished results).

For bacterial cell CL detection, strain XLU102 and *E. coli* strain BL21 (EMD Biosciences) competent cells were both transformed with the above selected pBADluc plasmids following standard protocols[20]. Overnight cultures of both strains were grown in LB broth containing the appropriate amount of ampicillin at 30 °C with vigorous shaking. The next day, the cultures were diluted 100 fold and grown until the early-log phase (OD_{600}~0.2).

Then L-arabinose was added to a final concentration of 0.2%. The bacteria continued to grow after induction for several hours, with a small amount of culture taken out every hour for real time CL detection and optical density (OD) measurement. Absorbance at 600 nm was measured on a Cary 300 UV-Visible Spectrophotometer (Varian Inc., Palo Alto, CA).

Instrumentation. The imaging system consists of an inverted light microscope (Nikon Diaphot 300, Fryer, Edina, MN) and a complex electron-multiplying microchannel plate (MCP) coupled ICCD (EEV 576 × 384, Princeton Instruments, Trenton, NJ) attached to the camera mount of the microscope. The ICCD camera was operated at –30 °C and read out at 430 kHz with 12-bit resolution. Gain of the intensifier chip was set at the maximum value of 10. A 100× oil-immersion objective (N/A 1.25, Nikon, Japan) was used for cell imaging. To keep the proper temperature for *in vivo* cell experiments, a heated stage insert (World Precision Instruments, Sarasota, FL) was placed on the microscope stage. For all bacterial cell experiments, the temperature was set at 30 °C. Bacterial cells were incubated in o-ring chambers on cover slips for microscopic observation. The chamber was created by sticking Teflon o-rings (Small Parts Inc., Miami Lakes, FL) to poly-L-lysine coated coverslips under sterile operations. The positively charged poly-L-lysine coating helps bacterial cells to stick onto the surface. In standard calibration tests when chemical reagents were added into the buffer, a 50 µl syringe (Hamilton, Reno, NV) was used. To keep the position consistent, the syringe tip was always placed right above the solution surface and in the microscope optical path. The whole system was placed in a dark box.

Standard Firefly Luciferase Calibration. Firefly luciferase standard solutions ranging from 4.56 to 228 nM were used in the standard calibration tests. 15 µl of the standard solution was injected by syringe into o-ring chambers (ID 3/16 inch) filled with 15 µl

reaction mixture, which is composed of 2 mM ATP and 2 mM D-luciferin in HBS buffer. Light generated by the reaction was recorded by the ICCD detector in sequential frames of 30 s exposure, with a dead time between two consecutive frames of about 0.5 s. In every experiment, enzyme standards were added at frame 3 and the first 2 blank frames were used as background. Blank movies were taken under the same conditions with HBS buffer placed in the chambers.

Bacterial Cell CL Detection. 1 µl aliquots of culture taken out every hour during growth periods were mixed with 9 µl HBS buffer and 10 µl 2 mM D-luciferin solution. The mixture was placed in o-ring chambers and incubated on the heated stage for 3 min. Then the chamber was immediately placed at the center of the microscope stage and the CCD was focused on the surface layer of the coverslip. Movies were recorded for about 20 min in consecutive frames of 30 s exposure. With the continuing loss of water by evaporation, bacteria started to become leaky, resulting in the emission of CL at around 12 min followed by a decrease as the dehydration process ended. The whole light emitting process usually lasted for about 2-3 min and was readily reproducible. Optical cell images were recorded after complete dehydration with 5 ms exposure.

For out-of-focus light detection, 20 µl aliquot of strain XLU102 growing culture was taken out after 3 h induction and kept on ice. Then experiments were performed with same procedure as above except that the CCD focus was placed 0-20 µm away from the coverslip surface. The focus was adjusted by rotating the fine focusing knob clockwise and counting the number of scale divisions, each of which gave 1 µm of vertical movement.

RESULTS AND DISCUSSION

Estimation of Single-Molecule Light Intensity. The theoretical amount of light produced from a single firefly luciferase molecule in 2 min can be calculated from the known enzyme properties. Firefly luciferase was reported to be a slow enzyme, with a specific activity k_{ES} of 0.1 U mg^{-1} (1 U = 1 μmol substrate min^{-1}).[21, 22] That means each mg of enzyme consumes 0.1 μmol of substrate in 1 min. The firefly luciferase we used has a molecular weight (*Mw*) of 120 kDa. At optimized conditions, the quantum yield *Y* is 0.88.[9] So during a 2 min exposure time, the number of photons produced, *N*, should follow:

$$N = 2k_{ES}MwY \quad (1)$$

So, each firefly luciferase molecule produces $N = 21$ photons in 2 min, but not all photons could reach the ICCD camera. The fraction *P* is determined by the microscope objective light collection efficiency E_o, lens and prism transmittance *T*, and intensifier quantum efficiency *E*. The objective light gathering ability is governed by the numerical aperture *NA*:

$$Numerical\ Aperture\ (NA) = n\sin(\alpha) \quad (2)$$

or,

$$\alpha = ASIN(NA/n) \quad (3)$$

Since the objective *NA* is 1.25 and the immersion oil refractive index is 1.4790, the objective half angular aperture α has a value of 57.69 degree, which equals 1.01 steradian. Fluorescence light emits in all directions randomly, but only the photons falling within the light cone of 2α are captured by the objective. So, the objective light collecting efficiency E_o is $2\alpha/4\pi = 0.16$. It is well known that a refractive-index difference across an interface

separating two media causes a reflection loss. Application of a quarter-wavelength thick antireflection coating having the appropriate refractive index can reduce the loss to $\approx 1.5\%$.[23] The optics on our microscope has a purplish tint, confirming the presence of single-layer coatings. So the total of 15 lens-air surfaces from the sample to the ICCD chip makes the transmittance $T = (1-1.5\%)^{15} = 0.797$. According to the Princeton Instruments technical note the intensifier quantum efficiency E_i at 560 nm, the emission wavelength of the ATP-firefly luciferase reaction,[9] is ≈ 0.45. Therefore, the overall fraction of light that could create a signal $P = E_o T E_i$, is 0.057. That means that out of the 21 photons produced from one enzyme molecule in 2 min, on the average only 1.2 photons finally create a count. The ICCD camera manual states that at the maximum gain the intensity count generated by one photon is about 70. So, the total intensity count from one enzyme molecule should be ≈ 84.

Standard Firefly Luciferase Calibration. For standard calibration, we optimized the ATP-firefly luciferase reaction conditions, i.e. temperature, reagent concentration and buffer, to obtain the lowest detection limit. The reaction occurred in the o-ring chamber on the coverslip once the firefly luciferase solution was added by syringe into the mixture of ATP and luciferin. Figure 1 illustrates a typical reaction time course. When enzyme was added at minute 1, a rapid increase in light output was observed due to a high local concentration. Then, after sufficient mixing, the light intensity fell to a plateau with a very slow decrease over time, suggesting zero-order reaction kinetics. This is expected since the substrates concentrations were considerably higher than the enzyme concentration.

To increase the signal-to-noise ratio, we processed the images by accumulating four frames into one combined frame using software ImageJ.[24] Frames of minutes 2.5 to 4 at the early plateau stage were combined into one image, and the average pixel intensity was

subtracted from the blank buffer image to give the signal intensity at each concentration. Since the signal is accumulated from four 30-s frames, the equivalent exposure time is 2 min. The process was repeated with different concentrations of firefly luciferase standards from three independent experiments to obtain the data listed in Table 1. The mean intensity is the average of three recorded signal intensities, each of which is the mean pixel intensity of all 576 × 384 pixels in one frame. So, although the pixel intensity has a standard deviation within one frame of ≈ 90 (data not shown), the standard deviation of averages from three independent experiments is only 1.665 (Table 1), which allows us to probe extremely low enzyme concentrations.

To interpret the data at the molecular level, we further adjusted the units of the concentrations and light intensities in Table 1. The concentrations were converted to number of molecules per 1 × 0.25 × 0.25 μm^3 volume. 0.25 × 0.25 μm^2 is the size of one pixel on the ICCD chip corrected for the magnification of 100×. So, the concentration values in the second column of Table 1 represent the number of molecules that are within 1 μm height in a pixel area. At the same time, the observed mean intensities in the third column are normalized by dividing by 84, the theoretical intensity count of one molecule as calculated previously. So, the normalized intensity in the fifth column refers to an estimated number of enzyme molecules based on calculation from the luminescence intensity.

Figure 2 displays the plot of the normalized intensity against firefly luciferase concentration in adjusted units. The smoothing spline curve of the data points in the figure showed a nonlinear relationship. At concentrations below 1.72 molecule/1 × 0.25 × 0.25 μm^3, the increase in normalized intensity was very slow; once the concentration reached ≈ 2, a substantial increase is observed. This result is consistent with recently published data from

the BioTek company.[25] The author measured luciferase enzyme luminescent activity using the Clarity™ luminescence microplate reader. The increase between 10^{-22} moles and 10^{-19} moles was substantially less than that observed from 10^{-19} to 10^{-14} moles. The author suggested that the reason for this downward hook-shape curve is that adsorption of enzyme molecules to the sides of the microplate well caused some of the enzyme activity to be sequestered or inhibited. The same explanation may be applicable to our result, as at lower concentrations a larger percentage of the enzyme may be adsorbed to the coverslip surfaces with compromised light production efficiency. Therefore, the increase in light intensity at extremely low concentrations is non-linear and nearly exponential. This explanation is based on the following assumptions: (1) most enzyme molecules were surface adsorbed to the slide at concentrations less than 2 molecules per 1 μm thickness; (2) the light production efficiency of adsorbed enzyme molecules was substantially reduced.

Figure 2 shows that our sensitivity is near the single-molecule limit. This is to be compared with the BioTek report, where their lowest detectable concentration is 1×10^{-22} moles. The roughly 60-fold sensitivity increase here comes from the great improvement in light collecting efficiency, from the usual 0.1% for commercial instruments to the high value of 5.7% in our system, and the ultra-sensitive ICCD employed.

We note in Figure 2 that for a concentration of 8.6 molecules/$1 \times 0.25 \times 0.25$ μm^3, the estimate total number of enzyme molecules from the normalized intensity is 128, indicating light from a solution thickness of > 15 (≈ 128/8.6) μm was included. That is because light from out-of-focus enzyme molecules could also reach the camera but with reduced efficiency. The rate of decrease in efficiency with respect to the out-of-focus distance is not known *a priori*. To solve this problem, we designed an out-of-focus light intensity detection

experiment making use of the luminescent dehydrating bacterial cells. The surface-adsorbed cells were placed at different distances from the focal plane and left to dry. With well controlled experimental conditions, the dehydration process is highly repeatable.[16] The recorded intensities of those pixels at known vertical cell locations were averaged for each focal distance and then normalized by dividing it with the value at the exact focus (distance = 0) to determine the change in light collection efficiency, as shown in Figure 3.

As predicted, the efficiency decreased with increasing out-of-focus distance. At a distance 20 μm from the focus, < 10% of the expected light intensity was collected. By fitting the data points with a smooth spline and integrating the area under the curve and then dividing that by the total distance of 20 μm, we estimate that the average light collection efficiency over 20 μm is ≈ 0.3. Since we placed the focus about 20 μm above the coverslip surface in all standard calibration experiments, the out-of-focus light originated from both above and below the focal plane, i.e., the total light gathering distance doubled to 40 μm. Therefore, the estimated concentration from the normalized intensity accounting for the light gathering distance and the correction factor 0.3 is 128/40/0.3 = 10.7 at the highest concentration, or 23% higher than the experimental concentration of 8.6. These are in reasonable agreement. This adjusted normalized intensity, shown as the rightmost y-axis in Figure 2, representing the estimated concentration is in the same unit as the x-axis (molecules/1 × 0.25 × 0.25 μm^3) in the plot. So, all the above standard data are self-consistent and support the previously stated theoretical value of 84 for single enzyme molecule CL. Thereupon this value is used in all subsequent single bacterial cell detection to quantify the enzyme molecule numbers.

Bacterial Cell CL Detection. Two types of stains were used, with the difference that

the XLU102 strain is modified to circumvent the all-or-nothing induction to get a homogeneous expression. The *araBAD* regulation has been shown to exhibit all-or-nothing induction. That is, at inducer concentrations below saturation levels, the cells that contain sufficient transporters to accumulate arabinose at the time the inducer is added are fully induced, while the rest of the cells undergo little or no induction. The reason is that induction is autocatalytic. The accumulated arabinose induces the synthesis of more transporters that uptake more arabinose, so those cells with transporter levels above the threshold self-accelerate the expression until fully induced, whereas those with insufficient transporters at the beginning can never catch up later on.[26] The XLU102 strain is deficient in both arabinose transport and arabinose degradation, so that the induction of arabinose transporter is uncoupled from that of the P_{BAD} promoter.[27] This strain is expected to have uniform gene expression under sub-saturating induction.

Being concerned with sensitivity, we still used 0.2% arabinose, a saturating induction concentration that is supposed to fully induce both strains. The growth of the two strains after induction is similar, as depicted in the OD_{600} curve (data not shown). The first two hours is the active growing log-phase, and hours 3-6 is the stationary phase when the exhaustion of available nutrients stops population growth. Every hour during growth, a small portion of the culture was taken out to perform the dehydration CL tests. The bacteria were left to dry on the microscope stage, with the complete process recorded in movies of consecutive 30-s frames. Usually the CL emission lasts around 2-3 min under the experimental conditions in this study.

An optical image was taken after complete dehydration (Figure 4A). Similar to the standard tests, four frames in the 2-min interval with the most intense CL were combined into

one CL image as shown in Figure 4B. The optical image was processed with software ImageJ in several steps to locate cell positions and to define cell particles. First, cell masks were created from the optical image to mark cells in solid black and the rest of the background in white. Second, since the mask and the CL image cannot completely overlap due to the separate optical paths, the cell mask was translated slightly to get the best superposition with the pseudo-colored CL images, as shown in Figure 4C. Third, selection of cells were preformed from the cell masks and applied onto the CL image to define individual bacterium, as illustrated in the tagged cells in Figure 4D, where only the outlines of the masks are displayed. Finally the integrated intensity, size, and mean pixel intensity for each tagged cell in the CL image was measured. The data for the two strains at different time points during growth were processed with Matlab and displayed as the plots in Figure 5. The reason we used cell masks from the optical images instead of directly counting the cells in the CL image is that (1) for some cells the CL light was so weak that it is hard to define the cell edges above the noisy background in the CL image, (2) for situations where most firefly luciferase is located in the middle of the cell, the CL cell image appears smaller than the actual cell size in the optical image, which in turn causes errors in cell-size correction.

The data in Figure 5 starts from 2 h after induction because CL from cells 1 h after induction was below the detection limit. Again, the integrated light intensities of individual cells were divided by 84, and the histograms of the normalized intensities from 100-200 cells at each time point were displayed in Figure 5, top row. The BL21 strain (left column) seems to express much less protein than the XLU102 strain (right column). This difference is obvious in Figure 6 when the median normalized integrated intensities at each time point of the two strains are compared. The highest value of ≈ 550 molecules/cell in the XLU102

strain is about 3 times higher than the highest value of ≈170 molecules/cell in the BL21 strain. The explanation is that the LacY proteins facilitated diffusion of arabinoses in XLU102 more efficiently than the arabinose transporters in BL21. Meanwhile, the accumulated arabinoses in XLU102 cannot be metabolized like in BL21. Therefore, the inducer arabinose concentration was kept at a much higher level in strain XLU102 than in BL21 to give a much higher expression level in the former. Compared to the reported value of around 600-1100 expressed proteins/cell for the $P_{lac/ara}$ system in a fully induced state,[7] our estimated median enzyme number of ≈ 550 ± 60/cell from fully induced XLU102 under the P_{BAD} promoter 2 hours after induction is reasonable, as P_{BAD} is expected to be a slightly less expressive promoter than $P_{lac/ara}$.[28, 29]

We can see from Figure 5, top row, that expression per cell in both plots were increasing when the cells are still actively growing at hour 2 to hour 3, but decreasing when the cells entered the stationary phase at hour 3 to hour 5, indicating that the stationary phase is not necessarily a period of quiescence. It is very likely that in the stationary phase cells are still dividing with expressed proteins randomly distributed to the daughter cells, therefore the amount of enzyme molecules per cell decreased and the distribution range is expanded in XLU102. This is confirmed in Figure 5, middle row that depict the cell size distributions. We can see that both strains keep decreasing in cell size with time, indicating the cells are dividing over time. Another phenomenon we noted from the top row is that although most BL21 cells have very low expression levels, there were a few exceptions that reached almost 2000 molecules/cell, which is also the highest level of a few XLU102 cells. After correcting those intensities with the cell sizes in the middle row, the anomalies disappeared (Figure 5, bottom row), suggesting that the high values are from unusual cell sizes, and not due to

exceptional intensive expression. This observation emphasizes that when comparing expression levels, it is necessary to correct the integrated intensities to account for the individual cell sizes.

One obvious difference between BL21 and XLU102 is that from hour 2 to 4, the distribution in BL21 is broader than that in XLU102. This is consistent with the fact that the expression of BL21 strain in nature is more heterogeneous than that of the modified XLU102 strain, even if both were fully induced. Then, starting from hour 5 to 6, the distributions in BL21 became narrower and the median values decreased. Since the size contribution has already been corrected for, a possible explanation is that the expression in BL21 stopped and the enzyme molecules were degraded. This is reasonable as the half-life for firefly luciferase is known to be about 4 h.[30] Meanwhile, the situation is reversed in XLU102: distributions were broadened and peak intensities increased, suggesting that in XLU102 arabinose was not metabolized so expression continued and more enzyme molecules were produced.

Finally, the 3-D surface plots of CL intensity at different growth times for 2 cells are shown in Figure 7 to reveal the internal firefly luciferase distributions within single cells. At early active growing stages, such as in Figure 7 B1/B2, the expressed firefly luciferase seems to be dispersed in many peaks of similar height around the whole cell. Then, with the cells entering the stationary phase, the luciferase seems to be concentrated to a few peaks at the center (C1) or at the poles (C2) of the cells. That is, the expressed proteins seem to be transported and located to certain cell positions over the growth period. The reason for this protein segregation phenomenon is unknown. However, it could be related to protein folding as suggested by Venkatesh et al.[31]

CONCLUSIONS

In this study, we have demonstrated how to quantify gene expression of individual bacterial cells with CL with sensitivity approaching single-enzyme molecules. This method is fast, convenient, and avoids many intrinsic problems associated with fluorescence detection, such as background, photobleaching or maturation time delay. Our single-cell data were normalized by the theoretical single-enzyme CL intensity based on the assumption that more than enough luciferin molecules diffused inside to react with fully active firefly luciferase. There is the possibility that these values need to be corrected if insufficient luciferin molecules are introduced into the cell or if the activity of the enzyme inside bacteria is different from that of the standards. These issues need to be evaluated with further experiments.

Although the present study is based on sampling a bacterial culture at regular time points during growth, it may be possible to observe real-time gene expression using this concept. For example, luciferin can be introduced into the bacteria via leakage during a brief period of dehydration. Then, the cells can be rehydrated and monitored by CL. We have shown[16] that such an operation does not cause rupture of the bacteria. Naturally, such studies will be limited to those organisms that can survive drying.[32, 33]

ACKNOWLEDGMENTS

E.S.Y. thanks the Robert Allen Wright Endowment for Excellence for support. The Ames Laboratory is operated for the U.S. Department of Energy by Iowa State University under Contract No. DE-AC02-07CH11358. This work was supported by the Director of Science, Office of Basic Energy Sciences, Division of Chemical Sciences.

REFERENCES

(1) Kaern, M.; Elston, T. C.; Blake, W. J.; Collins, J. J. Nature Reviews Genetics 2005, 6, 451-464.

(2) Remington, S. J. Nature Biotechnology 2002, 20, 28-29.

(3) Tsien, R. Y. Annual Review of Biochemistry 1998, 67, 509-544.

(4) Yu, J.; Xiao, J.; Ren, X. J.; Lao, K. Q.; Xie, X. S. Science 2006, 311, 1600-1603.

(5) Xue, Q.; Yeung, E. S. Nature 1995, 373, 681-683.

(6) Tan, W.; Yeung, E. S. Analytical Chemistry 1997, 69, 4242-4248.

(7) Golding, I.; Paulsson, J.; Zawilski, S. M.; Cox, E. C. Cell 2005, 123, 1025-1036.

(8) Greer, L. F.; Szalay, A. A. Luminescence 2002, 17, 43-74.

(9) Seliger, H. H.; Mcelroy, W. D. Archives of Biochemistry and Biophysics 1960, 88, 136-141.

(10) Wood, K. V.; DeLuca, M. Analytical Biochemistry 1987, 161, 501-507.

(11) Wang, Z.; Haydon, P. G.; Yeung, E. S. Analytical Chemistry 2000, 72, 2001-2007.

(12) Gruenhagen, J. A.; Yeung, E. S. Biochimica Biophysica Acta 2004, 1693, 135-146.

(13) Gruenhagen, J. A.; Lovell, P.; Moroz, L. L.; Yeung, E. S. Journal of Neuroscience Methods 2004, 139, 145-152.

(14) Aspinwall, C. A.; Yeung, E. S. Anal. Bioanal. Chem. 2005, 381, 660-666.

(15) Isailovic, D.; Li, H.-W.; Phillips, G. J.; Yeung, E. S. Applied Spectroscopy 2005, 59, 221-226.

(16) Zhang, Y.; Phillips, G. J.; Yeung, E. S. Anal. Chem. 2007, 79, 5373-5381.

(17) Siegele, D. A.; Hu, J. C. Proceedings of the National Academy of Sciences of the United States of America 1997, 94, 8168-8172.

(18) Goswitz, V. C.; Brooker, R. J. Membrane Biochemistry 1993, 10, 61-70.

(19) Bowers, L. M.; LaPoint, K.; Anthony, L.; Pluciennik, A.; Filutowicz, M. Gene 2004, 340, 11-18.

(20) Sambrook, J.; Russell, D. W. Molecular Cloning: A Laboratory Manual, Third Edition ed.; Cold Spring Harbor Laboratory Press: Cold Spring Harbor, NY, 2001.

(21) Wulff, K.; Haar, H.-P.; Michal, G. Luminescent Assays Perspectives in Endocrinology and Clinical Chemistry; Raven Press: New York, 1982.

(22) Schram, E.; Ahmad, M.; Moreels, E. Bioluminescence and Chemiluminescence Basic Chemistry and Analytical Applications; Academic Press: New York, 1981.

(23) Ingle, J. D. J.; Crouch, S., R. Spectrochemical Analysis; Prentice-Hall, Inc.: Upper Saddle River, New Jersey 07458, 1988.

(24) Rasband, W. S. In *http://rsb.info.nih.gov/ij/*; U. S. National Institutes of Health: Bethesda, Maryland, USA, 1997-2006.

(25) Held, P. In *http://www.nature.com/app_notes/nmeth/2006/063006/full.an1755.html*; Nature Methods: Application Notes, 2006.

(26) Morgan-Kiss, R. M.; Wadler, C.; Cronan, J. E. Proceedings of the National Academy of Sciences of the United States of America 2002, 99, 7373-7377.

(27) Khlebnikov, A.; Datsenko, K. A.; Skaug, T.; Wanner, B. L.; Keasling, J. D. Microbiology-Sgm 2001, 147, 3241-3247.

(28) Lutz, R.; Bujard, H. Nucleic Acids Research 1997, 25, 1203-1210.

(29) Guzman, L. M.; Belin, D.; Carson, M. J.; Beckwith, J. Journal of Bacteriology 1995, 177, 4121-4130.

(30) de Ruijter, N. C. A.; Verhees, J.; van Leeuwen, W.; van der Krol, A. R. Plant Biology 2003, 5, 103-115.

(31) Venkatesh, B.; Arifuzzaman, M.; Mori, H.; Suzuki, S.; Taguchi, T.; Ohmiya, Y. Photochemical & Photobiological Sciences 2005, 4, 740-743.

(32) Crowe, J. H.; Carpenter, J. F.; Crowe, L. M. Annu. Rev. Physiol. 1998, 60, 73-103.

(33) Crowe, J. H.; Hoekstra, F. A.; Crowe, L. M. Annu. Rev. Physiol. 1992, 54, 579-599.

Table 1. Standard firefly luciferase calibration data

Concentration (nM)	Concentration (# molecules in 1 × 0.25 × 0.25 μm^3)	Mean Intensity	Mean StdDev	Normalized Mean Intensity	Normalized Mean StdDev
0.00	0.00	1.14	1.7	0.01	0.020
4.56	0.17	10.4	2.6	0.12	0.031
11.4	0.43	12.2	5.2	0.15	0.062
22.8	0.86	24.9	5.1	0.30	0.061
34.2	1.29	54.7	3.2	0.65	0.038
45.6	1.72	168	34	2.0	0.40
114	4.30	2720	647	32.4	7.7
228	8.60	10800	1380	128	16.4

FIGURE CAPTIONS

Figure 1. Firefly luciferase reaction time course. Luciferin was added at 1 min. Intensity is the average pixel intensity with the background subtracted. Final firefly luciferase concentration: 45.6 nM. Final ATP concentration: 1 mM. Final D-luciferin concentration: 1 mM.

Figure 2. Firefly luciferase standard calibration curve. The intensity at each data point is shown in three Y scales: average pixel intensity (background subtracted) as the left Y-axis, the normalized intensity (obtained through dividing by the theoretical single-molecule CL value of 84) as the first right Y-axis, and an additional Y-axis of adjusted normalized intensity (obtained by dividing the normalized intensity by the light gathering distance of 40 μm and the collection efficiency 0.3). Error bars represent the standard deviation of three experimental measurements. The value of each point is listed in Table 1. Fitting curve: smoothing spline.

Figure 3: Out-of-focus light collection efficiency. Cells were placed at varying distances away from the focus, and the emitted CL light intensity was compared to the in-focus value to give the collection efficiency. Fitting curve: smoothing spline.

Figure 4. Single bacterial cell detection. All images were from one experiment of strain

XLU102 at 3 hours after induction. (A) Bright-field optical image taken after dehydration was completed. (B) Combined CL image of the 4 most intense CL frames. Effective exposure time after combination: 2 min. (C) Overlaid image of cell mask in solid black from optical image (A) and CL image in pseudo colors (B). (D) Processed CL image with the outline of cell masks showing tagged cells.

Figure 5. Strain BL21 and strain XLU102 CL detection. Histograms of normalized integrated intensity, size, and normalized mean pixel intensity measured for individual cells were shown in 3 rows, respectively. Those in the left column are from strain BL21 and those in the right column are from strain XLU102.

Figure 6. Expression level comparison. The median normalized integrated intensities at each time point of the two strains are plotted against the induction time. Error bars were obtained by multiplying the median cell sizes by the standard deviation, which was determined in blank buffer images binned with the median particle size. Stain BL21: diamond; strain XLU102: square.

Figure 7. 3-D surface plots and 2-D plots of CL intensities from 2 single bacterial cells. A1/A2: background. B1/B2: cells at 2 hours after induction. C1/C2: cells at 6 hours after induction. Each set contains two plots of the same cell, the upper one is 3-D and the lower one is 2-D. As the 3-D plots were rotated to the best observation angle, the cell orientations may be different in the 3-D plots from

those in the 2-D plots. The color is calibrated by the bottom scale bar to represent the number of molecules.

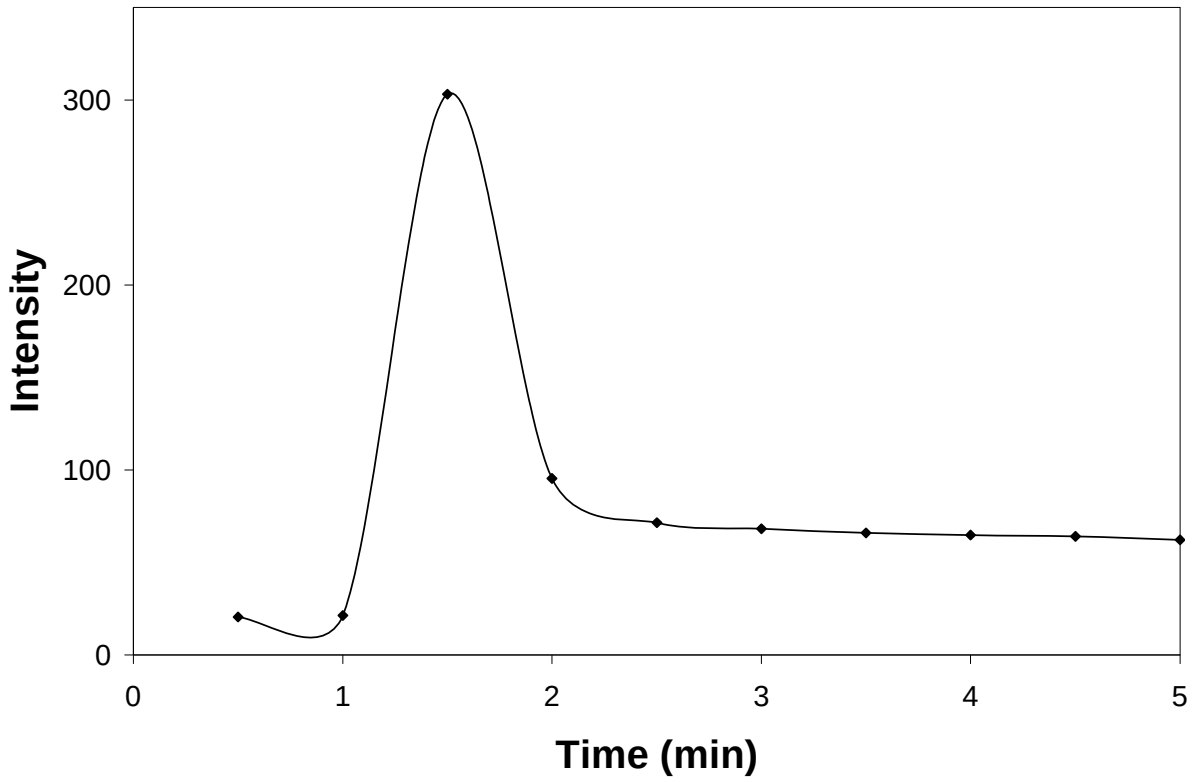

Figure 1.

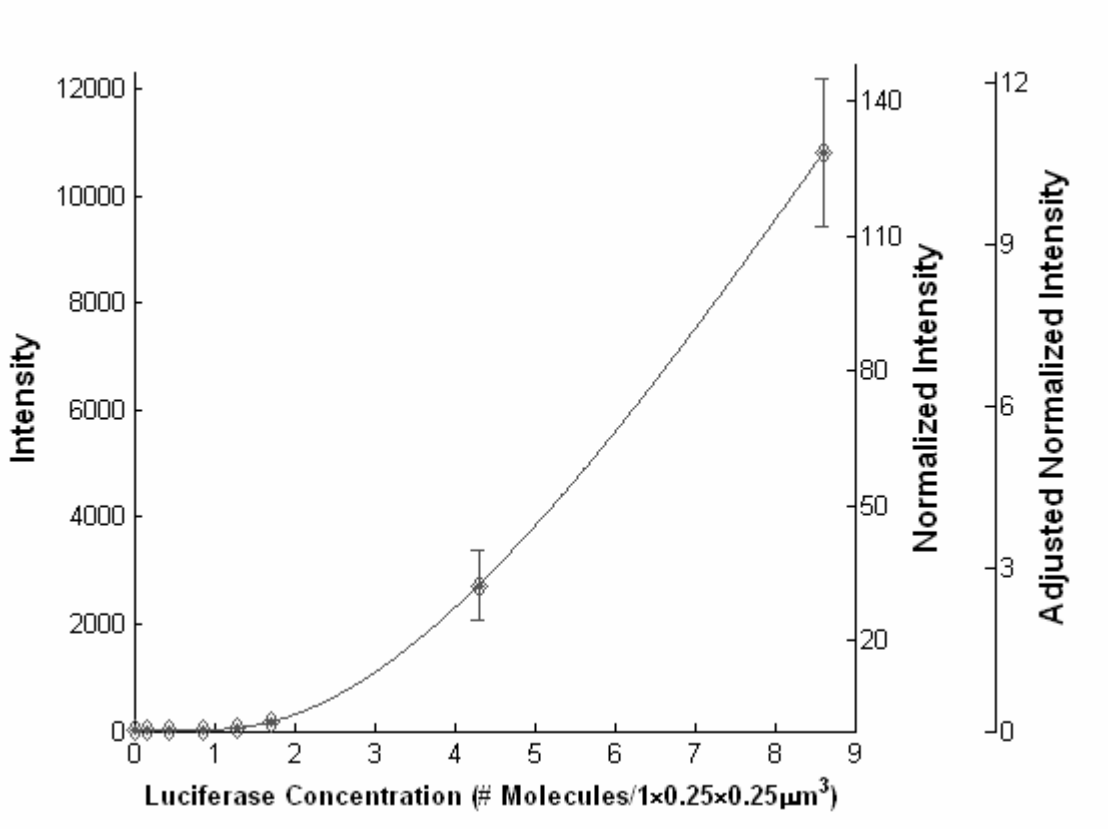

Figure 2.

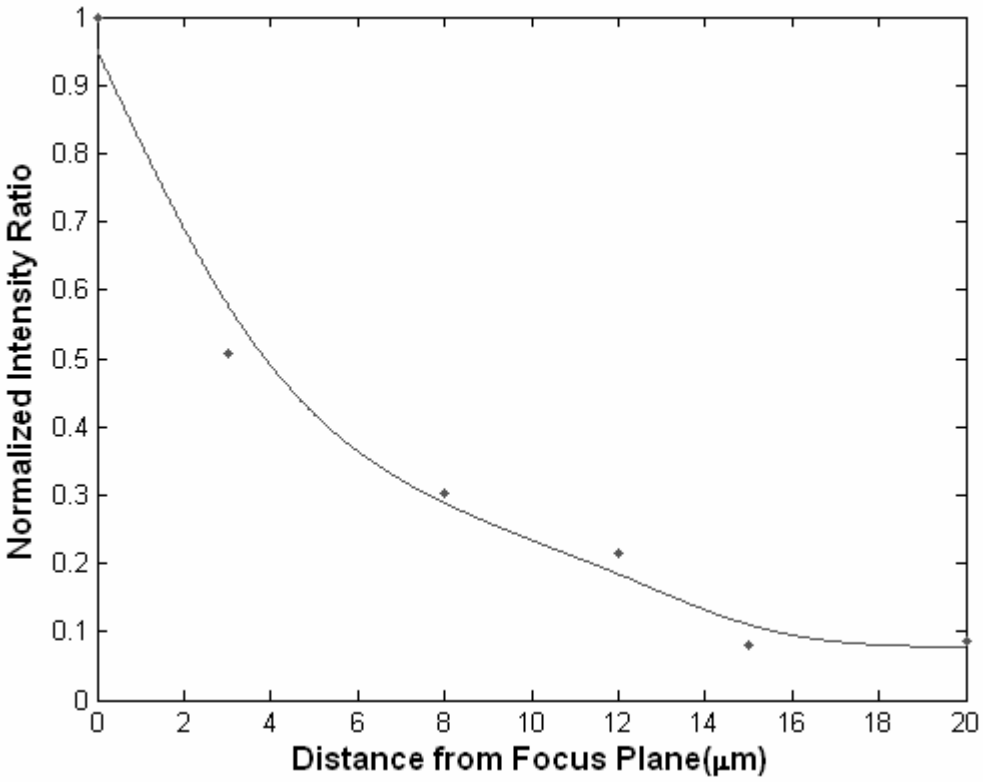

Figure 3.

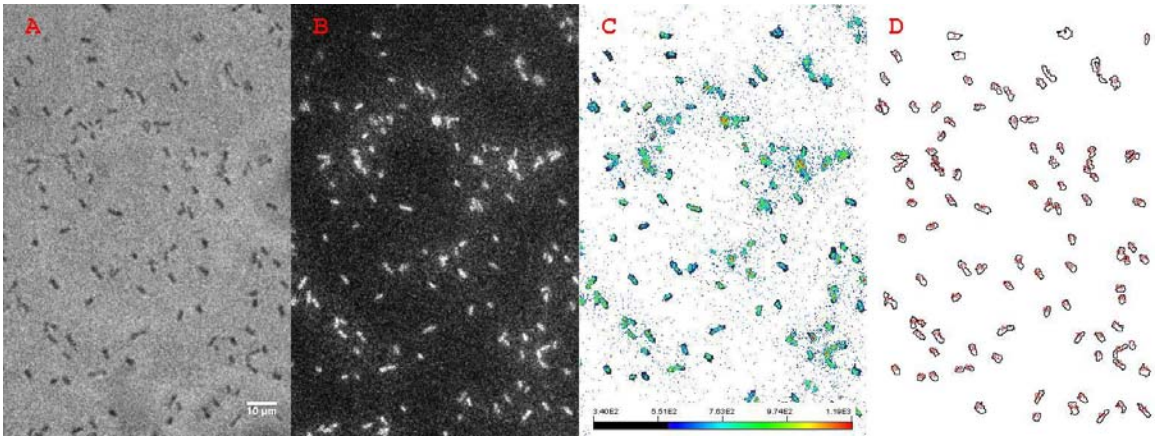

Figure 4.

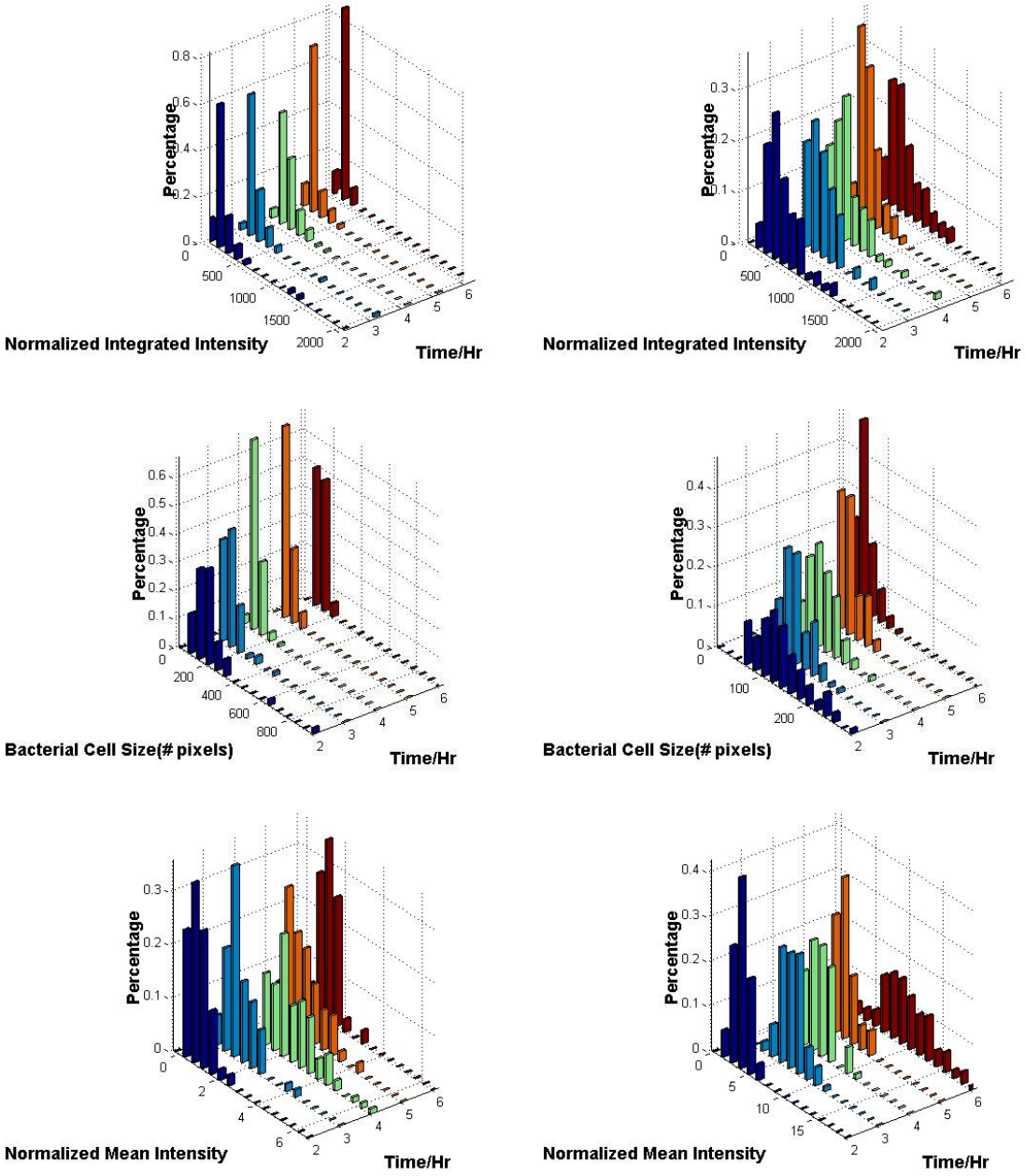

Figure 5.

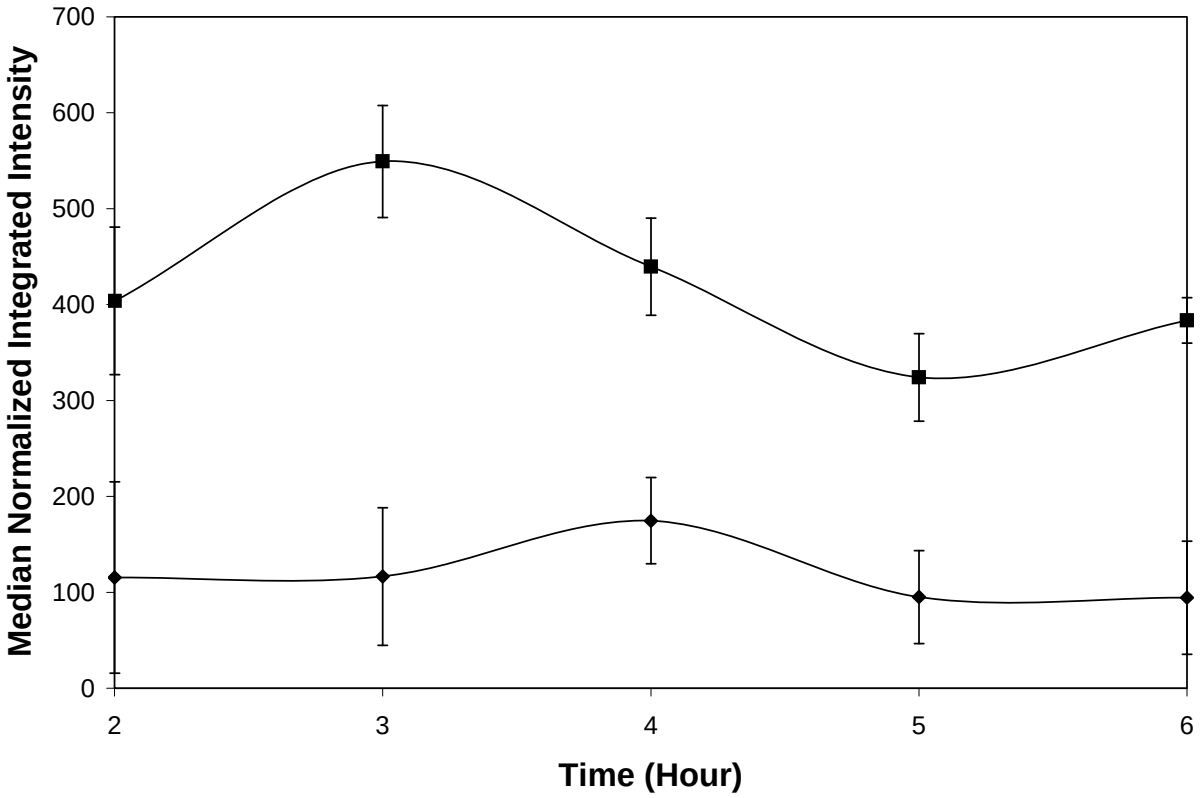

Figure 6.

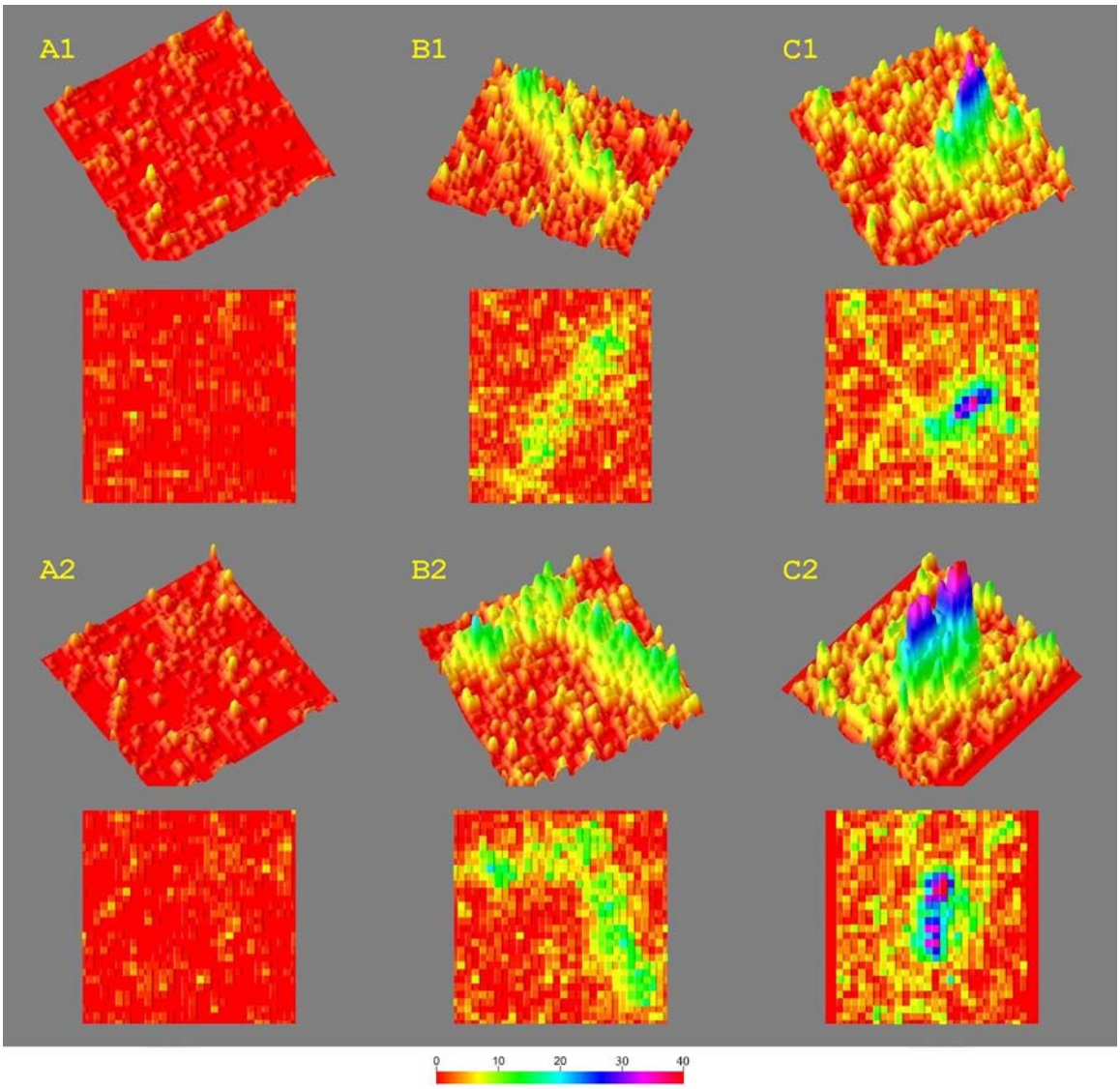

Figure 7.

CHAPTER 4. IMAGING LOCALIZED ASTROCYTE ATP RELEASE WITH FIREFLY LUCIFERASE IMMOBILIZED BEADS ATTACHED ON CELL SURFACE

A paper prepared for submission to Analytical Chemistry

Yun Zhang, Gregory J. Phillips, Qingxi Li and Edward S. Yeung

ABSTRACT

Extracellular adenosine triphosphate (ATP) functions as signaling molecules in many cell regulation processes. The traditional firefly luciferase assays measure the ATP release as a signal increase with time using a luminometer. Recently, advanced cell imaging techniques using charge-coupled device (CCD) cameras have enabled 2D high resolution detection providing both spatial and temporal information. Real-time imaging of ATP release from astrocyte cells has been reported. However, the observed chemiluminescence propagation wave reflects both ATP release and diffusion in the extracellular bulk solution. The dynamic ATP efflux at the cell surface could not be accurately measured. Hence we constructed biotinylated fused firefly luciferase proteins, immobilized the proteins on 1 μm beads, and attached the beads to the cell surface to detect ATP release from mechanically stimulated astrocyte cells. This novel detection method enables us to monitor the actual ATP concentration at the surface of single live cells. The localized ATP release was found to be

prominent but lasted only < 20 seconds, which is very different from the results obtained by free firefly luciferase detection.

INTRODUCTION

ATP efflux from cells has been extensively studied because of its biological importance in modulating autocrine and paracrine functions.[1-6] The mechanisms of ATP release into extracellular spaces are generally grouped into three categories. The first involves physical damage to healthy cells by tapping, stretching, and hypotonic stress. Since ATP is present in all cells at mM levels, the cytolysis of any cell could result in nonselective release of a high concentration ATP. The second mechanism occurs in many neuronal, neuroendocrine, or endocrine cells when ATP is released as signaling molecules via Ca^{2+} regulated exocytosis of nucleotides compartmentalized within synaptic vesicles or dense core granules.[7, 8] In the third situation, the probable route for ATP release is the efflux of cytosolic ATP via plasma membrane transport proteins.[9] A variety of methodologies have been developed for the characterization of these complex tissue responses. Chemiluminescence detection is the most widely used scheme for detecting ATP.[10, 11] The enzyme firefly luciferase catalyzes the reaction of ATP and the substrate D-luciferin in the presence of oxygen to produce light with high quantum efficiency. ATP can be detected in this way at the picomolar level.

In early-stage offline experiments, the extracellular medium is periodically collected in aliquots following stimulation of the cells and assayed with standard luciferase and D-luciferin to quantify the released ATP.[12, 13] This method dilutes ATP with the reagent solution and does not give accurate dynamic concentration information. An improved online

method was developed by Schwiebert et al.[14, 15] They used a luminometer to measure extracellular ATP levels in cultures of adherent cell monolayers grown in culture dishes. In this way ATP concentrations can be followed over time without perturbing the extracellular fluid. With recent live-cell imaging technologies, real time ATP secretion can now be observed at the single-cell level with charge-coupled device (CCD) cameras.[16, 17] By taking 2D movies (consecutive frames with 1 s temporal resolution), the ATP signaling process in live astrocyte cells was recorded both spatially and temporally.[8]

In those studies, ATP has been confirmed as an intercellular signaling molecule, but accurate quantitative evaluation and the underlying mechanisms remain unresolved. After release, ATP will immediately be diluted into the bulk extracellular solution, which results in the underestimation of the amount of ATP released. Meanwhile, several other factors make the situation even more complicated: ATP may be rapidly hydrolyzed at the extracellular surface by ecto-nucleotidase,[18, 19] or may be synthesized from extracellular ADP by disphosphokinase or adenylate kinase.[20-23] The detected ATP concentration is therefore a balance between the rates of release, hydrolysis, synthesis and dilution. To accurately measure the localized transient ATP release amount, Dubyak et al. proposed to detect ATP at the cell surface.[24, 25] They reported the use of a protein A-luciferase chimera that can be stably adsorbed onto the surface of intact cells via interactions with primary IgG antibodies directed against native surface antigens. However, the activities of luciferase fusion proteins were much lower that those of native luciferase and there were potential complications for antibody binding to some cell surface epitopes. An improved ATP sensing system with a luciferase fusion protein whose activity is highly conserved was described by Kobatake et al.[26] Firefly luciferase was fused with biotin acceptor peptide (BAP), which is a subunit of

acetyl-CoA carboxylase, that is posttranslationally modified with a biotin molecule covalently attached to a specific lysine residue.[27, 28] The biotinylated firefly luciferase was then immobilized to the cell surface via interactions with streptavidin for detecting localized ATP. Since there is no direct chemical modification of the enzyme, luciferase activity could be fully retained.[29, 30]

In this paper we modified the approach for attaching fused firefly luciferase to the cell surface. We engineered firefly luciferase similarly with a biotin targeting domain from a different bio-origin of *Klebsiella pneumoniae* oxaloacetate decarboxylase (KPBT).[31] The cell surface was again biotinylated with sulfo-NHS-biotin which binds to the N termini of cell membrane proteins. But, instead of using streptavidin solution to bind them, we used streptavidin beads of about 1 μm in diameter. Biotinylated enzymes were attached to the beads that have ~10 millions biotin binding sites each. Then, the residual uncovered sites on the beads interact with sulfo-NHS-biotin and attach to the cell surface. Concentrated firefly luciferase was thus accumulated within 1 μm at the cell surface in this way. Also, when using streptavidin molecules directly, the large streptavidin molecules alter the activity of cell membrane proteins because they cover the entire cell surface. By applying beads that only partially cover the cell surface, the same amount of firefly luciferase is immobilized via fewer linking sites, therefore affecting the cell membrane proteins less. In fact, our ATP release experiments using direct streptavidin linkage showed no signal (data not shown), while a clear signal was readily obtained by using beads.

To observe extracellular signaling and spreading of ATP and intercellular increase of calcium simultaneously, we stimulated astrocyte cells by poking and recorded chemiluminescence and fluorescence images alternately with an intensified CCD (ICCD)

camera at 1.5 s frame rate. Compared to free firefly luciferase solution detection, this method gives more accurate information about ATP amounts and decay time. We also studied rat hepatoma liver cell ATP release upon hypotonic stress, which follows the first mechanism (physical damage to cells for releasing cytosolic ATP). But recent studies have also implicated ATP as the autocrine signaling molecule in this situation.[4, 9] Our recorded ATP release from astrocytes showed a similar temporal profile but with a much lower amount, suggesting the second mechanism.

EXPERIMENTAL SECTION

Materials. Luciferase from firefly Photinus pyralis, D-luciferin, adenosine triphosphate (ATP), Luria-Bertani (LB) medium, ampicillin, and isopropyl β-D-1-thiogalactopyranoside (IPTG) were purchased from Sigma-Aldrich (St. Louis, MO). Hanks' balanced salt solution (HBSS), phosphate buffered saline (PBS), Fluo-4 NW calcium dye, pBAD TOPO TA Expression Kit and Champion pET Directional TOPO Expression Kit were purchased from Invitrogen (Carlsbad, CA). Qiaexpress Ni-NTA Fast Start Kit was purchased from Qiagen (Valencia, CA). Microcon centrifugal filter devices were purchased from Millipore. Bicinchoninic acid protein assay kit was purchased from Pierce (Rockford, IL). The medium used was LB supplemented with 100 μg/ml ampicillin. The plasmid pBESTluc™ was obtained from Promega (San Luis Obispo, CA). All chemical reagents were used without further purification.

Plasmid Construction. The biotinylated luciferase gene fusion vector, pET-KPBT-Luc (Figure 1) was constructed as follows. The *luc* gene was amplified from plasmid pBESTluc™ using PCR and the primers for the 5'-end of the gene (5'-

CACCGCGGAAGACGCCAAAAA

CATAAAGAAAGGCC-3') and the 3'-end of the gene (5'-TTCGTCATCGCTGAATACA

GTTAC-3'), and then ligated with pET100/D-TOPO vector following the Invitrogen directional TOPO cloning manual to generate the plasmid pET-Luc. The biotin targeting domain from

Klebsiella pneumoniae oxaloacetate decarboxylase (KPBT)[32] was amplified from a pKR46 (kindly provided by Dr. John Cronan, University of Illinois) by PCR and ligated into pBAD-TOPO using the pBAD TOPO TA Expression kit (Invitrogen). The relevant regions of the resulting plasmids were sequenced to confirm their configurations. A DNA fragment encoding KPBT was isolated from pBAD-KPBT by digestion with *Xba*I and *Spe*I, and inserted into pET-Luc digested with *Nhe*I, whose cut sites are compatible with *Xba*I and *Spe*I, yielding pET-KPBT-Luc. This plasmid encodes the KPBT-luciferase hybrid protein with a hexa-His-tag at the N-terminus. Expression of the hybrid protein is induced with IPTG.

Expression and purification of biotinylated luciferase. The constructed pET-KPBT-Luc plasmid was transformed into competent *E. coli* BL21 cells by heat shock. Transformed *E. coli* cells were grown overnight at 30 °C in 10 ml LB with ampicillin. The next day 250 ml media supplemented with ampicillin and 50 μM biotin was inoculated with the overnight 10 ml culture and grown until the early-log phase ($OD_{600} \sim 0.2$) to add the inducer IPTG to 0.2 mM. The induced bacteria culture continued to grow for an additional 5 h. Then the culture was harvested by centrifugation at 4000× g for 20 min. The cell pellet was frozen overnight at –20 °C. The next day the pellets were thawed on ice and his-tagged KPBT-firefly luciferase proteins were purified by metal-ion affinity chromatography using Qiaexpress Ni-NTA Fast Start Kit following the manufacturer's instructions. Finally the

proteins were collected in elution buffer of high salt concentration. To reduce the salt content for later detection, the buffer was exchanged into PBS using Microcon centrifugal filter devices. All of the above purification steps were performed at 4 °C. The purified biotinylated fused firefly luciferase was stored at 4 °C for two weeks. The concentration of the purified protein was determined with bicinchoninic acid protein assay kit.

Cell Culture. The primary astrocyte cell culture was prepared in the same manner as described by Wang et al.[8] Cortices of postnatal rat pups were dissected, and astrocyte cells were extracted and grown in modified minimal essential medium (MMEM) (Eagle's minimum essential medium (EMEM), 2 mM glutamine, 1 mM sodium pyruvate, 100 units/mL penicillin and 100 mg/mL streptomycin) supplemented with 10% fetal bovine serum at 37°C in CO_2 cell culture incubator until confluency. Then the flasks were rinsed with EBSS for three times, and applied with trypsin-EDTA solution to detach the cells. The detached cells were mixed with 6-8 ml MMEM and spun down at 1000 rpm for 10 min. The supernatant was discarded. The cell pellet was resuspended in MMEM and plated into o-ring chambers (ID 7/16 inch) on 22-mm cover slips. The chamber was created by sticking Teflon o-rings (Small Parts Inc., Miami Lakes, FL) to poly-L-lysine coated cover slips under sterile operations. The positively charged poly-L-lysine coating helps cells to stick onto the surface. The cells in the chambers on the cover slips were grown at 37°C in humidified 5% CO_2 incubator for about 4 days to reach confluency and were then ready for tests.

Rat hepatoma liver cell line was obtained from ATCC (Manassas, VA) and grown in EMEM medium supplemented with 10% fetal bovine serum. The propagation procedure followed the ATCC instructions. Then the cells were detached and plated into o-ring chambers on cover slips with the same handling procedure as described above.

Instrumentation. The imaging system consists of an inverted light microscope (Nikon Diaphot 300, Fryer, Edina, MN) and an electron-multiplying microchannel plate (MCP) coupled ICCD (EEV 576 × 384, Princeton Instruments, Trenton, NJ) attached to the camera mount of the microscope. The ICCD camera was operated at –30 °C and read out at 430 kHz with 12-bit resolution. The gain of the intensifier chip was set at the maximum value of 10. A 20× objective (N/A 0.75, Zeiss, Germany) was used for cell imaging. To keep the proper temperature for live-cell experiments, a heated stage insert (World Precision Instruments, Sarasota, FL) was placed on the microscope stage. For all cell experiments, the temperature was set at 30 °C. Cells were incubated in o-ring chambers on cover slips for microscopic observation. In standard calibration tests and rat hepatoma cell tests when chemical reagents or hypotonic buffer were added into the o-ring chamber, a 50 µl syringe (Hamilton, Reno, NV) was used. To keep the position consistent, the syringe tip was always placed right above the solution surface and in the microscope optical path. For in vitro astrocyte cell experiments, a mechanical tip was used to stimulate the cells. The mechanical tip was about 30 µm in diameter and was controlled by a micromanipulator. The whole system was placed in a dark box.

For alternate detection of calcium Fluo-4 fluorescence (FL) images and chemiluminescence(CL) images, a blue light emitting diode (LED) (Nichia, Detroit, MI) and a mechanical Uniblitz shutter (Edmund Optics, Barrington, NJ) next to it were put above the microscope stage in the microscope optical path. The shutter was closed to cut off light from the LED when the chemiluminescence image was collected, and opened to provide excitation when the fluorescence was captured. It was set with 50-ms exposure time and 3-s delay time. The ICCD camera was set to take consecutive frames of 1-s exposure time and 0.5-s delay

time in between frames. When experiments started, both ICCD and shutter were triggered simultaneously. The shutter was open for 5 ms in the first frame, providing light to induce fluorescence signal. Since the fluorescence intensity was much higher than the chemiluminescence signal (over 10×), the latter could be neglected in the image. Then, in the next frame, the shutter remained closed, so that only chemiluminescence was detected by the ICCD. Each detection cycle was 3 s and composed of one FL image and one CL image. That it, a 1-s exposure for the fluorescence image (actual LED exposure time was 50 ms) was recorded followed by a 0.5 s delay, then a 1-s exposure for chemiluminescence and 0.5 s delay, then another FL frame, etc.

Standard ATP Calibration with Free Firefly Luciferase. ATP standard solutions ranging from 0.2 to 200 μM were used in the standard calibration tests. 15 μl of the standard ATP solution was injected by syringe into the o-ring chamber (ID 3/16 inch) filled with 15 μl reaction mixture, which is composed of 2 mg/mL firefly luciferase and 2 mM D-luciferin in HBSS buffer. Light generated by the reaction was recorded by the ICCD detector in sequential frames of 1 s exposure, with a dead time between two consecutive frames of about 0.5 s. In every experiment, the first 10 blank frames were used as background and enzyme standards were added at frame 11. Blank movies were taken under the same conditions with HBSS buffer placed in the chambers. Each ATP data point was the average of triplicate measurements.

Standard ATP Calibration with Biotinylated Firefly Luciferase Immobilized on Beads. Biotinylated firefly luciferase was immobilized to MagnaBind Streptavidin Beads (Pierce, Rockford, IL) as follows. 20 μl MagnaBind Streptavidin Beads solution was pipetted into a microcentrifuge tube. The tube was placed in the MagnaBind Magnet to separate the

beads. The clear supernatant was removed. Then beads were rinsed three times with 200 µl PBS, and resuspended in 100 µl purified biotinylated fused firefly luciferase solution. The mixture was incubated at room temperature for 30 min with constant gentle mixing. Then biotinylated firefly luciferase immobilized beads were then separated magnetically and rinsed again three times with 200 µl PBS. The purified beads were resuspended in 200 µl PBS and 30 µl of that was applied to o-ring chambers (ID 3/16 inch) on poly-L-lysine coated cover slips to incubate for 10 min. Then, the solution was removed and only beads attached to cover slip surfaces were retained and treated with 15 µl 2 mM luciferin HBSS buffer. 15 µl of the standard ATP solution ranging from 2 to 2000 µM was injected by syringe into the o-ring chamber for the standard calibration tests. The experimental settings were the same as the above native firefly luciferase ATP calibration tests. Each ATP data point was the average of triplicate measurements.

In Vitro Astrocyte Imaging. The astrocyte cell culture was grown on cover slip chambers until confluency. For free firefly luciferase solution detection, the media MMEM was removed, and cells were rinsed three times with 200 µl HBSS. 200 µl Fluo-4 NW Calcium assay buffer supplemented with 2.5 mM probenecid was loaded into the chamber, and the cells were incubated at 37 °C for 45 min. Probenecid was used to reduce the fluorescence outside the cells by inhibiting the transport of Fluo-4 indicator out of the cell, and to block potential ATP release from astrocyte cells via multidrug resistance protein (MRP).[33] Then, the assay buffer was removed and the cells were rinsed again three times with HBSS. 200 µl solution of 1 mg/mL firefly luciferase and 2 mM D-luciferin in HBSS buffer were added onto the cells in the chamber. Stimulation to the cells to cause ATP release was via gentle tapping to the cell membrane with the mechanical tip in the same manner as

described elsewhere.[8, 34, 35] The alternating ATP chemiluminescence signal and calcium fluorescence signal were recorded sequentially with the ICCD camera at 1.5-s frame rate.

For local ATP release detection with firefly luciferase immobilized beads attached on the cell surface, the handling procedure is more complex. First the cell media was removed and cells were rinsed three times with 200 µl HBSS. 200 µl Fluo-4 NW calcium assay buffer supplemented with 2.5 mM probenecid was added into the chamber, and the cells were incubated at 30 °C for 50 min. Then cells were rinsed twice with HBSS and 200 µl 60 mM Sulfo-NHS-Biotin in HBSS was added. The cells were incubated at 30 °C for 10 min. At the same time, 20 µl MagnaBind Streptavidin Beads suspension was rinsed three times with 200 µl PBS using MagnaBind Magnet and resuspended in 200 µl Fluo-4 NW calcium assay buffer. The Sulfo-NHS-Biotin solution was removed from the cells and the prepared streptavidin beads solution was added to the cells rinsed twice with HBSS. The cells were incubated at 30 °C for 15 min with beads. Then the bead suspension was removed and cells were rinsed twice with HBSS to retain the surface attached beads only. 100 µl biotinylated firefly luciferase solution was loaded to the astrocyte cells bound with beads and incubated for another 15 min at 30 °C before it was removed. The cells were cleaned twice with 200 µl HBSS. Finally, cells with firefly luciferase immobilized beads were immersed in 200 µl 2 mM D-luciferin in HBSS buffer and were ready for detection. The whole treatment of cells took about 1.5 h. The detection procedure was the same as the above free firefly luciferase experiment. For control experiments, the same steps were used as described above, except that 2.5 µM streptavidin solution was used instead of streptavidin beads.

Monitoring Rat Hepatoma Liver Cell ATP Release upon Hypotonic Stress. The rat hepatoma liver cells cultured in cover slip o-ring chambers were rinsed three times with

200 µl HBSS and were loaded with 100 µl 1 mg/mL firefly luciferase and 2 mM D-luciferin HBSS buffer solution. 50 µl water was injected by syringe into the chamber to dilute the buffer to 67% concentration when chemiluminescence images were taken consecutively by the ICCD camera with 10 s exposure time.

RESULTS AND DISCUSSION

Characteristics and Immobilization of Biotinylated Firefly Luciferase. We constructed pET-KPBT-Luc (Figure 1) by fusing *luc* gene and biotin acceptor peptide gene KPBT, and inserted the DNA into pET100/D-TOPO vector. This vector was chosen because it contains T7 promoter, which produces high yields of recombinant proteins; also it includes a polyhistidine tag at the N-terminal of KPBT-Luc that allows highly selective purification of histidine-tagged fusion proteins using metal affinity columns. The KPBT-luciferase fusion proteins were highly expressed in induced *E. Coli* BL21 cell culture and biotinylated post-translationally to a specific lysine residue of the biotin domain.[36] The recombinant proteins purified with Ni-NTA column and SDS-PAGE showed high protein purity for the elution fractions. A 250 ml cell culture yielded 8.0 mg luciferase, which is about the amount of luciferase purified from 1600 fireflies by the method of Deluca and McElroy.[37] The molecular weight of KPBT-luciferase calculated from the amino acid sequence is 75.9 kDa, consistent with the molecular weight obtained from our MALDI-MS data, which is 76.0 kDa.

Storage conditions of KPBT-luciferase were studied. We found that freezing of the enzyme at –20 °C even just for a few days completely inactivated the enzyme, while refrigeration at 4°C retained more than 90% of the activity for 1-week storage. Using 50% glycerol could enable longer time storage of the enzyme at –20 °C without activity loss from

freezing-thawing cycles as suggested by Stewart et al.,[38] but glycerol interferes with the chemiluminescence reaction and must be removed from the enzyme before detection. Therefore, we prepared fresh KPBT-luciferase protein solutions that were stored at 4 °C, and used them within 1-2 weeks.

The enzymes were immobilized to beads via interaction of biotin and streptavidin. Considering that astrocyte cells are usually 20-30 μm in size, we used beads of about 1 μm. Magnabind streptavidin beads of this dimension were used because of the easy purification with magnetic field. Biotin binding to streptavidin has a dissociation constant $K_d = 10^{-15}$ mol/L, the strongest non-covalent biological interaction known.[39] The non-covalent binding avoids direct chemical modification of the enzyme, therefore retaining the enzyme activity. Furthermore, the reaction was rapid: maximal binding was reported to be reached within 30 min incubation.[29]

Standard ATP Calibration. Firefly luciferase light producing reaction with ATP, D-luciferin is the most efficient chemiluminescence system. We have reported detection of nanomolar ATP or a few thousands of firefly luciferase molecules in a single bacterium with an ultrasensitive ICCD imaging system.[16, 17] In this work, ultimate sensitivity was not the goal. We wanted to observe cell to cell communications, so a low magnification objective (20×) was used to image a larger cell culture area. Sensitivity was compromised, but ATP released from mammalian cells as signaling molecule was reported to be in the range of μM, i.e., within our detection limit.

The chemiluminescence intensity was plotted against added ATP concentration, as shown in Figure 3. The curves were nonlinear, possibly because surface adsorption caused the enzyme activity to be sequestered or inhibited.[17, 40] We fitted the data with a polynomial

equation, and used that to determine the cell-surface ATP amounts. When ATP was added to the mixture of firefly luciferase and D-luciferin in the o-ring chamber, a sharp increase in light intensity appeared within 1-2 s, followed by a signal decrease slowly over time to a plateau. The signal intensity at each concentration was calculated by subtracting the average pixel intensity of the peak intensity image with the average pixel intensity of the blank image (before ATP addition). For firefly luciferase immobilized on beads, the image results are different. Instead of the light intensity increasing over the entire image (Figure 2B), only those small dots representing beads showed bright chemiluminescence (Figure 2C). We carefully chose those bead locations with 10 pixel diameter circles, and recorded the average pixel intensity in these small areas. The signal intensity was obtained by subtracting the peak intensity with the blank intensity in the bead areas.

As a result of the smaller signal areas with beads, the lowest detectable concentration is lower for free enzyme (at 0.1 μM ATP with intensity 0.67) than for immobilized enzyme (at 10 μM ATP with intensity 35.2). That is because the average pixel intensity fluctuates more in smaller areas. The standard deviation of the mean pixel intensity from ten blank images of all 576 × 384 pixels in a frame is 0.10, but the same for 10 pixel diameter circles is 4.5. We also noticed that the chemiluminescence signal intensity is much higher with free firefly luciferase than with beads when high amounts of ATP is added (Figure 3). This is explained by the fact that light from out-of-focus enzyme molecules could also reach the camera but with reduced efficiency for free firefly luciferase. From our previous report, a fraction of the light from a distance of 20 μm from the focus was still collected.[17] However for firefly luciferase immobilized on beads, luciferase was bounded to a 1-μm thick surface layer. Since there was no light accumulation from out-of-focus layers, the intensity increase

at the thin layer was lower.

Monitoring Astrocyte ATP Release. Intercellular propagation of Ca^{2+} waves occurs among neurons and glial cells in the central nervous system (CNS) in response to mechanical or electrical stimuli to modulate cooperative cell activities.[41-44] Several studies have attributed the propagation of Ca^{2+} signals to the diffusion of intracellular and extracellular messenger molecules. Intercellular calcium wave propagation has been correlated with diffusion of small signaling molecules (Mw < 1000 Da), such as inositol triphosphate (IP_3) and Ca^{2+}, to cross gap junction channels among physically adjacent astrocyte cells.[45-48] An alternative pathway involves the release of ATP into the extracellular space, followed by the activation of Ca^{2+}-mobilizing P2Y nucleotide receptors in neighboring cells that may or may not be in contact.[8, 49, 50] In our study, confluent astrocyte cell cultures mechanically stimulated at a center cell were imaged alternatively with Ca^{2+} Fluo-4 fluorescence and ATP-firefly luciferase chemiluminescence, as shown in Figure 4 and 5. The two movies showed obvious differences in the ATP propagation pattern. From Figure 5, which shows localized ATP release at the cell surface with firefly luciferase immobilized beads, the ATP chemiluminescence propagation wave spread to a more limited area and disappeared faster than that by using free enzyme in Figure 4.

Regions of interest (ROI) 1-8 in each movie, at sequentially larger distances from the stimulation center, were chosen at cell locations with 10 pixel diameter circles. The average pixel intensities of the ROIs were plotted against time in Figure 6. Intensities of CL and FL of cells at the stimulation center reached the maximum immediately follow stimulation. Other cells responded with a delay time depending on the distance away from the stimulation center. Then the free-solution CL emission decayed slowly, > 1 min as in Figure 6 A1, while

with beads the intense CL burst lasted less than 20 s in Figure 6 B1. This indicates that the actual localized ATP release is strong but short in duration, followed by ATP attenuation by diffusion into extracellular spaces. By using the standard ATP calibration curve, we estimated from the bead experiments that the localized ATP concentration at the stimulation center is mM level, which is the approximate concentration of cytosolic ATP. At distances from 30-100 μm, which correspond to adjacent cells, the ATP concentration was about 150-20 μM. For cells > 100 μm away, the bead experiments did not give CL signal above background. The localized ATP concentrations are much larger than the ATP concentration of 20-1 μM obtained in free enzyme experiments, which agrees with our expectation that dilution does not affect the bead experiments. We can conclude that the true ATP release from astrocyte cells is a fast process that involves high concentrations of ATP in short bursts of seconds, which is consistent with the vesicle discharge time of seconds in stimulated exocytosis as recently reported.[51-53]

CL and FL propagation waves were evaluated by comparing the apparent diffusion coefficients assuming single-point source release. For a cell at distance x (μm) with peak intensity at delay time t (s) after wave initiation, the diffusion coefficient D ($\mu m^2/s$) = $x^2/4t$. The distance x was 1.25 times the pixel distance between the cell ROI and the stimulation center ROI since one pixel is 1.25 μm. The delay time was obtained by fitting the CL/FL intensity-time curve with smooth spline and subtracting the peak intensity time from the trigger time. Figure 7 displays the calculated CL and FL diffusion coefficients of 8 ROIs in the two experiments. The fact that the apparent diffusion coefficient keeps increasing with distance is in variance with diffusion being responsible for propagation and supports the mechanism of ATP and Ca^{2+} signaling occurring directly from cell to cell. The diffusion

speeds of CL and FL is also useful in understanding the relative contributions of intercellular and extracellular pathways in mediating the propagation of calcium waves. From Figure 7A, we can see that for short distances (< 120 μm), CL spread faster than FL, so extracellular ATP elevation evoked intracellular Ca^{2+} wave. However, for long distances (> 120 μm), synaptic transmission via gap junction channels is more effective, implying that intracellular Ca^{2+} increase induced ATP release. This conclusion also holds for the localized ATP propagation wave result in Figure 7B for distances < 100 μm. There, the ATP CL wave measured at the cell surface spread even faster than in the bulk solution, consistent with an extracellular CL pathway contributing more than the intracellular FL pathway at short distances. Whether the CL wave travels faster than the FL spread at distances > 100 μm was not determined in the beads experiment because of the inadequate CL detection sensitivity. We also note that the FL diffusion coefficient is lower when beads are attached by comparing Figure 7A and 7B, suggesting that the presence of beads may influence cell functions and caused a slower intracellular signaling speed.

Monitoring Rat Hepatoma Liver Cell ATP Release upon Hypotonic Stress.

During hypo-osmotic stress conditions, the rapidly swelling cells respond by active extrusion of osmolytes, such as K^+, Cl^- and small molecules, accompanied by the passive decrease in water, to return the cell to its original volume, a process referred to as 'regulatory volume decrease' (RVD).[54, 55] Some recent reports have suggested autocrine signaling through ATP release as a mechanism for cell-volume regulation. They showed that in rat hepatoma liver cell line, cell swelling increases membrane ATP permeability, meanwhile both Cl^- channel opening and cell volume recovery from swelling require stimulation of P2 receptors by extracellular ATP.[4, 9] We did similar experiments to observe ATP release from rat hepatoma

liver cells with hypotonic exposure, as shown in Figure 8. The cell shapes changed after the induced hypotonic stress (Figure 8 A1/A3), and ATP was released to the extracellular spaces (Figure 8 A2) to mediate the cell-volume change.

When firefly luciferase immobilized beads were used, extracellular ATP elevation was only confined to the cell regions (Figure 8 B2). Figure 9 clearly demonstrates the difference between the two types of experiments. For free enzyme (Figure 9 A1/A2), on-cell ROIs and off-cell ROIs showed similar ATP increase, which decayed slowly over a long time. However, for bead experiments, on-cell ROIs showed ATP release (Figure 9 B1) while off-cell ROIs displayed no ATP concentration change (Figure 9 B2). Also, the localized ATP release lasted only ~20 s in the bead experiments, similar to the astrocyte ATP release response with beads, but with much less released amounts. The net peak signal intensity increase was ~ 200, collected over 10 s. Using the ATP calibration curve of exposure time 1 s, we estimate the localized ATP release concentration to be around 10 μM, much less than the cytosolic ATP concentration, indicating that the mechanism of ATP release is not by physical damage on the cell membranes.

ACKNOWLEDGMENTS

E.S.Y. thanks the Robert Allen Wright Endowment for Excellence for support. The Ames Laboratory is operated for the U.S. Department of Energy by Iowa State University under Contract No. DE-AC02-07CH11358. This work was supported by the Director of Science, Office of Basic Energy Sciences, Division of Chemical Sciences.

REFERENCES

(1) Yin, J.; Xu, K. P.; Zhang, J.; Kumar, A.; Yu, F. S. X. *Journal of Cell Science* **2007**, *120*, 815-825.

(2) Ahmad, S.; Ahmad, A.; McConville, G.; Schneider, B. K.; Allen, C. B.; Manzer, R.; Mason, R. J.; White, C. W. *Free Radical Biology and Medicine* **2005**, *39*, 213-226.

(3) Yoon, M. J.; Lee, H. J.; Kim, J. H.; Kim, D. K. *Archives of Pharmacal Research* **2006**, *29*, 1032-1041.

(4) Wang, Y.; Roman, R.; Lidofsky, S. D.; Fitz, J. G. *Proceedings of the National Academy of Sciences of the United States of America* **1996**, *93*, 12020-12025.

(5) Coppi, E.; Pugliese, A. M.; Urbani, S.; Melani, A.; Cerbai, E.; Mazzanti, B.; Bosi, A.; Saccardi, R.; Pedata, F. *Stem Cells* **2007**, *25*, 1840-1849.

(6) Rossi, D. J.; Brady, J. D.; Mohr, C. *Nature Neuroscience* **2007**, *10*, 1377-1386.

(7) Coco, S.; Calegari, F.; Pravettoni, E.; Pozzi, D.; Taverna, E.; Rosa, P.; Matteoli, M.; Verderio, C. *Journal of Biological Chemistry* **2003**, *278*, 1354-1362.

(8) Wang, Z. Q.; Haydon, P. G.; Yeung, E. S. *Analytical Chemistry* **2000**, *72*, 2001-2007.

(9) Roman, R. M.; Wang, Y.; Lidofsky, S. D.; Feranchak, A. P.; Lomri, N.; Scharschmidt, B. F.; Fitz, J. G. *Journal of Biological Chemistry* **1997**, *272*, 21970-21976.

(10) Deluca, M.; McElroy, W. D. *Methods in Enzymology* **1978**, *57*, 3-15.

(11) Lundin, A. *Bioluminescence and Chemiluminescence, Pt C* **2000**, *305*, 346-370.

(12) Rojas, E.; Pollard, H. B.; Heldman, E. *Febs Letters* **1985**, *185*, 323-327.

(13) Detwiler, T. C.; Feinman, R. D. *Biochemistry* **1973**, *12*, 2462-2468.

(14) Schwiebert, L. M.; Rice, W. C.; Kudlow, B. A.; Taylor, A. L.; Schwiebert, E. M. *American Journal of Physiology-Cell Physiology* **2002**, *282*, C289-C301.

(15) Taylor, A. L.; Kudlow, B. A.; Marrs, K. L.; Gruenert, D. C.; Guggino, W. B.; Schwiebert, E. M. *American Journal of Physiology-Cell Physiology* **1998**, *44*, C1391-C1406.

(16) Zhang, Y.; Phillips, G. J.; Yeung, E. S., 2007; Vol. 79, pp 5373-5381.

(17) Zhang, Y.; Phillips, G. J.; Yeung, E. S. *Analytical Chemistry* **2008**, *80*, 597-605.

(18) Zimmermann, H. *Trends in Pharmacological Sciences* **1999**, *20*, 231-236.

(19) Zimmermann, H. *Naunyn-Schmiedebergs Archives of Pharmacology* **2000**, *362*, 299-309.

(20) Picher, M.; Boucher, R. C. *Journal of Biological Chemistry* **2003**, *278*, 11256-11264.

(21) Buxton, I. L. O.; Kaiser, R. A.; Oxhorn, B. C.; Cheek, D. J. *American Journal of Physiology-Heart and Circulatory Physiology* **2001**, *281*, H1657-H1666.

(22) Yegutkin, G. G.; Henttinen, T.; Samburski, S. S.; Spychala, J.; Jalkanen, S. *Biochemical Journal* **2002**, *367*, 121-128.

(23) Lazarowski, E. R.; Boucher, R. C.; Harden, T. K. *Journal of Biological Chemistry* **2000**, *275*, 31061-31068.

(24) Beigi, R.; Kobatake, E.; Aizawa, M.; Dubyak, G. R. *American Journal of Physiology-Cell Physiology* **1999**, *276*, C267-C278.

(25) Joseph, S. M.; Buchakjian, M. R.; Dubyak, G. R. *Journal of Biological Chemistry* **2003**, *278*, 23331-23342.

(26) Nakamura, M.; Mie, M.; Funabashi, H.; Yamamoto, K.; Ando, J.; Kobatake, E. *Analytical Biochemistry* **2006**, *352*, 61-67.

(27) Li, S. J.; Cronan, J. E. *Journal of Biological Chemistry* **1992**, *267*, 855-863.

(28) Cronan, J. E. *Journal of Biological Chemistry* **1990**, *265*, 10327-10333.

(29) Eu, J. Y.; Andrade, J. *Luminescence* **2001**, *16*, 57-63.

(30) Tatsumi, H.; Fukuda, S.; Kikuchi, M.; Koyama, Y. *Analytical Biochemistry* **1996**, *243*, 176-180.

(31) Jander, G.; Cronan, J. E.; Beckwith, J. *Journal of Bacteriology* **1996**, *178*, 3049-3058.

(32) Zen, K. H.; Consler, T. G.; Kaback, H. R. *Biochemistry* **1995**, *34*, 3430-3437.

(33) Darby, M.; Kuzmiski, J. B.; Panenka, W.; Feighan, D.; MacVicar, B. A. *Journal of Neurophysiology* **2003**, *89*, 1870-1877.

(34) Charles, A. C. *Journal of Neurochemistry* **1994**, *62*, S102-S102.

(35) Araque, A.; Parpura, V.; Sanzgiri, R. P.; Haydon, P. G. *European Journal of Neuroscience* **1998**, *10*, 2129-2142.

(36) Shenoy, B. C.; Wood, H. G. *Faseb Journal* **1988**, *2*, 2396-2401.

(37) Edluca, M.; McElroy, W. D. *Methods in Enzymology*; Academic Press: New York, 1978.

(38) Wang, C. Y.; Hitz, S.; Andrade, J. D.; Stewart, R. J. *Analytical Biochemistry* **1997**, *246*, 133-139.

(39) Green, N. M. *Methods in Enzymology* **1990**, *184*, 51-67.

(40) Held, P. In *Nature Methods: Application Notes*, 2006.

(41) Attwell, D. *Nature* **1994**, *369*, 707-708.

(42) Charles, A. C.; Kodali, S. K.; Tyndale, R. F. *Molecular and Cellular Neuroscience* **1996**, *7*, 337-353.

(43) Cornellbell, A. H.; Finkbeiner, S. M.; Cooper, M. S.; Smith, S. J. *Science* **1990**, *247*, 470-473.

(44) Kandler, K.; Katz, L. C. *Journal of Neuroscience* **1998**, *18*, 1419-1427.

(45) Churchill, G. C.; Louis, C. F. *Journal of Cell Science* **1998**, *111*, 1217-1225.

(46) Cotrina, M. L.; Lin, J. H. C.; Alves-Rodrigues, A.; Liu, S.; Li, J.; Azmi-Ghadimi, H.; Kang, J.; Naus, C. C. G.; Nedergaard, M. *Proceedings of the National Academy of Sciences of the United States of America* **1998**, *95*, 15735-15740.

(47) Scemes, E.; Suadicani, S. O.; Spray, D. C. *Journal of Neuroscience* **2000**, *20*, 1435-1445.

(48) Stout, C. E.; Costantin, J. L.; Naus, C. C. G.; Charles, A. C. *Journal of Biological Chemistry* **2002**, *277*, 10482-10488.

(49) James, G.; Butt, A. M. *European Journal of Pharmacology* **2002**, *447*, 247-260.

(50) Neary, J. T.; Kang, Y.; Willoughby, K. A.; Ellis, E. F. *Journal of Neuroscience* **2003**, *23*, 2348-2356.

(51) Araque, A.; Sanzgiri, R. P.; Parpura, V.; Haydon, P. G. *Journal of Neuroscience* **1998**, *18*, 6822-6829.

(52) Stenovec, M.; Kreft, M.; Poberaj, I.; Betz, W. J.; Zorec, R. *Faseb Journal* **2004**, *18*, 1270-+.

(53) Pangrsic, T.; Potokar, M.; Stenovec, M.; Kreft, M.; Fabbretti, E.; Nistri, A.; Pryazhnikov, E.; Khiroug, L.; Giniatullin, R.; Zorec, R. *Journal of Biological Chemistry* **2007**, *282*, 28749-28758.

(54) Jakab, M.; Furst, J.; Gschwentner, M.; Botta, G.; Garavaglia, M. L.; Bazzini, C.; Rodighiero, S.; Meyer, G.; Eichmuller, S.; Woll, W.; Chwatal, S.; Ritter, M.; Paulmichl, M. *Cellular Physiology and Biochemistry* **2002**, *12*, 235-258.

(55) Lang, F.; Busch, G. L.; Ritter, M.; Volkl, H.; Waldegger, S.; Gulbins, E.; Haussinger, D. *Physiological Reviews* **1998**, *78*, 247-306.

FIGURE CAPTIONS

Figure 1. Constructed plasmid, pET-KPBT-Luc. The biotin acceptor peptide from KPBT is fused to firefly luciferase and under control of the T7 promotor. As shown, sequences encoding a hexa-histidine tag are positioned at the 5' end of the gene fusion to facilitate purification of the recombinant protein.

Figure 2. Standard ATP detection. ATP was added by syringe into a mixture of D-luciferin and firefly luciferase in o-ring chambers on coverslips. (A) Blank image: no ATP was added. (B) Free firefly luciferase detection image: intense chemiluminescence light in the whole image when ATP was added to 2 mg/mL firefly luciferase and 2 mM D-luciferin. (C) Bead detection image: only bead locations show CL when ATP was added.

Figure 3: Firefly luciferase standard calibration curve. (A) Free firefly luciferase. (B) Firefly luciferase immobilized on beads. Fitting curve: polynomial.

Figure 4. Simultaneous monitoring of Ca^{2+} FL and ATP CL wave propagation using free firefly luciferase detection. The frame rate is 1.5 s. Exposure time for ATP is 1 s and that for Ca^{2+} is 50 ms. (a) Bright-field image of the astrocyte culture showing the mechanical tip positioned over a cell, followed by calcium fluorescence images in the upper two rows. (b) ATP chemiluminescence images in the lower two rows. Time 0 is when the

stimulation was applied. Scale bar at lower right: 50 μm.

Figure 5. Simultaneous monitoring of Ca^{2+} FL and localized ATP CL wave propagation using firefly luciferase immobilized on beads. The frame rate is 1.5 s. Exposure time for ATP is 1 s and that for Ca^{2+} is 50 ms. (a) Bright-field image of the astrocyte culture with beads attached to the cell surface showing the mechanical tip positioned over a cell, followed by calcium fluorescence images in the upper two rows. (b) ATP chemiluminescence images in the lower two rows. Time 0 is when the stimulation was applied. Scale bar at lower right: 50 μm.

Figure 6. Time course of ATP release and Ca^{2+} FL elevation in individual cells. Y-axis is the average pixel intensity of 10-pixel diameter circle ROIs at individual cell locations far from the stimulation center. (A1, A2): Time course of three ROIs in free firefly luciferase detection. A1, CL. A2, FL. (B1, B2): Time course of three ROIs in bead-immobilized firefly luciferase detection. B1, CL. B2, FL.

Figure 7. Diffusion coefficient at each ROI. After wave initiation by mechanical stimulation, the ATP CL and Ca^{2+} FL levels increased at each ROI sequentially from near to far from the stimulation center. The delay time t (s) of ROI at distance x (μm) to reach CL/FL intensity peak is dependent on the distance x. (A) D_{CL}/D_{FL} of each ROI from free firefly luciferase detection. (B)

D_{CL}/D_{FL} of each ROI from bead-immobilized firefly luciferase detection. D_{CL}: triangle. D_{FL}: square.

Figure 8. Monitoring rat hepatoma cell ATP release upon hypotonic stress. First row: free firefly luciferase detection. (A1): Bright-field image of cell before hypotonic stress. (A2): CL image of cells when hypotonic buffer was added. (A3): Bright-field image of cells after hypotonic stress. Second row: bead-immobilized firefly luciferase detection. (B1): Bright-field image of cells with beads attached. (B2): CL image of cells releasing ATP.

Figure 9. Time course of ATP release from cell regions and non-cell regions. (A1, A2): Free firefly luciferase detection. A1, ROIs on cell. A2, ROIs off cell. (B1, B2): Bead-immobilized firefly luciferase detection. B1, ROIs on cell. B2, ROIs off cell.

Figure 1.

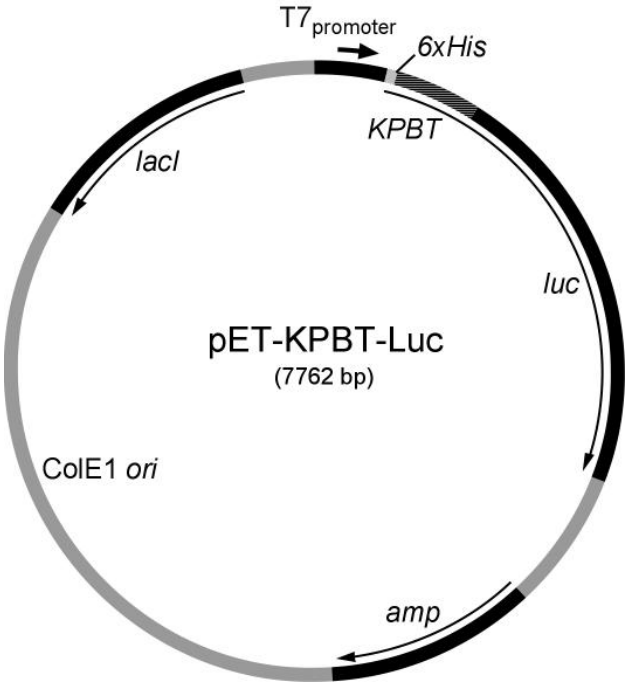

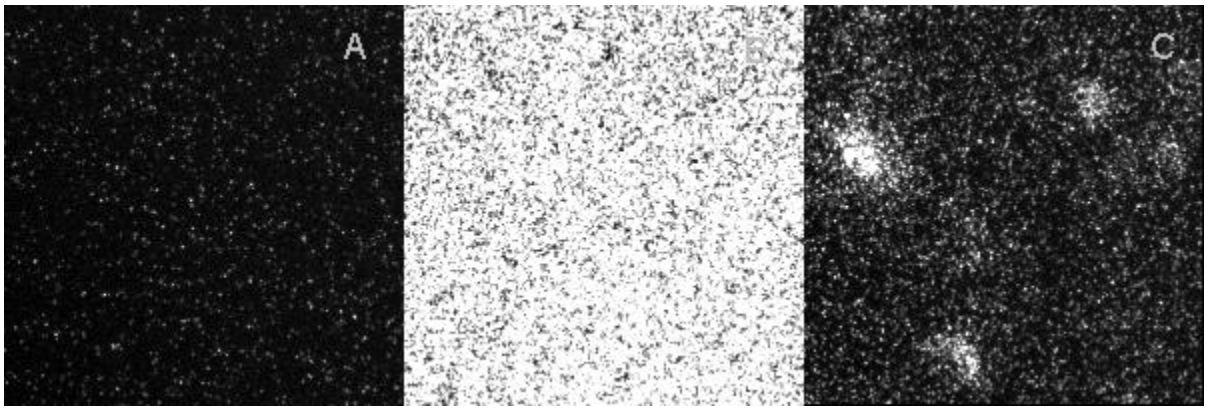

Figure 2.

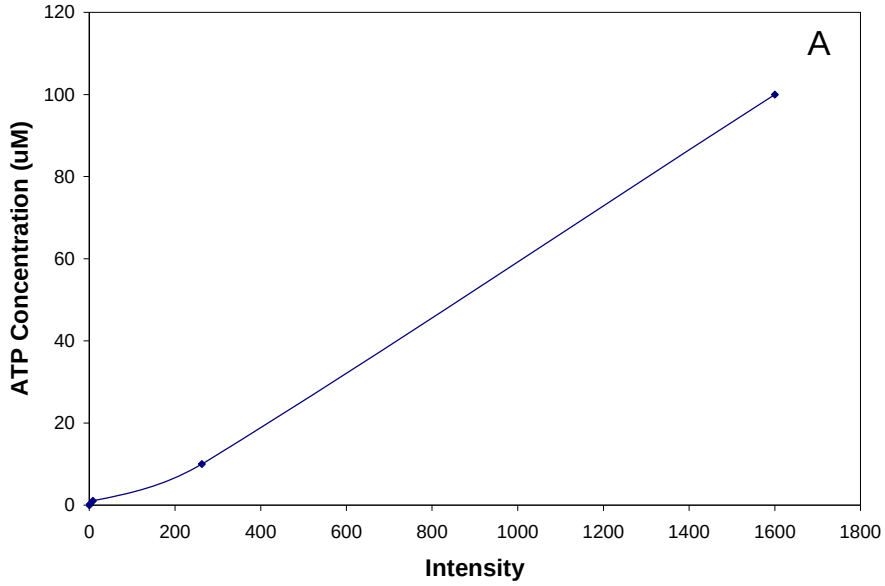

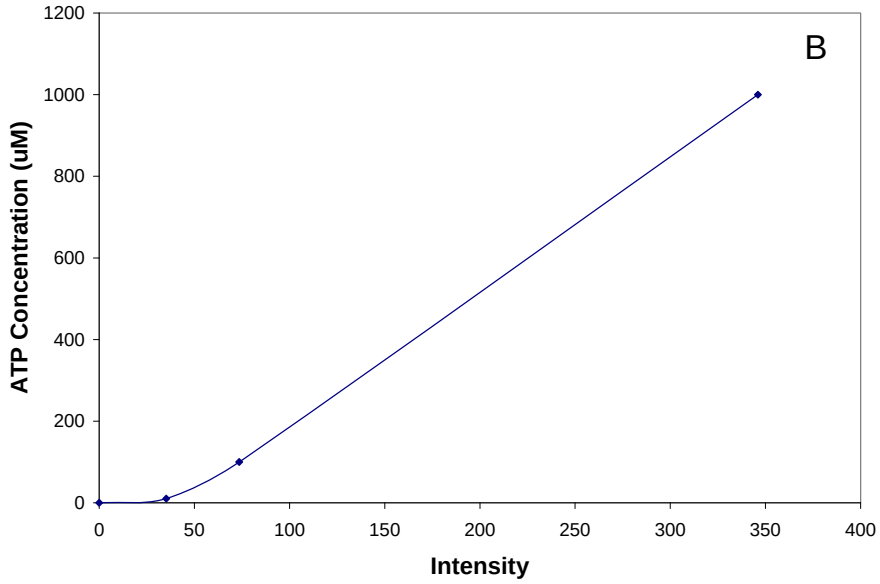

Figure 3.

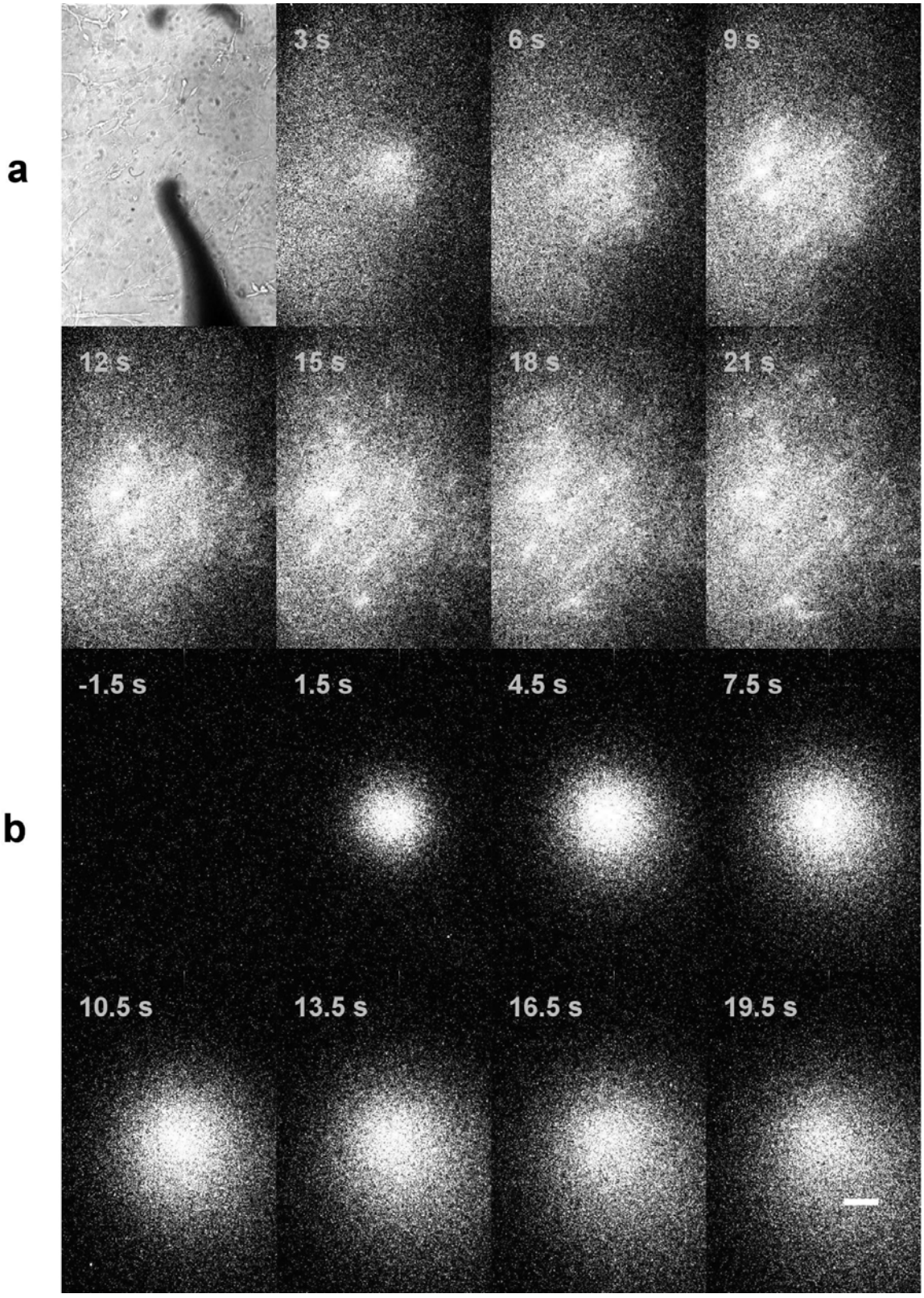

Figure 4.

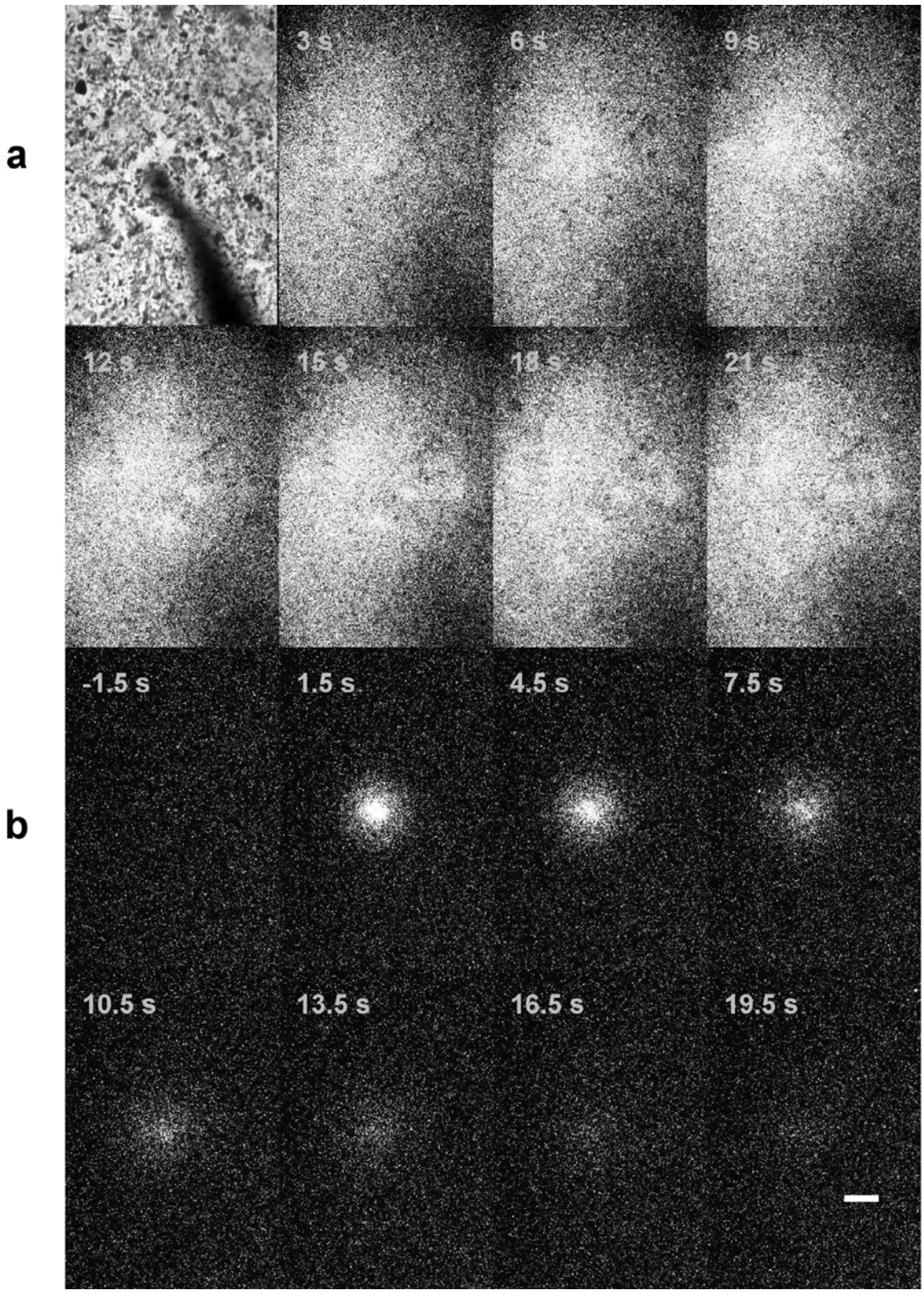

Figure 5.

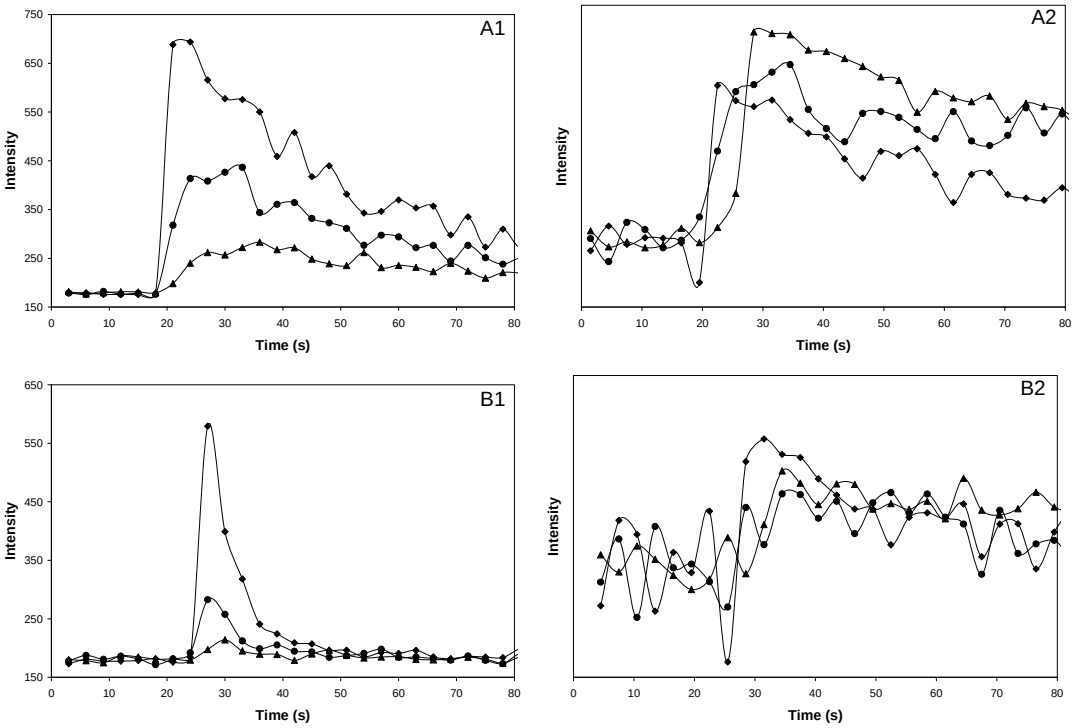

Figure 6.

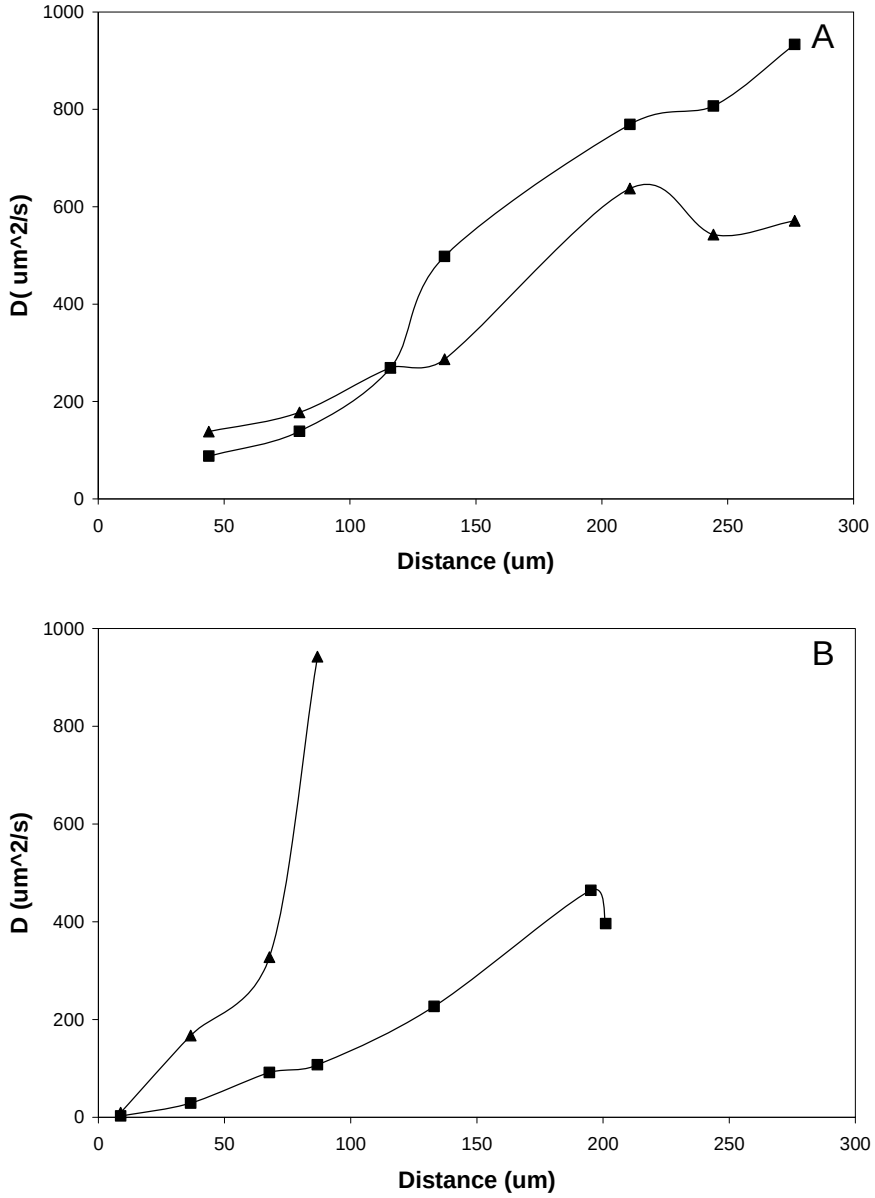

Figure 7.

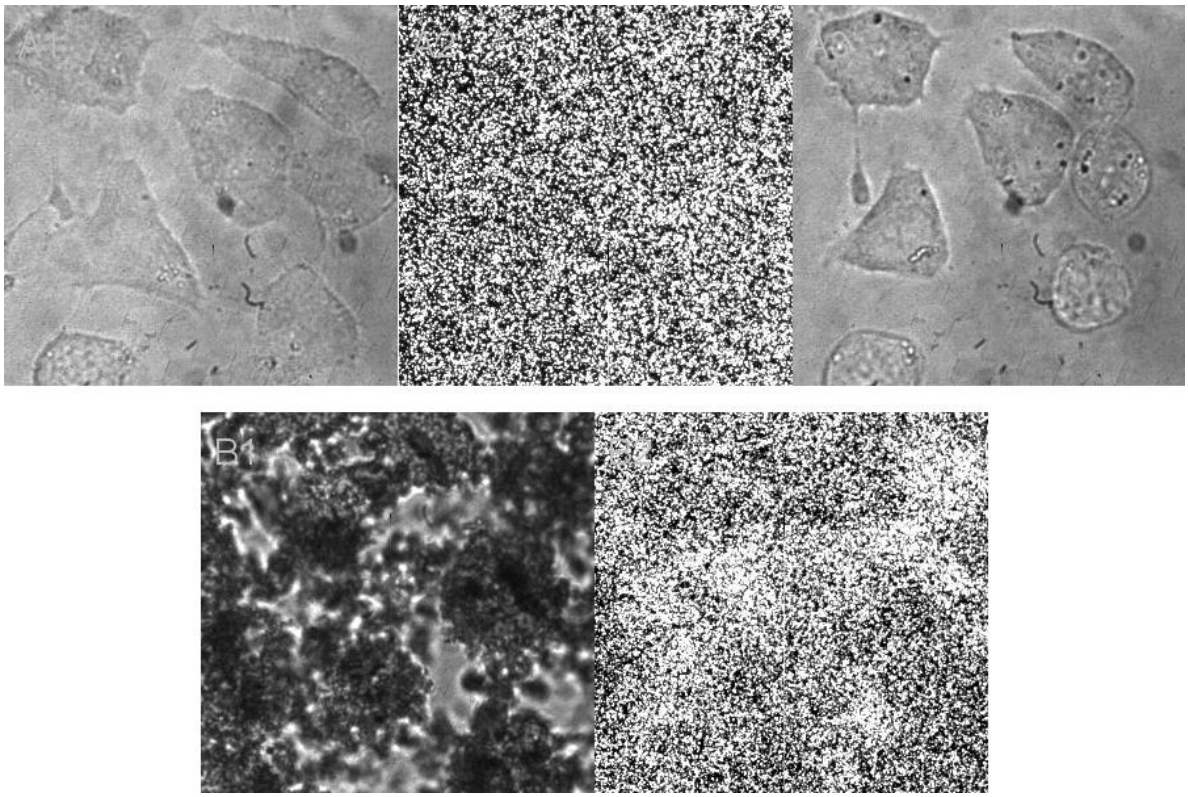

Figure 8.

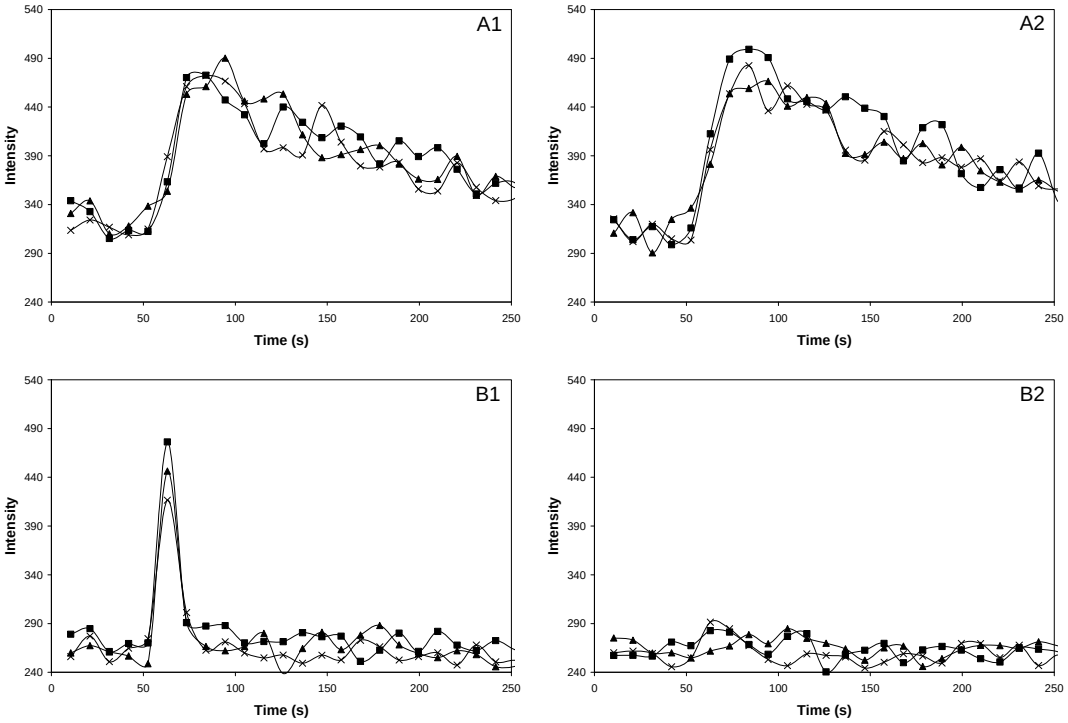

Figure 9.

CHAPTER 5. GENERAL CONCLUSIONS

The cell imaging field has been a hot research focus in the past decades. The achieved advances have dramatically transformed the biological sciences due to the dedicated work from multiple disciplines including chemistry, biology, physics, computer science, medicine, and pharmacology. The challenge for analytical chemists is to provide new cutting edge imaging technique that could probe single molecules or single organelles in single live cells non-invasively. Most of those approaches have been related to fluorescence detection since the cloning and expression of the revolutionary fluorescent GFP probe. CL cell imaging utilizing firefly luciferase as the reporter is a great alternative technique with good sensitivity and many advantages. And there is potential to improve the sensitivity and expand the applications of this technique.

We have demonstrated that 10^{-18} mole ATP and a few hundred firefly luciferase enzyme molecules inside single bacterium can be probed with CL imaging technique. And a new method of studying ATP release at the mammalian cell surface has been developed. The goal of our work in the future will be to improve the sensitivity to single firefly luciferase enzyme molecule level. To realize it we need to modify instrumentation in combine with computational manipulations to enhance image contrast. Meanwhile, ATP release mechanism can be further studied using our cell surface imaging technique by targeting at important biological questions. Other improvements on CL imaging technique may be developed depending on the needs of biologists.

ACKNOWLEDGEMENTS

First and foremost, I would like to express my sincere appreciation to my supervisor, Dr. Edward S. Yeung for his consistent help and guidance through the years in Iowa State University. Dr. Yeung set the example of a devoted scientist and a great man. He is intelligent, always challenges what is 'deemed to be true', never gives up when there seems no hope, and is patient and nice to all. These qualities make those years of working under his guidance a great pleasure for me.

I would also like to thank Dr. Houk, Dr. Phillips, Dr. Pohl, Dr. Schmidt-Rohr, Dr. Voytas and Dr. Porter for kindly serving on my committee and for all the guidance.

I am grateful for the collaboration work with Dr. Gregory Phillips, Xiaodong Lu, and Dr. Robert Doyle. My research involved a lot of molecular cloning and cell biology techniques. I could not have done this without their help in these fields.

It was also an enjoyable experience working with all the Young group members. Thank you for the support: Qingxi Li, Dr. Dragon Isailovic, Dr. Hungwing Li, Dr. Frank Li, Dr. Jiyoung Lee, Guoxin Lu, Slavica Isailovic, Dr. Bob Hsin, Dr. Hui Zhang, Dr. Aoshuang Xu, Jiangwei Li, Dr. Sangwon Cha, Dr. Ning Fang, Wei Sun and Wenjun Xie.

Finally, I would like to dedicate this dissertation to my family. My parents have supported and encouraged me all my life. They give me all the love without reservation and make me become what I am. And thanks to my beloved husband who inspired and encouraged me in work and in life. With his love and devotion, I am brave to take any challenges. Special thanks go to my unborn baby for accompanying me through those months and witnessing this moment.